Characterization of inflammatory signaling in the tumor microenvironment using SOCS3-U mice

I n a u g u r a l - D i s s e r t a t i o n

zur Erlangung des Doktorgrades

der Mathematisch-Naturwissenschaftlichen Fakultät

der Universität zu Köln

vorgelegt von
Philipp Justus Ackermann
aus Köln

Köln 2015

" *The true delight is in the finding out rather than in the knowing.*

- Isaac Asimov

Contents

List of Figures

List of Tables

List of Abbreviations

AAV	adeno associated virus
Alb	Albumin
AOM	Azoxymethane
BAC	Bacterial Artificial Chromosome
BW	body weight
cDNA	complementary DNA
CDS	coding sequence
cf.	confer
ChIP	chromatin immunoprecipitation
Ci	Curie
Cre	causes recombination (recombination enzyme)
CVD	cardiovascular disease
DEN	Diethylnitrosamine
DMEM	Dulbecco's modified eagle medium
DMSO	Dimethyl sulfoxide
DMF	Dimethylformamide
DNA	deoxyribonucleic acid
DSS	Dextransulfate
DTT	Dithiothreitol
EDTA	Ethylenediaminetetraacetic acid
ES cells	embryonic stem cells
EtOH	ethanol
F	Farad
FACS	fluorescence activated cell sorting
FCS	fetal calf serum
FLP	flippase (recombination enzyme)
FRT	FLP recognition target
(e)GFP	(enhanced) green fluorescent protein
i.p.	intraperitoneal
G418	Geneticin
HBSS	Hank's balanced salt solution
HCl	Hydrochloric acid
HSV	herpes simplex virus
IPTG	Isopropyl β-D-1-thiogalactopyranoside

IRES	internal ribosomal entry site
ITR	inverted terminal repeat
kb	kilo bases
kD	kilo Dalton
KO	knock out
LAH	left arm of homology
LB	lysogeny broth
LIF	leukemia inhibitory factor
loxP	locus of X-over P1
LPS	Lipopolysaccharide
M	molar
MEF	mouse embryonic fibroblast
MMC	Mitomycin C
mRNA	messenger ribonucleic acid
NaOH	Sodium hydroxide
NaCl	Sodium chloride
$Na_3C_6H_5O_7$	Sodium citrate
Na_3VO_4	Sodium orthovanadate
ORF	open reading frame
PAGE	Polyacrylamide gel electrophoresis
PBS	phosphate buffered saline
PCR	polymerase chain reaction
PMA	Phorbol 12-Myristate 13-Acetate
PMSF	Phenylmethanesulfonylfluoride
PVDF	Polyvinylidendifluorid
qPCR	quantitative polymerase chain reaction
rAAV	recombinant adeno associated virus
RAH	right arm of homology
RNA	ribonucleic acid
rox	region of cross-over
rpm	rounds per minute
RT	room temperature
ssDNA/RNA	single stranded DNA/RNA
SDS	sodium dodecyl sulfate
SEM	standard error of the mean
SOCS3	suppressor of cytokine signaling 3
STAT3	signal transducer and activator of transcription 3
Sv	sievert
TBS	tris buffered saline
TBS-T	tris buffered saline plus 0.1% Tween-20
TE	Tris-HCl EDTA

TG	transgene
Tk	thymidine kinase
UTR	untranslated region
UV	ultraviolet
V	Volt
WT	wildtype
X-Gal	5-bromo-4-chloro-3-indolyl-β-D-galactopyranoside

Abstract

Inflammatory signaling in the tumor microenvironment has been increasingly recognized to be a common, critical driving force for cancerogenesis. Unraveling inflammatory signaling in cancer initiation might give further insights into cancer formation to develop novel therapeutic treatment possibilities. This study introduces SOCS3-U, a novel reporter mouse line to conditionally visualize inflammatory signaling. The SOCS3-U modification was targeted to the endogenous suppressor of cytokine signaling 3 (SOCS3) locus, a negative feedback regulator of the JAK/STAT pathway highly upregulated by a variety of key inflammatory mediators. Here, a loxP flanked stop cassette in the first intron of SOCS3-U prevents the compound expression of SOCS3 and IRES-GFP. Thus, Cre-mediated recombination of the loxP flanked stop cassette leads to GFP expression in those cells that have upregulated SOCS3 expression. Moreover, the SOCS3 ORF has been flanked by rox sites to generate conditional SOCS3 knock-out mice in a Dre/rox-dependent manner, and the GFP configuration of SOCS3-U can be switched to firefly luciferase. In first experiments, SOCS3-U mice were used in mouse models of chemically induced colorectal and hepatocellular carcinoma to identify activation of distinct immune cell populations. These experiments demonstrate that SOCS3 negative M2 macrophages specifically upregulate CCL20 that attracts CCR6 expressing lymphocytes to the inflamed colon as a driving force for colorectal cancerogenesis. In the liver, inflammation promotes the formation of a hitherto unknown NK-T cell subpopulation that specifically upregulates IL-6Rα. Moreover, a novel generated AlbDre BAC transgenic mouse line creates hepatocyte specific SOCS3 knock-out mice via the Dre/rox system, providing the opportunity for sophisticated combinatory mouse models using more than one recombinase. Taken together, this study provides a

novel genetic tool for the universal visualization of inflammatory signaling *in vivo*.

Zusammenfassung

Entzündungsreaktionen im Tumormikromilieu werden mehr und mehr als gemeinsamer, entscheidender Katalysator in der Krebsentstehung erkannt. Die Netzwerke dieser Entzündungsreaktionen zu entschlüsseln verspricht daher neue Einblicke in die Krebsentstehung und könnte neue Behandlungswege eröffnen. In dieser Arbeit wird SOCS-U vorgestellt, eine neue Mauslinie um Entzündungsreaktionen konditional sichtbar zu machen. Die SOCS-U Modifikation wurde in den endogenen *suppressor of cytokine signaling 3* (SOCS3) lokus getargetet, einen sensitiven Rückkopplungshemmer des JAK/STAT Signalweges. Hier verhindert eine loxP flankierte stop Kassette im ersten Intron von SOSC3-U die kombinierte Expression von SOCS3 und IRES-GFP. Cre-abhängige Rekombination der loxP flankierten stop Kassette führt daher zu GFP Expression in Zellen, die SOCS3 hochreguliert haben. Zudem wurde der SOCS3 ORF mit rox Stellen flankiert, um Dre/rox abhängig konditionale SOCS3 Knock-out Mäuse zu erhalten. Darüber hinaus kann die GFP Konfiguration von SOCS3-U in eine Luziferase Konfiguration geändert werden. In ersten Experimenten wurden SOCS-U Mäuse in Mausmodellen von chemisch induziertem Darm- oder Leberkrebs eingesetzt, um eigenständige Untergruppen innerhalb verschiedener Immunzellarten zu identifiziert. Diese Experimente konnten zeigen, dass SOCS3-negative M2 Makrophagen spezifisch die Expression von CCL20 erhöhen, wodurch CCR6 exprimierende Lymphozyten in den entzündeten Darm angezogen werden und die Krebsentstehung fördern. In der Leber befördert eine Entzündung die Ausbildung einer bisher unbekannten NK-T-Zell Untergruppe, die spezifisch IL-6Rα hochreguliert. Des Weiteren kann eine neue Alb-Dre BAC transgene Mauslinie genutzt werden um Hepatozyten-spezifische SOCS3 Knock-out Mäuse mittels des Dre/rox Systems zu generieren, was die Möglichkeit

für elegante Mausmodelle mit mehr als einer Rekombinase ermöglicht. Zusammengenommen stellt diese Arbeit ein neues, genetisches Werkzeug zur universellen Identifizierung von Entzündungsreaktionen *in vivo* bereit.

1 Introduction

The development of a complex, higher organism from a single, fertilized oocyte is a vastly complicated process, and the evolution to multicellular organisms justifiably took place over the course of billions of years.

1.1 Inflammation associated cancerogenesis

Once an organism is fully developed, tissue growth is restricted to very defined areas harboring adult stem cells. Aberrations from this very controlled tissue growth are called neoplasms, which are further divided into benign neoplasms, whose growth does not spread -or metastasize- to neighboring tissues, and malignant neoplasms, which have the potential to metastasize to other tissues. Malignant neoplasia -or cancer- therefore does not constitute a singular disease, but rather encompasses uncontrolled cell growth in almost every tissue and invasion of these malignant cells into other tissues. The various cancer types display a high variability in incidence, mortality, severity, associated risk factors or geographical distribution (Fig. 1.1). There are, however, certain common hallmarks shared by all cancer types [seminally reviewed by Hanahan & Weinberg, 2011]. Cancer has been a constant burden on human health throughout history, with the earliest references preserved dating back to 3,000 BC [Hajdu, 2011].

In 2012, estimated 8.2 million cancer related deaths for the first time outpaced coronary heart diseases (7.3 million) and stroke (6.6 million), the undisputed leaders of the cardiovascular diseases (CVDs) and primary cause of death (17.5 million combined for CVDs), with 14.1 million new cancer cases world-wide [WHO, GLOBOCAN 2012, by Ferlay *et al.*, 2015]. Among cancers, colorectal cancer has the
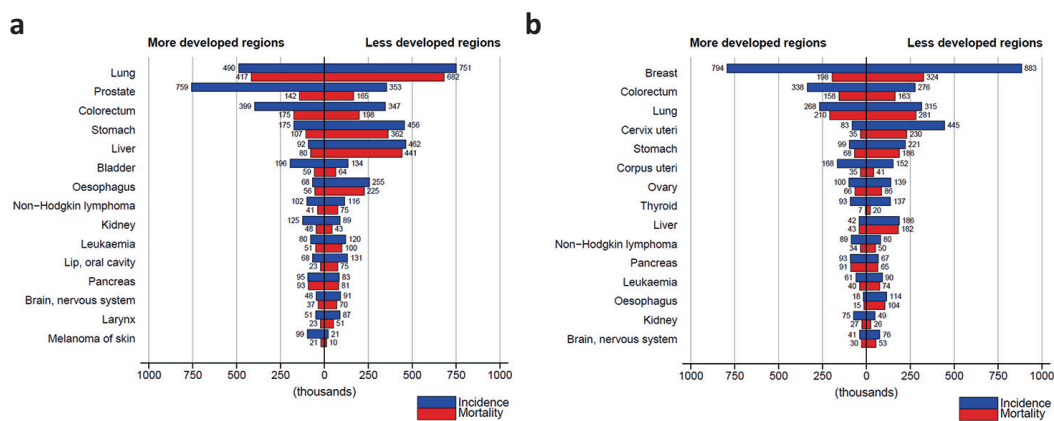
Figure 1.1: **Estimated world-wide new cancer cases and deaths in 2012**
Estimated new cancer cases (incidence) and deaths (mortality) world-wide for
2012, differentiated in more developed regions and less developed regions for
(a) males and (b) females [modified from Ferlay *et al.*, 2015]

third highest incidence (1.4 million new cases) with 694,000 deaths (mortality to incidence ratio of 0.49) in 2012, with a higher occurrence of about 55% in developed regions. Liver cancer ranks only fifth in incidence (782,000 new cases) but has a staggering mortality to incidence ratio of 0.95 (745,000 deaths), with higher occurrence in males and a strong bias towards less developed regions (83% of new cases). Most cancer types have a rather late onset and further deteriorate over time, and so the relative cancer occurrence is higher in developed regions; a trend which is likely to continue, given the increasing age-average of populations in developed regions. Consistently, European regions account for roughly 25% of cancer incidence and 20% of cancer deaths but accommodate only 10% of the global population.

1.1.1 Influence of the tumor microenvironment on cancerogenesis

In the last decades, our paradigm how we define cancer has substantially changed. Cancer is not anymore viewed as a few of out-of-control cells, but rather a network of different cell types surrounding and permeating masses of proliferating cells, almost forming tissue of their own. In fact, it is now believed that the interactions of cells of this so called tumor microenvironment with each other and the tumor cells are enabling cancerogenesis in the first place, a notion that becomes more apparent if the hallmarks of cancer are considered in more detail. Even if our conception of

tumors has broadened, the ability to proliferate and replicate indefinitely remains to be the prime hallmark of cancer cells. This includes a susceptibility to growth factors released by cancer cells themselves or immune cells in the tumor microenvironment, but also the ability to circumvent negative proliferation regulators, like contact inhibition. The classical countermeasure to a over-proliferating cell is for the cell to undergo apoptosis, either by cell-intrinsic mechanisms, or by ligand-induced, extrinsic apoptosis. A developing tumor therefore has to be able to both suppress the intrinsic apoptotic machinery, as well as to evade extrinsic apoptosis. The heightened replicative and proliferative potential of tumor cells requires a continuous supply of nutrients and oxygen, which the tumor achieves by inducing enhanced vascularization. The last step in tumorigenesis is the invasion and metastasis of hitherto unaffected tissues, which can also be facilitated by non-tumor cells within the microenvironment [Gocheva *et al.*, 2010].

Immune cells infiltrate the tumor microenvironment in high numbers and inhere a critical role in tumorigenesis, albeit a dichotomous one. Developing tumors need to escape destruction by immune cells, as becomes apparent if the increase in cancer formation upon immunodeficiency is considered [Vajdic & van Leeuwen, 2009]. Continuous inflammation however has tumor promoting functions, in that immune cells can release reactive oxygen species which can induce DNA damage in cancer cells, contributing to the genomic instability and mutagenesis [Maeda & Akaike, 1998]. Additionally, immune cells secrete various cytokines and chemokines into the tumor microenvironment, some of which, e.g. EGF (epidermal growth factor), VEGF (vascular endothelial growth factor) or FGF2 (basic fibroblast growth factor), actively induce proliferation. This is especially true for cells of the innate immune system, which is heavily involved in wound healing and tissue remodeling. Consequently, tumors have been long compared to „wounds that do not heal" [Dvorak, 1986].

Very similar to the inflammatory response to a wound, a developing tumor attracts and activates leukocytes to the afflicted tissue [Mantovani *et al.*, 2004].

Amongst the first leukocytes recruited are neutrophils, followed by monocytes differentiating into macrophages. These macrophages will then strongly secrete growth factors and cytokines into the tumor microenvironment, impacting on the endothelial, epithelial and mesenchymal cells in the vicinity [Coussens & Werb, 2002]. Additional cytokines and chemokines are secreted from the tumor cells, e.g. IL-6 (interleukin-6) and CSF-1 (colony stimulating factor 1), which push the differentiation of myeloid cells to tumor associated macrophages (TAMs) [Allavena *et al.*, 2000]. Although TAMs kill neoplastic cells via phygocytosis to a certain extent upon IL-2 or IL-12 stimulation, they also release angiogenic and lymphangiogenic factors that stimulate neoplasia [Schoppmann *et al.*, 2002]. The tumor microenvironment is generally recognized as having high levels of IL-10, blocking cytotoxic T-lymphocytes, and TGF-β (transforming growth factor beta), while having low levels of IL-12 and a defective T_H1 response [Germano *et al.*, 2008]. The low levels of the anti-carcinogenic IL-12 coincides with an increase in pro-carcinogenic IL-23, mediated by STAT3 (signal transducer and activator of transcription 3) [Kortylewski *et al.*, 2009]. Likewise, TAMs have a strong bias towards the M2 polarization [Mantovani *et al.*, 2002], skewed by the survival-factor NF-κB (nuclear factor κ-light-chain-enhancer of activated B cells) [Hagemann *et al.*, 2008].

1.1.2 Hepatic inflammation drives hepatocellular carcinogenesis

The vast majority (85%-90%) of liver cancer is represented by hepatocellular carcinoma (HCC) [El-Serag, 2011], which is mainly driven by cirrhosis after hepatitis B (HBV infection) or C (HCV infection), prolonged alcohol consumption or non-alcoholic steatohepatitis (NASH) [Donato *et al.*, 2002; Yoshioka *et al.*, 2004; Sherman, 2005]. Common hallmark of cirrhosis is an enhanced inflammation, and elevated serum levels of IL-6 can be found in patients with HBV, HCV or sustained alcohol consumption [Khoruts *et al.*, 1991; Kakumu *et al.*, 1991; Malaguarnera *et al.*, 1997], whereas obesity generally is increasingly recognized as a state of chronic low grade inflammation [Hotamisligil *et al.*, 1993]. Persistent inflammatory signal-

ing in the liver leads to wide-spread hepatocyte death, which is compensated by increased proliferation, further contributing to carcinogenesis [Bisgaard & Thorgeirsson, 1996]. NF-κB, mediating the effect of proliferation on the balance of proliferation and apoptosis, has consequently been recognized as a tumor promoter in inflammation-associated cancerogenesis [Pikarsky *et al.*, 2004]. Consistently, high levels of the catalytic subunits IKKα (IκB kinase α) and IKKβ are a prerequisite for malignancy in hepatocellular carcinoma [Jiang *et al.*, 2010].

Hepatocyte specific deletion of IKKβ increases chimcally-induced, via injection of the carcinogen diethylnitrosamine (DEN), HCC development, possibly due to enhanced cell death due to an elevated JNK (c-Jun N-terminal kinase) activity and concomitant ROS (reactive oxygen species) accumulation, consistently accompanied by increased hepatocyte proliferation [Maeda *et al.*, 2005]. Interestingly, IKKβ ablation both in hepatocytes and Kupffer cells (KCs) has the opposite effect and decreases DEN-induced HCC susceptibility, while exhibiting higher levels of liver injury and cell death and no detectable IL-6 upon DEN injection. Kupffer cells, liver resident macrophages, are important inflammatory contributors and the major source for proliferation stimulating mitogens in the liver [Fausto, 2000]. Increasing levels of IL-1α, released from dying hepatocytes, induces IL-6 release from KCs, elevating the inflammatory tone and subsequently causing even more hepatocyte death and resulting hyperproliferation, a potential driving force for HCC development [Naugler *et al.*, 2007; Sakurai *et al.*, 2008]. Compellingly, this effect is more pronounced in males, mirroring the enhanced risk for men to develop HCC, whereas the IL-6 release by KCs in females is inhibited by high levels of estrogen [Mantovani, 2007]. In line with the tumor promoting effect of a hepatocyte specific IKKβ deletion, loss of the NF-κB regulatory subunit IKKγ in hepatocytes causes steatohepatitis and spontaneous HCC development [Luedde *et al.*, 2007]. Additionally, hepatocyte specific deletion of the TLR (toll-like receptor) signaling mediator MyD88 (myeloid differentiation primary response gene 88) reduces DEN-induced HCC formation via decreased activation of both NF-κB and JNK pathways [Ströhle,
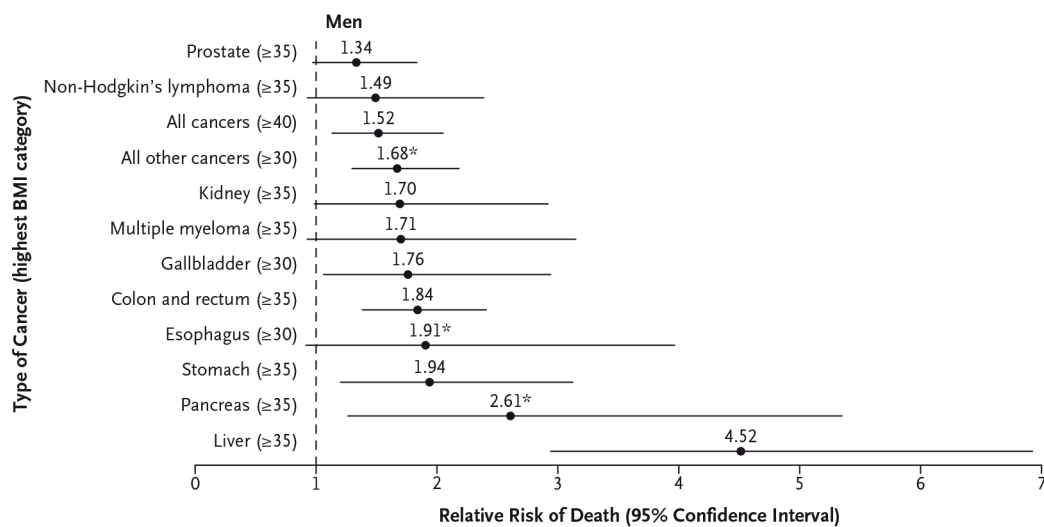
Figure 1.2: **Increased risk of cancer related death upon obesity in men**
Relative risk to die a cancer related death upon obesity depicted for a high body mass index (BMI, in parentheses) compared to reference category (BMI between 18.5 and 24.9) in men. Asterisks indicate non-smoking group. [from Calle *et al.*, 2003]

2012].

Obesity is a major risk factor for hepatocellular carcinoma

Obesity has been recognized as a state of chronic low grade inflammation and increases the risk of almost all cancers, with varying severity for individual cancer types per gender [Calle *et al.*, 2003]. People with a body mass index (BMI, $\frac{weight[kg]}{height^2[m]}$) of at least 40 had dramatically increased death rates for all cancers combined (52% for men and 62% for women respectively) compared to men and women with normal weight (BMI between 18.5 and 24.9). Amongst men, a BMI of at least 35 increases the relative risk to die from liver cancer 4.52 fold, the strongest increase in relative risk of death for all cancers (Fig. 1.2). As a consequence, an estimated 90.000 death per year in the USA are attributed to a BMI greater than 25.

In line with the obesity-associated increased risk of developing liver cancer, high-fat diet (HFD) fed rats develop not only NASH but have a higher incidence of pre-cancerous markers and pre-neoplastic lesions upon DEN injection [Wang *et al.*, 2009]. Consistently, HFD feeding aggravates spontaneous HCC development upon

hepatocyte specific IKKγ deletion in mice [Wunderlich *et al.*, 2008]. NASH development as a cause for HCC is furthermore dependent on the non-canonical NF-κB pathway, as LIGHT (TNFsF14) secretion from NK-T cells promotes hepatic lipid uptake and ultimately leads to cancer formation [Wolf *et al.*, 2014]. The exacerbated tumorigenesis accompanying obesity is reversed in a whole body IL-6 knock-out, in line with the previously demonstrated role for IL-6 in DEN-induced HCC formation [Park *et al.*, 2010]. Interestingly, in contrast to the IL-6 deletion, whole body IL-6Rα deletion fails to exert a protective effect on obesity promoting HCC development [Gruber *et al.*, 2013]. On normal chow diet (NCD), IL-6 signaling inhibits GSK-3β, a serine/threonine protein kinase targeting the key anti-tumor regulator Mcl-1 for polyubiquitinylation by MULE (Mcl-1 ubiquitin ligase E3), thereby prohibiting hepatocyte apoptosis and promoting cancerogenesis. In concert with decreased GSK-3β activity upon IL-6 signaling, expression of MULE and PP-1α, a GSK-3β activating protein phosphatase, is inhibited in a pSTAT3 dependent manner. Loss of IL-6Rα therefore protects from DEN-induced HCC formation by destabilizing Mcl-1, subsequently increasing apoptosis of damaged hepatocytes. Obesity aggravates tumor formation in the liver by further stabilizing Mcl-1 in an IL-6 independent manner, enabling continued proliferation of malformed hepatocytes.

Intriguingly, a hepatocyte specific IL-6Rα deletion does not confer protection from DEN-induced HCC development even on NCD, whereas T-cell specific IL-6Rα ablation (IL-6R$\alpha^{\text{T-KO}}$) protects from DEN-induced HCC even under obese conditions [Gruber, 2013]. The function of effector T-cells is tightly controlled by regulatory T-cells (T$_{\text{reg}}$s), and combined IL-6 and IL-1 signaling is required to release effector T-cells from T$_{\text{reg}}$-mediated repression and mount both a strong T$_{\text{H}}$1 and T$_{\text{H}}$17 response [Nish *et al.*, 2014; Schenten *et al.*, 2014]. Consequently, T$_{\text{reg}}$ depletion via *i.p.* injection of an α-CD25 antibody in the tumor initiation phase completely abrogates the protective effect of IL-6R$\alpha^{\text{T-KO}}$ on DEN-induced HCC development [Gruber, 2013].

1.1.3 Inflammatory bowel disease and gut microbiota

Although increased inflammation in the tumor microenvironment is a characteristic of every cancer type, some cancers show an especially high association of chronic inflammation with cancerogenesis. Colorectal cancer (CRC) develops predominantly after continuos inflammatory bowel disease, e.g. chronic ulcerative colitis or Crohn's disease [Jess *et al.*, 2005; Danese *et al.*, 2011]. Development of CRC is recapitulated in a mouse model of colitis associated cancerogenesis (CAC), where mice are injected with the procarcinogen azoxymethane (AOM) and tumorigenesis is promoted by induction of colitis with dextran sulfate sodium salt (DSS) application [Tanaka *et al.*, 2003]. The enhanced inflammatory profile upon colitis exerts a deleterious effect on tumorigenesis, as becomes apparent in light of an enterocyte specific IKKβ deletion. Loss of IKKβ and therefore canonical NF-κB ablation dramatically reduces AOM/DSS induced tumor formation by 75% [Greten *et al.*, 2004]. While the inflammatory tone is unaffected, IKKβ is required for Bcl-X$_L$ (B-cell lymphoma-extra large) expression, thus IKKβ ablation protects from CRC development via enhanced apoptosis. Interestingly, IKKβ deletion in the myeloid lineage also protects from AOM/DSS induced tumor formation, albeit to a smaller extent, but does so by reducing the inflammatory tone.

Inflammation in the colon is furthermore affected by the gut microbiome, which is in constant contact with the colonic mucosa, the tissues with the highest proliferative capacity, completely renewing the single-cell epithelial layer every 4-5 days [van der Flier & Clevers, 2009]. The gut microbiome in the large intestine contains over 10^{11} cells per g content and can differ greatly between individuals, further influenced by the dietary composition [Louis *et al.*, 2014]. Metabolites produced by gut microbiota can have both protective and deteriorating effects, highlighting the importance of a healthy gut microbiome. Short-chain fatty acids (SCFAs), like butyrate and propionate, can inhibit histone deacetylases in colonocytes and immune cells, affecting signal transduction via transcription factors, ultimately leading to a downregulation of pro-inflammatory cytokines, like IL-6 and IL-12, and thereby

counteracting tumorigenesis [Chang *et al.*, 2014]. Additionally, SCFAs are implicated in driving the differentiation of FoxP3$^+$ (forkhead box P3) T$_{reg}$s, which exert an inflammation controlling effect [Smith *et al.*, 2013]. Furthermore, butyrate signaling can inhibit NF-κB activation and selectively drive apoptosis in malformed cells [Thangaraju *et al.*, 2009].

Conflicting data however show a tumor-promoting effect of butyrate in a mouse model of mutations both in the Apc (adenomatous polyposis coli) and Msh2 (MutS homolog 2) genes [Belcheva *et al.*, 2014]. Other detrimental metabolites, like hydrogen sulfite or bile acid, on the other hand, drive the expression of pro-inflammatory cytokines and can cause DNA damage in colonocytes [Roediger *et al.*, 1997; Islam *et al.*, 2011]. Elevated levels of these pathogenic microbiota will eventually lead to their detection by dentritic cells via microorganism-associated pattern (MAMPs), subsequently promoting a T$_H$17 mediated IL-23 upregulation, concomitantly downregulating IL-10 [Grivennikov *et al.*, 2012]. This continuing inflammatory signaling, caused by pathogenic bacteria, can lead to loss of colonocyte barrier function, enabling the efflux of gut microbiota from the colon lumen into the submucosa, ultimately further driving inflammatory signaling.

The diverse effects of the various microbiota, often dependent on a very fine-tuned balance between tumor-promoting and -inhibiting bacteria, sometimes even controversial effects of the same metabolite (e.g. butyrate), place the gut microbiota at a very delicate position in tumorigenesis, substantiated by microbiota affecting the efficacy of immunotherapy against other cancer entities [Garrett, 2015].

1.2 Supressor of cytokine signaling 3 (SOCS3)

Inflammatory signaling, whether it being pro- or anti-inflammatory, is a very important tool for an organism to elicit a strong, specific and rapid response to a particular stimulus, and it is therefore paramount to tightly control both its onset as well as termination. Cytokines are potent mediators of inflammatory signaling and are a cornerstone of the immune response, but can also control proliferation or

contribute to tissue remodeling. Cytokines are usually kept in low concentrations but can be released in high quantities in a very short amount of time, so that their effect on their respective target tissues runs at peak efficiency. The intracellular effect of cytokine signaling can have a profound impact on various other signaling cascades as well as dramatically change gene expression, so unchecked inflammatory signaling can very well exceed the deleterious effects of its cause, and is in some cases fundamental part of the problem in the first place. Eukaryotic cells have therefore a wide array of ways to terminate inflammatory signaling at their disposal, one of it being the SOCS family of eight proteins.

1.2.1 SOCS mediated cytokine signaling feedback inhibition

The SOCS family of proteins comprises eight proteins, SOCS1-7 and CIS (cytokine-inducible Src-homology 2-containing protein). The eponymic SOCS1 was first described in parallel by three groups in 1997 [Starr *et al.*; Naka *et al.*; Endo *et al.*], and CIS in 1995 [Yoshimura *et al.*]. The shared functional significance of the SOCS protein family members as negative feedback inhibitors is reflected in their structural similarity (Fig. 1.3), containing a central SH2 (Src homology 2) domain and a highly conserved SOCS box at the C-terminus [Hilton *et al.*, 1998]. SOCS1 and SOCS3 contain an additional, conserved kinase inhibitory region (KIR domain) at their N-terminus [Yasukawa *et al.*, 1999]. The respective domains dictate three potential routes of dissipating inflammatory signaling for SOCS proteins.

Mechanism of SOCS3 negative feedback regulation

The most prominent domain is the C-terminal SOCS box, which can interact with the elongin B/C heterodimer and cullin-5 to form an E3 ubiquitin ligase [Zhang *et al.*, 1999; Zheng *et al.*, 2002]. SOCS proteins can utilize this domain to directly target cytokine receptors, JAKs (janus kinases) or downstream mediators of inflammatory signaling for degradation [Kamura *et al.*, 2004]. Although there are certain targets for SOCS3 E3 ligase activity known [Williams & Palmer, 2012], the affinity
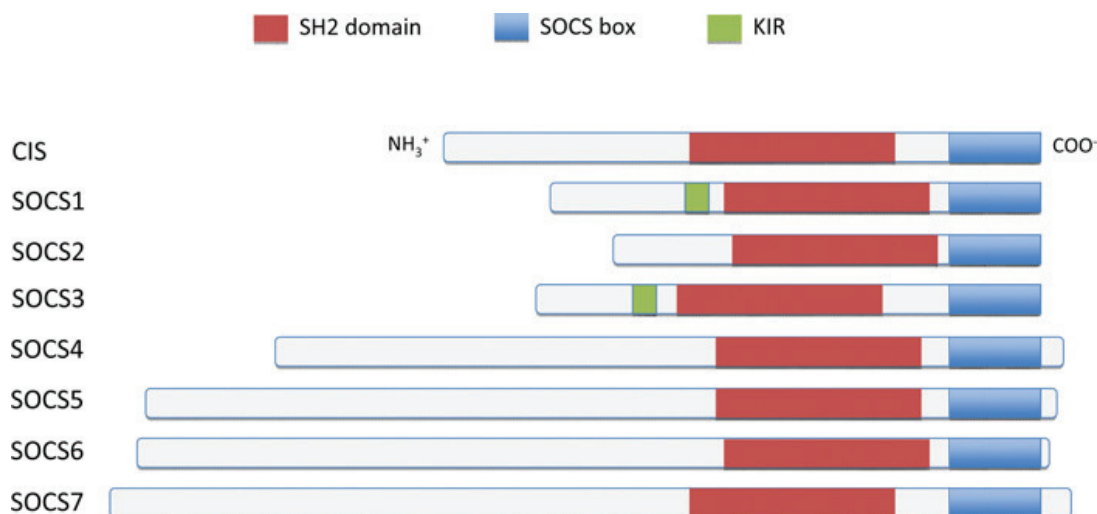
Figure 1.3: **Structural overview of the SOCS protein family**
CIS and SOCS1-7 share a central SH2 domain and a C-terminal SOCS box. SOCS1 and SOCS3 contain an additional KIR domain at the N-terminus. [modified from Galic *et al.*, 2014]

of SOCS3 for cullin-5, and thereby ultimately its E3 ligase activity, is comparably low [Babon *et al.*, 2009], indicating that SOCS3 is inhibiting inflammatory signaling rather through its SH2 or KIR domains than an E3 ligase activity via its SOCS box. SOCS proteins are inhibitors of cytokine signaling through the JAK/STAT pathway and are able to rapidly decrease activated STAT transcription factors. IL-6 stimulation leads to phosphorylated STAT3 (pSTAT3) in hepatocytes with one or two copies of SOCS3 within 15 minutes and persists for 2h, which is prolonged to 4h in the absence of SOCS3 [Croker *et al.*, 2003]. SOCS proteins bind with their SH2 domain to phosphotyrosines on various cytokine receptors, e.g. pY757 on gp130 (glycoprotein 130), pY800 on IL-12Rβ2 (IL-12 receptor β 2) or pY985 on the leptin receptor (LepR) in case of SOCS3, with a much higher affinity than JAKs, thereby competitively inhibiting binding and subsequent activating phosphorylation of JAKs [Nicholson *et al.*, 2000]. SOCS proteins with a KIR domain, like SOCS3, can also directly bind and inhibit JAKs (Fig. 1.4). In fact, SOCS3 specifically binds receptor/JAK dimers, which, together with the selective affinity for certain receptors, may explain why SOCS3, although being able to bind to three of the four JAK/STAT kinases (JAK1, JAK2 and TYK2, but not JAK3), does not inhibit signal-
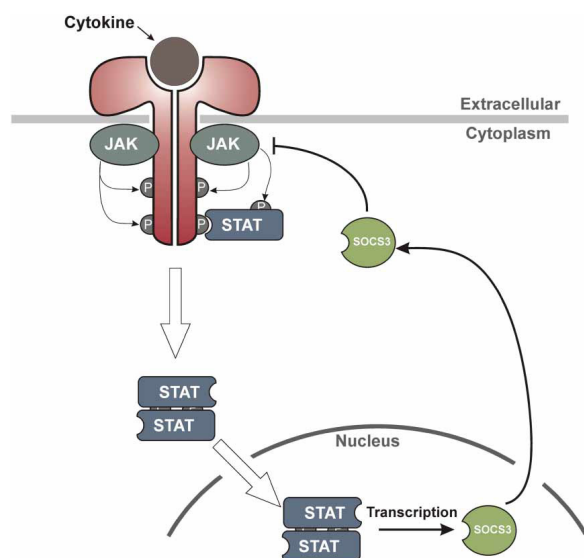
Figure 1.4: **Mechanism of SOCS3 feedback inhibition on JAK/STAT signaling**
Binding of the ligand induces dimerization and subsequent activation of associated JAKs. JAK phosphorylation of the respective receptor β-chains triggers recruitment and phosphorylation of downstream STAT signaling mediators. Phosphorylated STAT dimers translocate to the nucleus and activate target gene expression, including SOCS3. SOCS3 translocates to the plasma membrane and inhibits JAK/STAT signaling. [from Babon & Nicola, 2012]

ing by all cytokines utilizing those kinases [Kershaw *et al.*, 2013].

SOCS3 expression is induced by various stimuli

SOCS3 expression is mainly induced by signaling through the JAK/STAT pathway, but is upregulated differentially in response to the respective upstream mediator of JAK/STAT signaling. *i.v.* injection of IL-6 results in an upregulation of SOCS3 mRNA in mouse livers within 20 minutes and returns to basal levels after 8 h [Starr *et al.*, 1997]. The SOCS3 promoter contains two STAT1/STAT3 responsive elements [Auernhammer *et al.*, 1999] and is most prominently induced by IL-6 type cytokines. Apart from IL-6, IL-11 and LIF as IL-6 type cytokines, SOCS3 is also upregulated by leptin [Bjørbaek *et al.*, 1998], TNFα [Emanuelli *et al.*, 2001], CNF [Bjørbaek *et al.*, 1999], insulin [Emanuelli *et al.*, 2000] and resistin [Steppan *et al.*, 2005]. Expression of SOCS3 is also activated by IL-10 derived pSTAT3, but SOCS3 does not inhibit signaling by IL-10, a cytokine with classical anti-inflammatory capacities [Yasukawa *et al.*, 2003; Lang *et al.*, 2003; Niemand *et al.*, 2003].

SOCS3 activity is efficiently terminated by post-translational modification

The efficient inhibition of JAK/STAT signaling by SOCS3 requires an equally efficient termination of that inhibition, in order to normalize the transcriptome of the target cell and prime it for an upcoming, novel signaling event. Whereas JAK/STAT inhibition by SOCS3 will prevent further *de novo* expression, SOCS3 is post-translationally regulated through several mechanisms. The SOCS3 SH2 domain contains an unstructured region containing a PEST sequence [Babon *et al.*, 2005], a motif commonly associated with a short protein half-life [Rogers *et al.*, 1986]. Furthermore, SOCS3 is tyrosinephosphorylated at residues Y204 and Y221 in the SOCS box, inhibiting the interaction of SOCS3 with elongin C and targeting SOCS3 for proteasome-mediated degradation [Haan *et al.*, 2003]. Proteasomal degradation of SOCS3 can also be achieved via polyubiquitination at SOCS3 K6, a conserved residue absent in a naturally occurring truncated form of SOCS3 via alternative translation after ER stress or activated protein kinase (PKR) [Sasaki *et al.*, 2003].

Furthermore, SOCS3 is regulated by promoter methylation and miRNA action [Boosani & Agrawal, 2015]. miR-122, the most abundant miRNA in the liver, is a potent regulator of SOCS3 activity, although the mechanism is not completely elucidated. Conflicting reports in Huh7 HCC cells show either an increased SOCS3 promoter methylation in the absence of miR-122, resulting in silencing of SOCS3 expression and subsequently enhanced phosphorylation of STAT3 upon interferon-α (IFN-α) stimulation [Yoshikawa *et al.*, 2012], or binding of miR-122 to the 3'UTR of SOCS3 mRNA and thereby a post-transcriptional SOCS3 inhibition [Gao *et al.*, 2015]. SOCS3 inhibition by promoter methylation has been observed in several colorectal cancer cell lines, where the methyltransferase DNMT1 downregulates SOCS3 expression via hypermethylation in an IL-6 dependent manner [Li *et al.*, 2012]. Blocking DNMT1 increases SOCS3 expression in unchallenged cells, rendering them susceptible to IL-6 induced SOCS3 upregulation. A SOCS3 downregulation by hypermethylation can also also be observed during the progression of lung

cancer in rats [Liu *et al.*, 2010] and humans [He *et al.*, 2003]. SOCS3 promoter analyses from various human HCC cell lines revealed aberrant methylation in three cell lines, and six out of 18 primary HCC samples [Niwa *et al.*, 2005]. The responsible methylation site co-localizes with a conserved STAT binding site, approximately 500 bp upstream of the translation start site, providing a possibility for efficient ablation of STAT induced SOCS3 expression. Moreover, SOCS3 is a direct target of miR-483-5p, an intronic miRNA in the IGF2 locus, in murine Hepa1-6 hepatoma cells, substantiating SOCS3's function both in metabolism as well as cancerogenesis [Ma *et al.*, 2011]. Consistently, an upregulation of miR-802 under obese conditions indirectly increases SOCS3 expression by downregulating the transcription factor Hnf1b [Kornfeld *et al.*, 2013]. Furthermore, diabetic patients exhibit a decrease in miR-185 plasma levels, negatively correlating with blood glucose levels and SOCS3 expression [Bao *et al.*, 2015]. An inhibition of miR-185 in the pancreatic beta-cell line MIN6 results in a decreased glucose stimulated insulin secretion, reduced cell growth and viability and ultimately increased apoptosis. SOCS3 is a direct target of miR-185, as co-tranfection of a SOCS3-expressing plasmid and miR-185 restores the metabolic phenotype. miR-185 additionally has already been implicated in cancer progression of various human cancer entities, namely non small cell lung cancer [Takahashi *et al.*, 2009], colorectal cancer [Liu *et al.*, 2011], ovarian-, renal- and breast-cancer [Imam *et al.*, 2010] and gastric cancer [Li *et al.*, 2014], though no connection to SOCS3 is reported. A miR-203 knock-down in breast cancer tissues however enhances SOCS3 expression and increases apoptosis [Ru *et al.*, 2011].

SOCS3 function is indispensable for the developing organism

SOCS3 functions at the heart of several highly important signaling pathways, and as such plays a crucial role in embryonic development. Consequently, a homozygous whole body knockout of SOCS3 is lethal between embryonic days 11 and 13 (E11-E13), due to placental deficiency [Roberts *et al.*, 2001]. Conditional knockouts, using the Cre/loxP system, have been utilized to elucidate the contribution

of SOCS3 to individual cell types or signaling processes.

1.2.2 SOCS3 controls immune cell differentiation

Function of both the innate as well as adaptive immune system relies heavily on inflammatory signaling, whether immune cells are attracted by chemokine signaling to a site of infection or whether their maturation to elicit are more defined response is induced by interleukins or other cytokines. SOCS3 function, like that of other suppressors of cytokine signaling, is very important in many immune cell types. SOCS3 is constitutively expressed in CD4$^+$ naïve T-cells and maintains their quiescent state [Yu *et al.*, 2003]. Stimulation of naïve T-cells with hen egg lysozyme decreases SOCS3 expression and concomitantly upregulates IL-2 production, which is in line with an observation that elevated SOCS3 action inhibits CD28-mediated IL-2 production and proliferation in T-cells via its SH2 domain [Matsumoto *et al.*, 2003]. Conflicting data demonstrate hyperproliferation of CD8$^+$ T-cells from gp130^{Y757F}/gp130^{Y757F} mutant mice (where SOCS3 cannot bind to, and thereby inhibit signaling through, the gp130 receptor) in response to T-cell receptor (TCR) signaling, suggesting an impact of SOCS3 on IL-27 signaling rather than TCR- or CD28-mediated signaling to modulate T-cell proliferation [Brender *et al.*, 2007]. An inverse correlation between SOCS3 and IL-2 expression corroborates an implication for SOCS3 in T$_H$ cell lineage commitment, where high levels of SOCS3 expression have been found in the T$_H$2 subtype, which does not express IL-2, and only very low levels in IL-2 secreting T$_H$1 cells [Egwuagu *et al.*, 2002]. SOCS3 function in T$_H$ cell lineage commitment is further substantiated by an enhanced T$_H$2 development, measured by enhanced IL-4 in combination with suppressed IFN-γ production, upon SOCS3 overexpression and consistently T$_H$2 suppression alongside SOCS3 haploinsufficiency [Seki *et al.*, 2003]. Enhanced SOCS3 action in T$_H$2 cells leads to a reduction of IL-12 induced STAT4 activation by binding to pY800 on IL-12Rβ2, subsequently inhibiting IFNγ secretion and maintaining the T$_H$2 commitment [Yamamoto *et al.*, 2003].

SOCS3 and T_H17 cell development

The classical concept of naïve CD4+ T-cells developing either into T_H1 or T_H2 cells had to be modified with the recognition of IL-17 secreting CD4+ T-cells as a separate subtype, consistently termed T_H17, which is negatively regulated by T_H1 and T_H2 cells [Harrington *et al.*, 2005; Park *et al.*, 2005]. Development of T_H17 cells is driven by dendritic cells secreting IL-23, a heterodimeric cytokine sharing subunit p40 with IL-12 and also signaling through the IL-12β1 receptor [Aggarwal *et al.*, 2003]. An investigation of the T_H1/T_H2 polarization in context of a SOCS3-deficiency via MMTV-cre (mammary tumor virus-cre) [Hennighausen *et al.*, 1995] revealed no changes compared to the wild-type, but enhanced STAT3 phosphorylation upon IL-23 stimulation and a subsequent induction of IL-17 secretion [Chen *et al.*, 2006]. Similar results were obtained when TGF-β stimulation of naïve CD4+ T-cells increased T_H17 development by decreasing SOCS3 expression, thereby also prolonging pSTAT3 signaling [Qin *et al.*, 2009]. An elevated secretion of TGF-β from SOCS3-deficient CD4+ T-cells was already implicated in the development of T_H3 cells [Kinjyo, 2006], but later connected to an increased IL-17 production upon siRNA mediated SOCS3 down-regulation in CD4+ T-cells [Moriwaki *et al.*, 2011]. The inhibitory effect of SOCS3 on T_H17 T-cell development was further substantiated by LIF (leukemia inhibitory factor) treatment of CD4+ T-cells and the subsequent SOCS3 and ERK upregulation, abrogating pSTAT3 signaling essential for T_H17 T-cell proliferation [Cao *et al.*, 2011], as well as impaired IL-17 production upon SOCS3 overexpression in T lymphocytes [Romain *et al.*, 2013].

T_H cell proliferation is globally suppressed bei CD4+CD25+FoxP3+ T_{reg}s, which do not show SOCS3 expression [Pillemer *et al.*, 2007], despite their expression of and signaling through IL-6Rα [Doganci *et al.*, 2005]. Stimulation of T_{reg}/T_H co-cultures with IL-2 and IL-6 inhibits the T_{reg}-mediated T_H cell suppression, due to dominant effects of the cytokines on T_H cells. Further analyses demonstrated that, since SOCS3 mRNA is indeed expressed also in T_{reg}s, SOCS3 protein levels have to be kept low by post-translational modification. The inverse correlation of SOCS3

levels and IL-2 signaling observed in T_H cells seems to also be reflected in T_{reg}s, where IL-2 signaling is crucial for their homeostatic maintenance [Fontenot *et al.*, 2005]. Rapid SOCS3 upregulation in T_{reg}s upon infection could therefore mediate the release of T_H cells from T_{reg}-mediated suppression. Furthermore, SOCS3 deletion in dendritic cells (DCs) selectively promotes FoxP3$^+$ T_{reg}s by increasing TGF-β1 production, suggesting SOCS3 as a key regulator of the DC-mediated balance between regulatory and effector T-cells [Matsumura *et al.*, 2007].

SOCS3 promotes M1 macrophage polarization

Macrophages are part of the innate immune system, and act both as antigen-presenting cells (APCs) as well as mediators of the immune response of infiltrating leukocytes. Macrophages can be differentiated into „classically activated" (M1) macrophages and „alternatively activated" (M2) macrophages [reviewed by Mosser & Edwards, 2008]. M1 macrophages are considered anti-microbial and cytotoxic and are induced by a combination of IFN-γ and pro-inflammatory stimuli like LPS or TNF-α, whereas M2 macrophages function mainly in tissue-repair and are induced by IL-4 or IL-10. Polarization to either subtype renders the macrophage unresponsive to the inducers of the respective other subtype [Erwig *et al.*, 1998]. In line with the differentiating functions of M1 vs. M2 macrophages, 80% of infiltrating macrophages in the acute stage of nephrotoxic nephritis express either SOCS1 or SOCS3, with the majority expressing SOCS3 [Liu *et al.*, 2008]. Markedly, bone-marrow derived macrophages (BMDMs) stimulated with IFN-γ exclusively express SOCS3, whereas IL-4 stimulated BMDMs selectively upregulate SOCS1. Responsiveness to M2 inducing IL-4 signaling is restored upon siRNA mediated SOCS3 knock-down, demonstrating a function for SOCS3 in maintaining M1 polarized macrophages. A correlation between SOCS3 expression and M1 polarization is substantiated by a strong co-expression of SOCS3 and the M1 marker iNOS (nitric oxide synthase) in infiltrating, glomerular macrophages in nephritis [Arnold *et al.*, 2014]. siRNA mediated SOCS3 depletion results in an upregulation of M2 markers

like arginase-1 or mannose receptor. A potential mechanism for unresponsive-ness of M1 macrophages to M2 inducing stimuli in context of SOCS3 activity is provided by observations from peritoneal macrophages obtained from *db/db* mice, where IL-4 induced, IRS-2 (insulin receptor substrate)/PI3K (phosphoinositide 3-kinase)-association-dependent upregulation of IL-1Rα is attenuated by a chronic SOCS3 overexpression [O'Connor *et al.*, 2007]. Consistently, macrophages from IL-4R$\alpha^{-/-}$ mice showed an upregulation in SOCS3 protein levels [Whyte *et al.*, 2011]. Conflicting data show an enhanced M1 macrophage polarization upon myeloid-specific SOCS3 deletion, although an upregulation of SOCS3 in macrophages upon M1 inducing cytokine stimulation is confirmed [Qin *et al.*, 2012]. Furthermore, a myeloid-specific deletion of SOCS3 promotes both T_H1 and T_H17 response of CD4$^+$ T-cells. Interestingly, responsiveness of SOCS3 deficient macrophages to IL-4 stim-ulation is not assessed.

$T_H1/2$ cytokines IFN-γ and IL-4 are also released in large amounts by stim-ulated NK-T cells, which are an abundant T-cell subpopulation in the liver. A lymphocytic overexpression of SOCS3 using the lck (lymphocyte specific protein tyrosine kinase)-promoter in T and NK-T cells (Lck-SOCS3 tg) results in decreased serum IFN-γ and IL-4 levels, without affecting lymphocyte numbers oder cyto-toxic activity, when Lck-SOCS3 tg mice are subjected to a Concanavalin-A (ConA) induced model of hepatitis [Nakaya *et al.*, 2009]. Lck-SOCS3 tg mice are protected from ConA induced hepatitis, and exhibit decreased phosphorylation of STAT1 and STAT3 specifically in NK-T cells, and not in T-cells. This leads to suppression of cytokine release from NK-T cells, ultimately suggesting a protective effect against liver injury for SOCS3 expression in NK-T cells, as opposed to SOCS3 action in hepatocytes, where a deletion of SOCS3 protects against ConA induced hepatitis [Ogata *et al.*, 2006b].

1.2.3 SOCS3 regulates energy homeostasis

The regulation of energy homeostasis is a very complex machinery, encompass-

ing the central control by the arcuate nucleus in the hypothalamus, as well as peripheral control in tissues like liver, skeletal muscle or adipose tissue. Abundant energy in form of elevated blood glucose levels triggers the release of insulin from the pancreas, which signals both on neurons in the arcuate nucleus to modify food intake as well as on peripheral tissues like the liver, to suppress gluconeogenesis, or skeletal muscle to take up glucose. With food intake constantly exceeding energy consumption, ever increasing amounts of adipocytes will be stored in the adipose tissue, which correlates with their proportional secretion of leptin, the „satiety hormone". The intricate network of energy homeostasis is under extensive investigation for many decades now and reviewed constantly and manifold [e.g. Karatsoreos *et al.*, 2013; Friedman, 2014].

Both insulin and leptin upregulate SOCS3 expression, and both their intracellular signaling cascades are in turn regulated by SOCS3. A deletion of SOCS3 in neuronal precursor cells with nestin-cre or synapsin-cre results in increased and prolonged tyrosinephosphorylation of STAT3 upon leptin administration [Mori *et al.*, 2004]. This enhanced leptin sensitivity leads to increased expression of proopiomelanocortin (POMC) in neurons, which secrete the anorexigenic neuropeptide α-MSH. Consequently, leptin administration results in reduced food intake and a greater weight loss in mice with neuronal SOCS3 deficiency. Furthermore, weight gain upon HFD feeding is decreased and insulin sensitivity maintained in the absence of SOCS3 in neurons. A more specific deletion of SOCS3 in POMC neurons of the arcuate nucleus results in a very similar phenotype, namely enhanced leptin sensitivity and glucose tolerance upon NCD and reduced weight gain, due to increased energy expenditure, and improved insulin sensitivity on HFD [Kievit *et al.*, 2006]. Another brain region involved in feeding behavior is the ventromedial hypothalamus (VMH), whose neurons abundantly express steroidogenic factor 1 (SF-1). Deletion of SOCS3 with a SF-1-cre consistently leads to enhanced leptin sensitivity, reduced food intake and improved insulin sensitivity [Zhang *et al.*, 2008].

As for the peripheral impact on energy homeostasis, obesity has been increas-

ingly recognized as a state of chronic low grade inflammation [Hotamisligil *et al.*, 1993; Xu *et al.*, 2003]. Increased circulating cytokine levels under obese conditions, as assesed in mice lacking the leptin receptor (*db/db* mice), subsequently upregulate SOCS3 in hepatocytes [Ueki *et al.*, 2004a]. Increased expression of SOCS3 in the liver inhibits insulin signaling by blocking the IRS1 binding site pY960 on the insulin receptor, resulting in insulin resistance [Emanuelli *et al.*, 2001]. Consequently, a hepatocyte specific SOCS3 knock-out increases insulin stimulated IRS1 phosphorylation [Senn *et al.*, 2003] and thereby protects from IL-6 induced insulin resistance [Torisu *et al.*, 2007; Sachithanandan *et al.*, 2010], whereas an overexpression of SOCS3 leads to insulin resistance by reducing IRS1 and IRS2 phosphorylation [Ueki *et al.*, 2004b].

The protective effect on energy homeostasis of attenuated SOCS3 function in hypothalamus and liver is, to a lower extent, also present in other peripheral tissues. A knockout of SOCS3 in the white adipose tissue (WAT) shows only a mild protection of obesity induced insulin resistance in female mice [Palanivel *et al.*, 2012], while a SOCS3 deletion in skeletal muscle results in an increased peripheral glucose disposal and partially protection from insulin resistance [Jorgensen *et al.*, 2012]. Furthermore, a whole body SOCS3 haploinsufficiency (*SOCS3*$^{+/-}$) conveys enhanced leptin sensitivity and protection from diet-induced obesity [Howard *et al.*, 2004].

1.2.4 SOCS3 is heavily involved in cancerogenesis

The interplay between metabolism, inflammation and cancer puts SOCS3 in a key position to influence tumorigenesis. As a hepatocyte specific SOCS3 deletion in the ConA-induced hepatitis model, prolonging intracellular signaling after cytokine stimulation, protects from liver injury by upregulating Bcl-X$_L$ and thereby decreasing apoptosis, loss of SOCS3 in hepatocytes and the resulting escape from apoptosis exacerbates DEN-induced HCC formation [Ogata *et al.*, 2006b]. A similar aggravation of DEN-induced HCC formation can be observed upon SOCS3 hap-

loinsufficiency. Interestingly, SOCS3 depletion in both liver parenchymal as well as non-parenchymal cells together exacerbates not only HCC formation, but also ConA-induced hepatitis via TGF-β1 upregulation [Ogata *et al.*, 2006a]. Consistently, a hepatocyte specific gp130 knock-out ameliorates acute inflammation upon high-dose DEN-injection, demonstrated by decreased serum ALT/AST (alanine and aspartate transaminases) levels as well as less IL-6 and oncostatin M (OSM) in liver protein lysates [Hatting *et al.*, 2015]. HCC initiation 24 weeks after regular-dose DEN-injection is unchanged compared to wt, but differences are visible in HCC progression, 40 weeks after DEN-injection. Tumor tissue shows less nodules, a tendency for less tumor associated inflammation, less DNA damage and decreased TGF-β expression.

A similar, tumor-suppressive function for SOCS3 has been assigned in colorectal cancer (CRC) formation. An intestinal epithelial cell (IEC)-specific SOCS3 deletion ($SOCS3^{IEC-KO}$) results in a strong hyperproliferation and hyperplasia after treatment with colitis-inducing DSS [Rigby *et al.*, 2007]. Consistently, SOCS3 overexpression in intestinal epithelial cell lines inhibits proliferation. Additional AOM injection into DSS-treated $SOCS3^{IEC-KO}$ mice results in increased tumor formation, initiated by elevated levels of nuclear pSTAT3 and NF-κB, ultimately increasing IEC proliferation and tumorigenesis. Risk of CRC formation, among other cancers, has additionally been found to be elevated in obesity [reviewed in Renehan *et al.*, 2008]. Interestingly, genetically obese, leptin-deficient (*ob/ob*) mice subjected to the AOM/DSS model develop more tumors, comparable to HFD-fed wild-type animals, than lean animals, but have a decreased tumor size at later stages despite overt obesity [Endo *et al.*, 2011]. Consistently, LepR-deficient (*db/db*) mice also exhibit a decreased tumor frequency and size compared to HFD-fed animals, despite being obese. The protective effect of loss of leptin signaling is mediated by lack of pSTAT3 activation and subsequently decreased activation of proliferation in concert with increased apoptosis. Similar observations can be made for gastrointestinal epithelial cell-specific SOCS3 deletion, initiating hyperproliferation via continuos

leptin signaling and subsequent pSTAT3 activity [Inagaki-Ohara *et al.*, 2014]. Furthermore, leptin signaling has been found to impact on CD133$^+$Nanog$^+$ Tumor initiating stem cells (TISCs), which strongly express the LepR [Feldman *et al.*, 2012], providing a mechanism how increased serum leptin levels under obese conditions can promote tumorigenesis.

1.3 Site specific recombination & conditional gene targeting

Biological and medical research nowadays heavily relies on the use of genetically modified organisms to study role and function of genes, both protein-coding and non-coding. A series of giant leaps in laboratories around the world in the last 40 years advanced the field from studying individual organisms with random, naturally occurring mutations to custom made, gene-targeted mice harboring artificially introduced mutations with nucleotide precision [establishment of gene targeting extensively reviewed by Mario Capecchi, 2005]. The specific disruption of any target gene, now termed conventional gene targeting, is a vastly powerful tool to examine gene function, taking full advantage of the sequenced mouse genome [Mouse Genome Sequencing Consortium *et al.*, 2002]. But even this technique, unthinkable mere 30 years ago, has certain limitations when it comes to a very fine tuned analysis of gene functions or the investigation of essential genes. Utilizing site specific recombinase (SSR) systems in gene targeting, termed conditional gene targeting, can alleviate restrictions imposed by conventional gene targeting [Kühn *et al.*, 1995; Rajewsky *et al.*, 1996].

1.3.1 Mechanism of site specific recombination

With the use of conditional gene targeting and site specific recombination, gene disruption is elevated from a basic, whole body deletion to a more sophisticated control of the genetic modification, including excision, insertion or inversion of DNA fragments with full spatial and temporal control. Site specific recombinases can be found in several organisms where they have varying functions. SSR systems
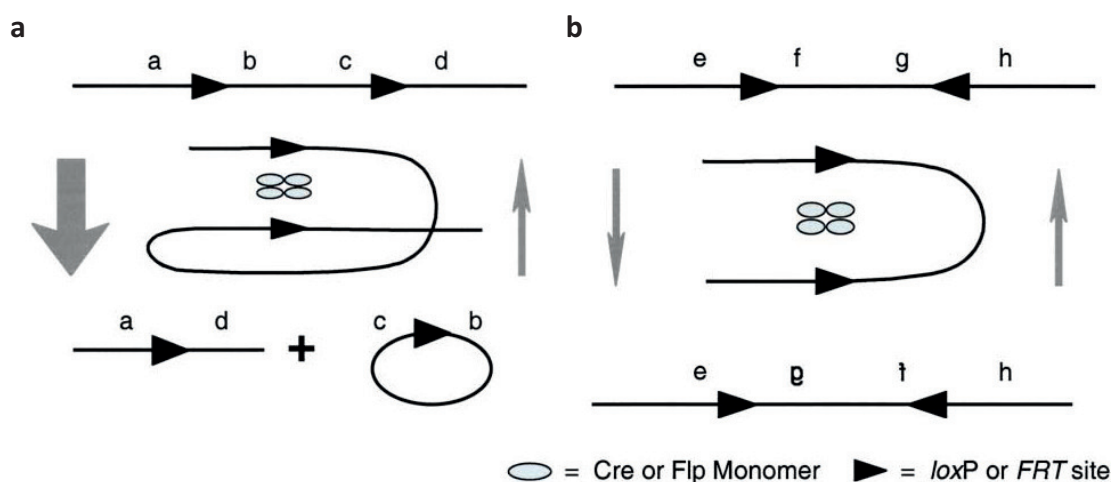
Figure 1.5: **Site specific recombination events**
Site specific recombination requires two recombinase target sites, indicated by black arrows, within the DNA and can either result in excision/insertion or inversion, determined by the relative orientation of the target sites. (a) Two target sites in tandem orientation will result in the excision of the flanked DNA regions, b and c, as a circular DNA fragment with one target site and the other target site within the remaining DNA. Insertion of the circular DNA fragment is possible but unfavored. (b) Two target sites facing each other will result in an inversion of the flanked DNA regions, f and g, and an otherwise unchanged DNA structure, enabling further inversions of the flanked DNA regions. [modified from Branda & Dymecki, 2004]

most commonly used in transgenic mice are members of the λ integrase superfamily of SSRs, like Cre/loxP from bacteriophage P1 [Sternberg & Hamilton, 1981] or Flp/frt from *Saccharomyces cerevisiae* [Andrews *et al.*, 1985]. Recombination by both Cre and Flp follow a common mechanism (Fig. 1.5): Site specific recombinase tetramers recognize 34 bp DNA regions, composed of two 13 bp palindromic sequences, called inverted repeats, flanking an 8 bp non-palindromic core sequence, called spacer, determining the overall orientation of the recombinase target site. Recombination requires two such target sites, where the recombinase introduces strand cleavage, exchange and ligation. The target site orientation determines the exact recombination event, either facilitating strand excision/insertion in case of two target sites facing the same direction, or strand inversion in case of two target sites facing each other. An inversion reaction can occur multiple times, since the DNA structure is not changed after the recombination event.

Generally, a combination of two transgenic mouse lines is used to utilize site

specific recombination and conditional gene targeting in mice. One mouse will express the respective recombinase, using a specific promoter to determine the site of recombination. The promoter will either convey a spatial control of recombinase expression, differentiating between so called deleter-strains, expressing the recombinase under a ubiquitous promoter, vs. expressing the recombinase under a tissue-specific promoter. Recombinase expression can also be under temporal control using an inducible promoter, to allow targeting of genes essential for development. By using post-translational methods of protein induction, spatial and temporal control of recombinase activity can even be combined. Taken together, expression of the recombinase usually determines the „condition" of conditional gene targeting.

A second mouse harbors recombinase target sites within its genome, whose recombination can have various effects. A conditional knock-out allele would have several exons flanked by recombinase target site to induce strand-excision in the presence of the recombinase, ideally introducing a frameshift in the open reading frame to completely abolish gene transcription. A conditional knock-in allele on the other hand would have a transcriptional STOP-cassette flanked by recombinase target sites introduced between the promoter and the first exon, enabling transcription of the downstream target gene only in the presence of the recombinase. Recombinase target sites facing each other are usually used to switch the expression of one particular gene to another, this way either exchanging gene of interest expression with expression of a reporter gene, or a mutated version of the same gene.

1.3.2 Dre/rox is a novel recombinase system distinct from Cre/loxP

The Cre/loxP system is the undisputed incumbent of the site specific recombinases, with the vast majority of conditional mouse lines employing Cre driver lines and loxP-based target alleles. Cre excels at both efficiency as well as versatility, when compared to other tyrosine recombinases like Flp or the larger serine recom-

binases such as ΦC31. Flp matches Cre in versatility, being able to mediate excision/insertion as well as inversion, but, as a protein from *Saccharomyces cerevisiae*, is significantly less efficient in mammalian cells, due to a decreased thermostability [Buchholz *et al.*, 1996]. A mutated form Flp-e with increased thermostability shows improved efficiency [Buchholz *et al.*, 1998], but still does not match Cre. Large serine recombinases like ΦC31 not only lack some of Cre's high efficiency, but also are less versatile, in that they only mediate a directed, irreversible integration [Belteki *et al.*, 2003], rendering them well suited for cassette exchange strategies, but not to cover the diverse applications of Cre. Recently *de novo* synthesized, codon-optimized versions of Flp and ΦC31, termed Flp-o and ΦC31-o, further raise their efficiency to be „similar to Cre" but, especially for Flp-o, still cannot quite match it [Raymond & Soriano, 2007].

Sequencing of four P1-related phages, which are maintained as an extrachromosomal plasmid like P1 and should therefore also have a recombinase system to resolve phage DNA dimers after replication [Austin *et al.*, 1981], to identify Cre homologs revealed a closely related site specific recombinase system in the phage D6, termed Dre/rox [Sauer & McDermott, 2004]. Dre recombinase shares 39% similarity with Cre recombinase, and requires the unique rox target site for recombination. The 32 bp rox site consists of two 14 bp inverted repeats, separated by a directional 4 bp spacer, as compared to the 34 bp loxP site, with about 55% sequence homology to loxP. The Dre/rox system was subsequently adopted and analyzed further in bacteria, *in vitro* and *in vivo* [Anastassiadis *et al.*, 2009]. Complete recombination between rox sites in bacteria is only achieved in the presence of Dre recombinase, neither in the absence of Dre, nor in presence of Cre recombinase. Likewise, Dre recombinase does not mediate recombination between loxP sites. Similar results were obtained with eukaryotic expression vectors and cell lines *in vitro*, successful recombination happens exclusively for the Cre/loxP combination or Dre/rox, respectively. The combined efficiency and specificity of Dre/rox was also observed *in vivo* (Fig. 1.6). Lastly, an inducible Dre system was constructed utilizing the mod-
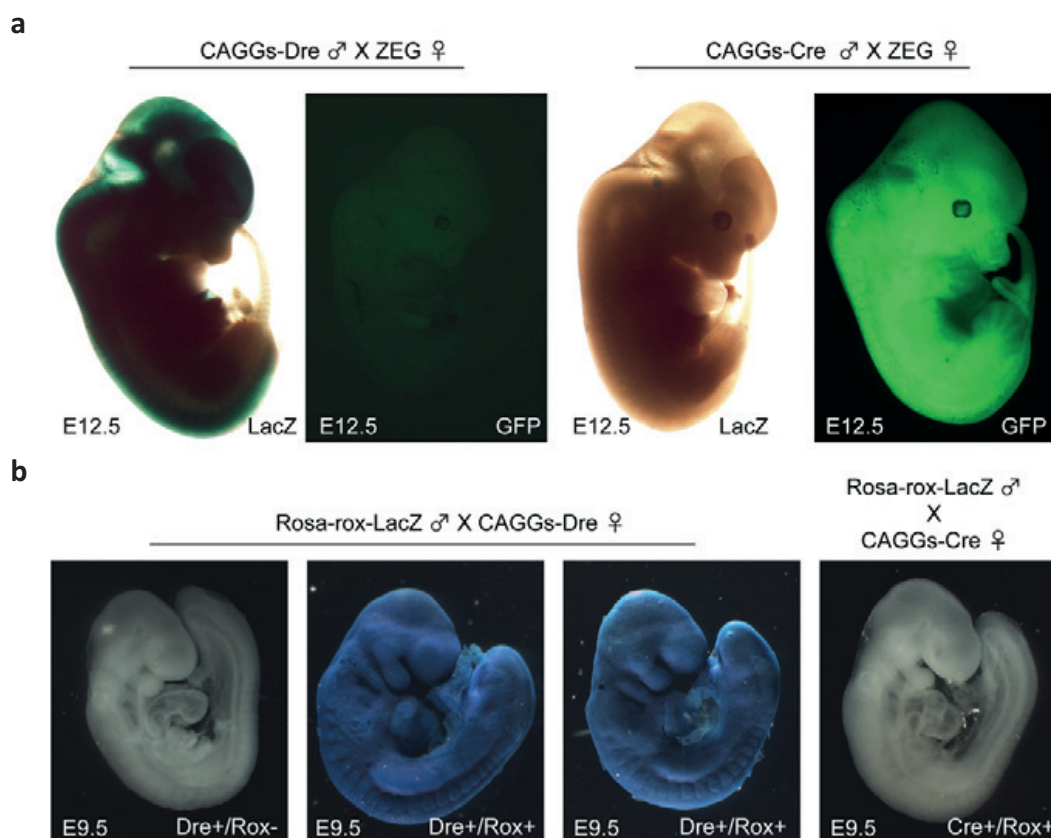
Figure 1.6: **Dre specificity** *in vivo*
CAGGs-Dre and CAGGs-Cre mice, expressing the respective recombinase under the ubiquitous CAGGs promoter, were either crossed to ZEG mice, expressing lacZ before and GFP after successful excision of a loxP-flanked STOP-cassette, or Rosa-rox-lacZ mice, expressing β-galactosidase after successful excision of a rox-flanked STOP-cassette. (a) LacZ staining and GFP epifluorescence indicate that Dre recombinase does not recombine loxP sites in mice. (b) Likewise, Cre does not recombine rox sites in mice. [modified from Anastassiadis *et al.*, 2009]

ified progesterone ligand-binding domain developed for the Cre*PB [Wunderlich *et al.*, 2001].

1.3.3 Generation of transgenic mice by BAC recombineering

The utility of conditional mouse models and the usage of site specific recombinases critically depends on the specificity of the recombinase driver line. This becomes especially evident if the recombinase is supposed to be expressed under the control of a tissue-specific promoter, where it is important that every regulatory promoter element is functional. Red/ET cloning, also called recombineer-

ing, is a rapid procedure to create a tissue-specific, transgenic mouse line [Zhang *et al.*, 1998]. Bacterial artificial chromosomes (BACs) are available ready-to-buy in a host *E. coli* strain from the BACPAC Resources Center. By introducing a plasmid containing the recombination proteins Redα and Redβ coding sequences from bacteriophage λ into the *recA⁻* host bacteria, the BAC carrying bacteria are recombination competent if expression from the plasmid is induced by arabinose addition [Muyrers *et al.*, 1999]. The gene of interest, in this case the recombinase, is amplified by PCR with 50 bp homology arms corresponding to the translation-start of the respective driver gene on the BAC. Successful recombination will result in a modified BAC, expressing the recombinase under the full, endogenous promoter of at least 5 kbp upstream of the transcription-start. Pronucleus injection of the modified BAC gives rise to a founder line with full penetrance upon successful BAC integration into the genome.

1.4 Objectives

In recent decades, Inflammatory signaling has become increasingly recognized as a key system both under cancerous as well as obese conditions. Our immune system is struggling to keep a very delicate balance between initiating cell death and promoting tissue remodeling by inducing cell proliferation. In this regard, members of the innate as well as the adaptive immune system secrete a large variety of inflammatory mediators, cytokines and chemokines, into target tissues and the blood stream, signaling on parenchymal and non-parenchymal cells alike. Only the complex interaction of the various inflammatory mediators present, the source of the respective cytokine or chemokine and the exact target cell, determines whether innate and adaptive immune response act in concert or with diametral consequences.

In order to analyze the role of inflammatory signaling of the various immune cell subpopulations in cancer initiation, promotion and progression, as well as to monitor cancer cell fate, this study aims to develop a universal reporter tool to visualize inflammatory signaling both *in vivo* and *in vitro*. Although different cancer entities can vary greatly in onset, severity and mortality, there are certain hallmarks on the cellular level which can be exploited. Suppressor of cytokine signaling 3 (SOCS3) is a negative feedback regulator of, among others, the JAK/STAT signaling pathway, and its expression is upregulated by a plethora of inflammatory mediators. Inflammatory signaling can therefore be visualized by utilizing the endogenous SOCS3 promoter to drive expression of reporter proteins.

Aim of this thesis is the generation of the universal reporter mouse line SOCS3-U and to use it in mouse models of chemically induced cancerogenesis. Utilizing SOCS3-U in combination with different Cre-driver lines to activate only specific immune cell subpopulations, this study should give a more detailed insight into the contribution of the respective cell types, its inflammatory mediators and their impact on cancer initiation, promotion and progression.

2 Materials and Methods

Standard methods of molecular biology were performed according to established protocols [Green & Sambrook, 2012] if not stated otherwise.

2.1 Genetic Engineering

Cloning of polynucleotides was done using PCR, restriction digest and DNA ligation (T4 DNA ligase, NEB, Frankfurt, Germany). Table 2.2 lists all primers utilized for cloning and table 2.3 lists all restriction endonucleases. Amplicons generated by PCR were cloned into the pGEM-T-Easy vector system (Promega, Madison, WI, USA) and sequenced if not stated otherwise. Sequencing was done by GATC Biotech (Konstanz, Germany) either utilizing T7 and SP6 primers provided by the company for sequencing of pGEM inserts, or using the primers listed in table 2.4.

All cloning procedures were performed with XL-10 Gold Ultracompetent cells (Agilent, Santa Clara, USA). Bacteria were cultivated in LB-medium or on LB-agar at 37°C if not stated otherwise. Table 2.1 contains a list of contents for bacterial cultures.

Table 2.1: Bacterial Cultures

Content	Stock	Working concentration
LB	powder	25 g/l
LB-agar	powder	35 g/l
Ampicillin	50 mg/ml H_2O	50 μg/ml
Tetracycline	5 mg/ml 70% EtOH	50 μg/ml
Chloramphenicol	20 mg/ml 70% EtOH	20 μg/ml
Kanamycin	50 mg/ml H_2O	50 μg/ml
X-Gal	40 mg/ml DMF	40 μg/ml
IPTG	0.1 M in H_2O	0.2 mM

2.1.1 Cloning of targeting constructs

Cloning PCRs were done with the High Fidelity PCR Master (Roche Diagnostics, Mannheim, Germany) according to the manufacturer's instructions. Standard reaction conditions generally were: 50 μl reaction mix, containing 50 pmol of each primer and at least 50 ng DNA template. The thermocycler was programmed according to the specific PCR with an annealing temperature fitting the respective primers and an elongation time of 1 min/kb amplicon.

Table 2.2: Cloning Primer

Description	Primer	Sequence 5'-3'
SOCS3-U	5MluRL	AAAACGCGTTAACTTTAAATAATTGGCATTATT TAAAGTTAGCCGGCAGTGACCGAGG
	3MluRL	ACGCGTTAACTTTAAATAATGCCAATTATTTAA AGTTATGGCTCCACTTGAAAGAAGCTG
	5RsrLA	AAACGGTCCGAAGCTTAGACTGGCCTCAAAT
	3PacLA	TTTTTAATTAAGATATCCAACCCCAGACAGTCT CTTC
	5RVRA	AAAGATATCGGCGCGCCGTTTAAACATTTAAA TGGAGCAAAAGGGTCAGAGGGG
	3RVRA	TTTACCGGTATCCAGGGCTGAGGAGG
	5AgeRA	AAAACCGGTATCGGCGCGCCGTTTAAA
	3AgeRA	TTTACCGGTATCCAGGGCTGAGGAGG
	5SwaLuc	AAAATTTAAATGAAGTTCCTATTCCGAAGTTCC TATTCTCTAGAAAGTATAGGAACTTCCTTTGCT CTCTGCAGGCCACCATGGAAGACGCCAAAAA CATAA
	3AscLuc	AAAGGCGCGCCTTAAACTTACAATTTGGACTT TCCGCC
Alb-Dre	5AlbDre	TGTTGTGTGGTTTTTCTCTCCCTGTTTCCACAG ACAAGAGTGAGATCGCCACCATGGGTAAGAA GAAGA
	3AlbDre	ATAACTTACAGGCCTTTGAAATGTTGTTCTCCC AAATCATTATACCGATGGAGGATTTAATATTTC TGACGC
	5Alb	GTCTCCGGCTCTGCTTTTTCCAGG
	3Alb	TGTTCTCCCAAATCATTATACCG
	3Dre	TACTCCCTAGCCATCTCAGGAGAGAT

Restriction digest was either performed in a 50 μl reaction mix for cloning or 10 μl reaction mix for analysis. Analytic restriction digests contained around 500 ng DNA, restriction digests for cloning around 5 μg DNA. Linearized DNA vectors were dephosphorylated using Antarctic phosphatase (NEB, Frankfurt, Germany). Separation of DNA fragments was done by agarose gel electrophoresis. DNA fragments were extracted with the QIAEX II gel extraction kit (Qiagen, Hilden, Germany).

Table 2.3: Restriction Endonucleases

Enzyme	Supplier	Recognition Sequence
AgeI-HF	NEB	A∣CCGGT
AscI	NEB	GG∣CGCGCC
AsiSI	Fermentas	GCGAT∣CGC
AvrII	NEB	C∣CTAGG
EcoRV-HF	NEB	GAT∣ATC
PacI	NEB	TTAAT∣TAA
PvuI-HF	NEB	CGAT∣CG
SwaI	NEB	ATTT∣AAAT
PI-SceI	NEB	*homing endonuclease*

For sequencing analysis, 500 ng DNA [20 ng/μl] were sent to GATC Biotech. Custom primer were sent at 10 μM concentration.

Table 2.4: Sequencing Primer

Description	Primer	Sequence 5'-3'
SOCS3-U	5SOCS1	GTGCGCAAGCTGCAGGAGAG
	5SOCS2	TGTGTACTCAAGCTGGTGCA
	5SOCS3	GTAGCTCCCAGTGAGCCAGG
	5LA1	CTATCACAGTGTCTCACTGG
	5LA2	ATCTCCATCTGTGAGCATCT
	5LA3	CTCAATCACCTGCTCTTATC
	5LA4	GAGTGATAAGGTAGTAGTTA
	5LA5	CTGCCAGAAACCAGCCTTCT
	5LA6	CAGCTCTCCGTCGAGGTCCC
	5LA7	TCGCCACTGAGGACACCGGA
	5RA0	TAAACATTTAAATGGAGCAA
	5RA1	GAACTTGTTTGCGCTTTGAT

Table 2.4 – continued from previous page

Description	Primer	Sequence 5'-3'
	5RA2	GGCTAGGAGACTCGCCTTAA
	5Luc1	CAGTAAGCTATGTCTCCAGA
	5Luc2	GTTGGTACTAGCAACGCACT
	5Luc3	TAGAATCCATGATAATAATT
	5Luc4	CGTATCTCTTCATAGCCTTA
	3Luc1	ATATGTGCATCTGTAAAAGC
	3Luc2	CCGGTTATGTAAACAATCCGGA
Alb-Dre	5Alb	GTCTCCGGCTCTGCTTTTTCCAGG
	3AmplifyFlp	AGCCAGAAGTCAGATGCTCA
	DreSeqJ	TGCTGTCTAGATCTGAGAGACT
	DreSeq0j	CCTGGTATTTTAAAATAGTT
	DreSeq1j	TCTCATAGGGCCTGCCTGCT
	DreSeq2j	TAGCTTAGGTCAGTGAAGAG
	DreSeq3	TCCACTCCTGGGCTAGATGG
	DreSeq4	GTGGGAGACCTGGACCAGAC
	DreSeq5	AAAGCCTGAGACACTGATGA
	3DreSeq	TCTCCGGATTCTCCTCATGGC
	Drerevneu	GCGGTGGTCCTCCTAGAC

SOCS3-U targeting construct

SOCS3 CDS was amplified using the primers 5MluRL and 3MluRL from genomic DNA and ligated into the pGEM-T-Easy Vector System. The amplicon was cut from the pGEM backbone with MluI and ligated with the common Stop-eGFP-ROSA-CAGs [SERCA, Klisch, 2006] plasmid, cut with AscI. The resulting intermediate was cut with NheI and EcoRV and the 5.7 kb fragment was ligated with the GK12TK plasmid [Wunderlich *et al.*, 2010], cut with AvrII and PmeI. The SOCS3 LAH was amplified using the primers 5RsrLA and 3PacLA from genomic DNA. The amplicon was cut from the pGEM backbone with PvuI and PacI and inserted into the GK12TK-SOCS3 intermediate, cut with PacI. The SOCS3 RAH was amplified using the primers 5RVRA and 3RVRA from genomic DNA, which served as template for a second amplification using the primers 5AgeRA and 3AgeRA. Firefly luciferase CDS was amplified using the primers 5SwaLuc and 3AscLuc from the pTE-Luc plasmid [Jordan *et al.*, 2011]. The amplicon was cut from the pGEM back-

bone with AscI and SwaI and inserted into the pGEM-RA intermediate, cut with AscI and SwaI as well. The RA-Luc intermediate was cut from the pGEM backbone with AgeI and inserted into the GK12TK-SOCS3-LA intermediate, cut with AgeI as well.

Alb-Dre recombinant BAC

Construction of the Alb-Dre recombinant BAC was performed via Red-E/T recombination [Muyrers *et al.*, 1999]. Dre CDS and a neomycin resistance cassette were amplified using the primers 5AlbDre and 3AlbDre from the pTE-Dre-neo/kana [Tim Klöckener, University of Cologne] plasmid. The resultant DNA fragment contains 50 bp homology arms with the endogenous Alb locus.

1.4 ml LB medium containing chloramphenicol were inoculated with 30 μl overnight culture of Alb-BAC carrying bacteria and cultivated for 3 h at 37°C. Cells were centrifuged for 30 sec at 11,000 xg, 4°C. Cells were washed with 1 ml chilled water and centrifuged again. The cell pellet was resuspended in 20-30 μl chilled water. Resuspended cells were mixed with 3 μl pSC101-BAD-gbaA [100-200 ng/μl]. Cells were transformed via electroporation (1350 V, 10 μF, 600 Ω). Electroporated cells were resuspended in 1 ml LB medium and incubated for 70 min at 30°C. Cells were plated on LB agar plates containing tetracycline and chloramphenicol and incubated over night at 30°C. Colonies were picked and incubated in LB medium containing tetracycline and chloramphenicol over night at 30°C. 1.4 ml LB medium containing tetracycline and chloramphenicol were inoculated with 30 μl overnight culture and incubated at 30°C until an OD_{600} of 0.15 was reached. 20 μl L-Arabinose were added and the cells incubated for 60 min at 30°C. Cells were then incubated at 37°C until an OD_{600} of 0.4 was reached. Cells were centrifuged for 30 sec at 11,000 xg, 4°C. Cells were washed with 1 ml chilled water and centrifuged again. The cell pellet was resuspended in 20-30 μl chilled water. Resuspended cells were mixed with 3 μl linearized, recombinant DNA fragment [100-200 ng/μl]. Cells were transformed via electroporation (1350 V, 10 μF, 600 Ω). Electroporated cells were

resuspended in 1 ml LB medium containing 20 μl L-Arabinose and incubated for 70 min at 37°C. Cells were plated on LB agar plates containing kanamycin and incubated over night at 37°C. Colonies were picked and checked for correct insertion of the recombinant fragment. Recombinant BACs were linearized with PI-SceI and purified with the NucleoBond® Xtra BAC kit (Macherey-Nagel, Düren, Germany) for transfection.

2.1.2 Cell culture

All cells utilized were maintained in an incubator with constant conditions (95% humidity, 37°C, and 10% CO_2 saturation), while handling and passaging of cells was performed under a sterile hood (Hera Safe KS 12, Heraeus Instruments). Bruce4 embryonic stem cells [ES-cells, Köntgen & Stewart, 1993] were used for all transfection and kept on a confluent layer of mouse embryonic fibroblasts (MEFs). MEFs were passaged three times and treated with mitomycin C (MMC, Sigma-Aldrich) to serve as feeder cells for ES cells to maintain their pluripotency. Growth medium for ES cells was changed every day and every 2-3 days in case of MEFs. Contents of the various growth media are listed in table 2.5.

Passaging of cells

MEFs were passaged upon confluence, ES-cells at 85% confluency or at least every three days to maintain pluripotency. Cells were washed twice with PBS and incubated with trypsin-solution (0.05% trypsin, 0.02% EDTA in PBS) at 37°C for 5 min. Trypsin digest was stopped with 1:1 FCS-containing medium. Cells were centrifuged (270 xg, 5 min, 4°C) and seeded on fresh plates. MMC-treated MEFs were seeded on gelatin-coated (0.2% gelatin in PBS, $\geqq$ 5 min at 37°C) plates to enhance adherence. Cells were counted in a C-Chip Neubauer improved counting chamber (Peqlab, Erlangen, Germany) if indicated.

Freezing and thawing of cells

For cell freezing, cells were trypsinized and centrifuged as described before. The cell pellet was resuspended in FCS containing 10% DMSO and stored at -80°C for short term storage or liquid nitrogen for long term storage. Frozen cells were thawed 1:40 in the appropriate culture medium, centrifuged and seeded in fresh medium on the appropriate dish.

Transfection

Medium of the ES-cells was changed 2-3 hours prior to transfection. 40 μg targeting construct were linearized with AsiSI, purified with isopropanol precipitation and resuspended in 400 μl PBS under sterile conditions. 10^7 ES-cells were trypsinized and also resuspended in 400 μl PBS. ES-cells and linearized plasmid were mixed in an electroporation cuvette (0.4 cm) for transfection (230 V, 500 μF, ∞ Ω; GenePulser Xcell™, Bio-Rad, München, Germany). Cells were incubated for 5 min at RT and subsequently resuspended in ES-medium and seeded on four 10 cm dishes with feeder cells. Selection with G418 and counterselection with ganciclovir for correct integration of the targeting construct started two days post transfection and was carried out for seven days. Picking of colonies was performed nine days post transfection.

Picking of colonies

ES-cells were washed twice with PBS prior to picking colonies. Cells were picked in 40 μl PBS and transferred to a 96-well plate (round bottom) containing 25 μl trypsin solution. Picking was stopped once the 96-well plate was full or at least 30 minutes after picking the first colony. Cells were incubated for 5 min at 37°C and trypsin reaction was stopped with 100 μl ES-medium. 50 μl each were transferred to three 96-well plate (flat bottom) with feeder cells and incubated for three days. Two plates were frozen at -80°C (25 μl trypsin solution plus 25 μl FCS containing 20% DMSO) and the third one split on three gelatin-coated 96-well plates (flat

bottom). Cells were incubated until confluency, where two plates were washed twice with PBS and frozen at -20°C. The third plate was washed twice with PBS and incubated in ES-cell lysis buffer (10 mM Tris-HCl, 10 mM EDTA, 10 mM NaCl, 0.5% N-Lauroylsarcosine, 4% Proteinase K) over night at 56°C. DNA was precipitated by adding 100 μl isopropanol and 30 min incubation at RT. The supernatant was discarded and the pellet washed with 200 μl 70% EtOH, dried for 30 min at 37°C and resuspended in 25 μl TE plus RNAse A. 10 μl restriction digest mastermix (3,5 μl buffer, 2 μl enzyme, 0.01 μl 1 M DTT, 0.02 μl spermidine, 4.5 μl H$_2$O) were added and incubated over night at 37°C for Southern blot analysis (cf. 2.1.3).

HTNC transduction

Cre-mediated recombination *in vitro* was performed with a transducible His-TAT-NLS-Cre (HTNC) protein [Peitz *et al.*, 2002]. Cells were seeded on culture plates and grown to about 95% confluency. 1 μM HTNC was applied for 16-20 hours in DMEM / PBS [1:1] without antibiotics or supplements.

Growth media

Growth media were prepared under sterile conditions and stored at 4°C.

Table 2.5: Cell Culture Media

Medium	Contents	Supplier
ES-medium	DMEM with L-Glutamine	Gibco
	15% FCS	Biochrom AG
	1 mM Sodium Pyruvate	Gibco
	1x Non-essential Aminoacids	Gibco
	10 U/ml LIF supernatant	-
	0.1mM β-Mercaptoethanol	Gibco
	2 mM L-Glutamine	Gibco
	100 U/ml Pen-Strep	Gibco
	300 μg/ml G418 (*if indicated*)	Gibco
	2 mM Ganciclovir (*if indicated*)	Sigma-Aldrich
EF-medium	DMEM plus Glutamax	Gibco
	10% FCS	Biochrom AG

Table 2.5 – continued from previous page

Medium	Contents	Supplier
	1 mM Sodium Pyruvate	Gibco
	1x Non-essential Aminoacids	Gibco
	100 U/ml Pen-Strep	Gibco
Hepatocyte-medium	DMEM with L-Glutamine	Gibco
	10% FCS	Biochrom AG
	1 mM Sodium Pyruvate	Gibco
	1x Non-essential Aminoacids	Gibco
	100 U/ml Pen-Strep	Gibco
Hepatocyte-fasting-medium	DMEM with L-Glutamine	Gibco
	4% FCS	Biochrom AG
	1 mM Sodium Pyruvate	Gibco
	1x Non-essential Aminoacids	Gibco
	100 U/ml Pen-Strep	Gibco

2.1.3 Southern blot analysis

Gel electrophoresis and blotting

10-15 μg digested genomic DNA was loaded on an 0.8% agarose gel and run over night at 30 V. The gel was incubated for 20 min in 0.25 M HCl for depurination. DNA was blotted on Hybond-XL™ charged nylon membrane (GE Healthcare, Freiburg, Germany) by alkaline capillary transfer with 0.4 M NaOH over night. The membrane was then washed for 20 min in 2x SSC (SSC: 300 mM NaCl, 30 mM $Na_3C_6H_5O_7$) buffer and cross-linked at 80°C for 40 min.

Labeling and hybridization

DNA fragments of the respective Southern probes were amplified by PCR or restriction digest (cf. table 2.6). Radioactive labeling with 25 μCi α^{32}P-dCTP of 150 ng DNA was performed with the Ladderman DNA Labeling Kit (Takara Bio, Shiga, Japan). The membrane was incubated in 30 ml pre-hybridization solution (1 M NaCl, 50 mM Tris-HCl pH 7.5, 10% dextransulfate, 1% SDS, 250 μg sonicated

salmon sperm DNA) for 4 h. The labeled probe was added and the membrane hybridized at 65°C over night. The membrane was washed in increasingly stringent Southern wash solution (2x SSC ↘ 0.5x SSC, plus 0.1% SDS) until the radioactive signal was below 30 mSv. Detection of the radioactive signal was done with Kodak MS hypersensitive films after over night exposure at -80°C.

Table 2.6: Southern probes

Probe	Source	Amplification
SOCS3-U LA1	genomic DNA	5'-GATATCTCTGAATGCATCCAAGTTCTG-3'
		5'-GATATCGATGCACAGCCAGCTTCTCA-3'
SOCS3-U RA1	genomic DNA	5'-GATATCACATGCTATGGCACACGTGT-3'
		5'-GATATCCTGGGATGAAGTTCCTTGTC-3'
Neo^R	A-04 plasmid*	5'-TGAATGAACTGCAGGACGAGGCA-3'
		5'-GCCGCCAAGCTCTTCAGCAAT-3'

* Mao *et al.*, 1999

2.2 Protein Biochemistry

2.2.1 Protein extraction

Proteins from tissues or cells were extracted in organ lysis buffer (50 mM HEPES, 1% Triton X-100, 50 mM NaCl, 0.1 M NaF, 10 mM EDTA, 10 mM Na$_3$VO$_4$, 0.1% SDS, 2 mM benzamidine, 10 μl/ml aprotinine, 2 mM PMSF, proteinase inhibitor cocktail, pH 7.4). Final protein lysates were diluted in organ lysis buffer and 4x SDS loading dye (250 mM Tris-HCL pH 6.8, 10% SDS, 87% glycerol, 200 mM DTT, 0.04% bromphenol blue).

Protein extraction from tissues

Organs were extracted from mice and a small part was incubated in 1 ml organ lysis buffer. The tissues were homogenized using an Ultra Turrax homogenizer (IKA, Staufen, Germany). The homogenate was centrifuged at 17,000 xg for 60 min at 4°C. Protein concentration of the cleared homogenate was determined using a NanoDrop ND-1000 UV-Vis Spectrophotomoter (Thermo Fisher Scientific Inc.,

Schwerte, Germany) and adjusted to 10 μg/μl.

Protein extraction from cells

Cells were washed twice with PBS and scraped from the dish in an appropriate amount of organ lysis buffer. Cells were homogenized using a Vibrax VWR basic (IKA, Staufen, Germany) at 1000 rpm for 20 min at 4°C. The homogenate was centrifuged at 17,000 xg for 60 min at 4°C. Protein concentration of the cleared homogenate was determined using a NanoDrop ND-1000 UV-Vis Spectrophotomoter (Thermo Fisher Scientific Inc., Schwerte, Germany) and adjusted to 10 μg/μl.

2.2.2 Western blot analysis

SDS-polyacrylamide gel electrophoresis (SDS-PAGE)

Isolated proteins were separated by size via SDS-PAGE. Resolving gels contained 10% acrylamide if not stated otherwise. Gel electrophoresis was carried out in SDS running buffer (25 mM Tris, 200 mM glycine, 3.5 mM SDS) at 100 V for 2 h. 1.5 mm gels were used and loaded with PageRuler Prestained Protein Ladder (Thermo Fisher Scientific Inc., Schwerte, Germany) and 100 μg protein per sample.

Western blot

Proteins were blotted from polyacrylamide gels onto PVDF-membrane (Bio-Rad, Munich, Germany) at 100 mA for 1 h. Membranes were blocked with 1% blocking reagent (Roche, Mannheim, Germany) in TBS-T for 1 h at RT. Incubation with the primary antibody in 0.5% blocking reagent was performed over night on a rotator at 4°C. Membranes were washed thrice in TBS-T for 10 min at RT and subsequently incubated with the appropriate secondary antibody in 0.5% blocking reagent for 1 h at RT on a rotator. Membranes were washed thrice in TBS-T for 10 min at RT and subsequently incubated in 10 ml Pierce ECL Western Blotting Substrate (Perbio Science, Bonn, Germany) for 1 min at RT. Detection of luminescence was performed

using Amersham Hyperfilm chemiluminescent film (GE Healthcare, Little Chalfont, UK). Membrane stripping was done in stripping solution (65 mM Tris-HCl pH 6.8, 2% SDS, 0.7% β-Mercaptoethanol) for 30 min at 56°C if indicated. Table 2.7 contains a list of all antibodies used.

Table 2.7: Antibodies for Western blot

Antibody	Cat.No.	Supplier
Monoclonal anti-α-Tubulin	T6074	Sigma-Aldrich
phospho-STAT3 (Y705) (D3A7) XP Rabbit mAb	9145	Cell-Signaling
SOCS3 Antibody	2923	Cell-Signaling
α-Rabbit IgG (whole molecule) Peroxidase Conjugate	A6154	Sigma-Aldrich
α-Mouse IgG (whole molecule) Peroxidase Conjugate	A4416	Sigma-Aldrich

2.3 Molecular Biology

2.3.1 quantitative Real-Time PCR

Quantitative Real-Time PCR was performed with the QuantStudio™ 7 Flex Real-Time PCR System (Applied Biosystems®, Foster City, USA).

mRNA isolation

mRNA from tissues and cells was isolated using the RNAeasy kit (Qiagen, Hilden, Germany). Tissues were homogenized using an Ultra Turrax homogenizer (IKA, Staufen, Germany), cells were homogenized with using QIAshredder columns (Qiagen). DNA was digested on-column with the RNase-Free DNase Set (Qiagen). Instructions given by the manufacturer were followed for all kits. RNA concentration was assessed by measuring absorption at 260 and 280 nm using a NanoDrop ND-1000 UV-Vis Spectrophotomoter (Thermo Fisher Scientific Inc., Schwerte, Germany) and adjusted to 200 ng/μl.

cDNA synthesis and qPCR setup

1 μg RNA was was reversely transcribed with High-Capacity cDNA Reverse

Transcription kit (Applied Biosystems, Foster City, USA) and amplified using Taq-Man Gene Expression Master Mix with TaqMan Assay-on-demand kits (Applied Biosystems) following the instructions given by the manufacturer. Realtime probes used for gene expression analysis are listed in table 2.8. Relative expression was determined for target mRNA and samples were adjusted for total mRNA content by quantitative PCR for the housekeeping gene hypoxyanthine guanine phosphoriboysl transferase (*HPRT*). Calculations were performed by comparative method ($2^{-\Delta\Delta C_T}$) [Livak & Schmittgen, 2001].

Table 2.8: Realtime Taqman probes

Symbol	Transcript Name	Probe
Ccl20	Chemokine (C-C motif) ligand 20	Mm01268754_m1
Cd4	Cluster of differentiation 4	Mm00442754_m1
Cd8a	Cluster of differentiation 8	Mm01182107_g1
Csf1	Colony stimulating factor 1	Mm00432685_m1
Il17ra	Interleukin-17 receptor A	Mm00434214_m1
Il6ra	Interleukin-6 receptor α chain	Mm00439653_m1
Socs3	Suppressor of Cytokine Signaling 3	Mm00545913_s1
Tnfsf14	Tumor necrosis factor superfamily member 14	Mm00444567_m1
Hprt	Hypoxanthin-phosphoribosyl-transferase	Mm00446968_m1

2.3.2 Flow cytometry

Quantitative flow cytometry was performed either with the MACSQuant® VYB and MACSQuant® Analyzer 10 flow cytometers (both by Miltenyi Biotech, Bergisch Gladbach, Germany) or FACSCalibur™ (3.5, 3.6) flow cytometer (BD Bioscience, Heidelberg, Germany). Cell sorting was done with the FACSVantage™ SE (3.8, 3.13) or FACSAria™ II (3.9) cell sorters (both by BD Bioscience, Heidelberg, Germany).

Extracellular staining

Isolated non-parenchymal cells were treated with Trustain fcX™ for 15 min at 4°C. Cells were centrifuged at 400 xg for 5 min at 4°C. The pellet was resuspended in 100 μl FACS-buffer with Trustain fcX™ and the appropriate antibody for extracel-

lular staining (cf. table 2.9). Cells were stained for 30 min at 4°C, and the reaction was stopped by adding 400 μl FACS-buffer. Cells were centrifuged at 400 xg for 5 min at 4°C and resuspended either in 200 μl FACS-buffer for analysis or 200 μl fix-perm buffer for intracellular staining.

Intracellular staining

Cells were incubated in fix-perm (#00-5123, eBioscience) for 30 min at RT and subsequently washed three times with 200 μl perm-buffer (#00-8333, eBioscience). Staining with the appropriate antibody (cf. table 2.9) was performed in 50 μl perm-buffer for 30 min at 4°C. Cells were washed twice in 200 μl perm-buffer and resuspended in 200 μl FACS-buffer for immediate analysis or IC-fix (#00-8222, eBioscience) for over night storage.

Table 2.9: Antibodies for FACS

Antibody	Cat.-No.	Supplier
Trustain fcX™ (anti-mouse CD16/32)	101320	Biolegend
APC anti-mouse NK-1.1	108709	BioLegend
Brilliant Violet 421™ anti-mouse CD3ϵ	100336	Biolegend
LIVE/DEAD® Fixable Aqua Dead Cell Stain Kit	L34957	Applied Biosystems
FITC anti-mouse NK-1.1	108705	Biolegend
PE/Cy7 anti-mouse F4/80	123114	Biolegend
PE/Cy7 anti-mouse TCR β	109222	Biolegend
PE anti mouse/rat CD126 (IL-6Rα chain)	115805	BioLegend
PE-CF594 anti-mouse CD3ϵ	562332	BD Horizon™

Magnetic cell isolation and cell separation

T-cells were separated from other non-parenchymal cells by MACS separation using CD90.2 microbeads (#130-049-101, Miltenyi Biotech) and LS columns (#130-042-401, Miltenyi Biotech). Instructions by the manufacturer were followed.

Stimulation of Cytokine-production

Cytokine production of isolated T-cells was stimulated *in vitro* prior to intra-

cellular staining. T-cells were resuspended in 2 ml stimulation medium (DMEM, 10% FCS, 50 mg/ml PMA, 500 ng/ml Ionomycin, 1 μl/ml GolgiPlug™), seeded on a 6-well dish and incubated at 37°C for 6 h.

2.4 Animal handling

2.4.1 Animal care

Mice (*Mus musculus*, C57Bl/6N) were housed in a virus-free facility at 22-24°C on a 12 h light / 12 h dark cycle. Animals were fed standard rodent chow (Teklad Global Rodent 2018; 53.5% carbohydrates, 18.5% protein, 5.5% fat (12% calories from fat); Harlan, IN, USA). All animals had access to water and food ad libitum. Procedures and euthanasias were reviewed by the animal care committee, approved by local government authorities (Tierschutzkommission acc. §15 TSchG of the Landesamt für Natur, Umwelt und Verbraucherschutz Nordrhein-Westfalen) and were in accordance with NIH guidelines.

2.4.2 Genotyping

Isolation of genomic DNA

Mouse tail biopsies for genotyping were taken at weaning age (D18-D25) and subsequently digested in 600 μl tail lysis buffer (100 mM Tris-HCl pH 8.5, 5 mM EDTA pH 8.0, 0.2% SDS, 200 nM NaCl) containing proteinase K (1/100) at 56°C over night. DNA was precipitated using 600 μl 100% isopropanol and centrifugation at 17,000 xg. Afterwards, DNA was washed with 500 μl 70% ethanol, centrifuged at 17,000 xg and dried. The DNA pellet was resuspended in TE buffer (10 mM Tris-HCl pH 7.5, 1 mM EDTA) containing RNase A (1/1000).

Polymerase chain reaction

For genotypic analysis, polymerase chain reaction (PCR) was performed on tail DNA using the primers given in table 2.10. For PCR DreamTaq PCR MasterMix and

DNA polymerase (Fermentas/Fisher Scientific Germany GmbH, Schwerte, Germany) was used. Standard PCR contained approx. 50 ng DNA, 25 pMol of each primer, 25 μM dNTP mix and 1 unit DNA polymerase in a 25 μl reaction mix.

Table 2.10: Genotyping Primer

Mouse Line	Primer	Sequence 5′-3′
SOCS3-U	5SOCS3U1	TTTTCTCTGGGCGTCCTCCTAG
	3SOCS3U2	AGCGCATCGCCTTCTATCGCC
	5SOCS3U3	CTGGATCTGACATGGTAAGTAAGCTT
	3SOCS3U4	CCGCACAGCGGCCGCTAC
	3SOCS3U5	CAAGCGGCTTCGGCCAGTAAC
	3SOCS3U6	AATTGTTCCAGGAACCAGGGC
	5SOCS3U7	CCGCGATCAATTCGGTACCG
Alb-Dre	5Alb2	GAGTGTAGCAGAGAGGAACC
	3Alb	TGTTCTCCCAAATCATTATACCG
	3Dre	TACTCCCTAGCCATCTCAGGAGAGAT
Universal Dre	DreSeqJ	TGCTGTCTAGATCTGAGAGACT
	Drerevneu	GCGGTGGTCCTCCTAGAC
Universal Cre	mom0137	CTGCAGTTCGATCACTGGAAC
	mom0138	AAAGGCCTCTACAGTCTATAG
	oIMR6694	TCCAATTTACTGACCGTACA
	oIMR6695	TCCTGGCAGCGATCGCTATT
Rosa-RedTomato	oIMR9020	AAGGGAGCTGCAGTGGAGTA
	oIMR9021	CCGAAAATCTGTGGGAAGTC
	oIMR9103	GGCATTAAAGCAGCGTATCC
	oIMR9105	CTGTTCCTGTACGGCATGG

2.4.3 Mouse experiments

STAT3 signaling

STAT3 signaling was induced by *i.p.* injection of upstream ligands, where indicated, at the following concentrations: 50 ng/g IL-6, 20 ng/g TNFα, 250 ng/g LPS. Ligands were dissolved in PBS at a concentration corresponding to an injection volume of 10 μl/g.

DEN-injection

long-term chronic Diethylnitrosamin (DEN) injection of 25 mg/kg BW [2.5 mg/ml H_2O] was performed in male mice *i.p.* 14 days after birth. Treated animals were sacrificed and their livers analyzed either 4 or 8 month post injection. *short-term* acute DEN injection of 100 mg/kg BW [10 mg/ml H_2O] was performed in male mice *i.p.* 8-12 weeks after birth. Treated animals were sacrificed and their livers analyzed 0, 1, 2, 3 or 10 days post injection.

AOM/DSS treatment

Mice were injected *i.p.* with 10 mg/kg BW [1 mg/ml PBS] azoxymethane (AOM) and had their drinking water supplemented with 2.5% [w/v] dextransulfate for 5 days. Treated animals received pure drinking water for additional 3 days before they were sacrificed and their colons analyzed.

Isolation and cell culture of primary hepatocytes

Mice were anesthetized and their liver perfused via vena cava with EBSS-perfusion buffer (0.5 mM EGTA in EBSS) for 5 min, followed by perfusion with 50 ml EBSS-collagenase buffer (10 mM HEPES, 15 mg Collagenase IV, 2 mg trypsin inhibitor in EBSS). Afterwards, hepatocytes were released from cell association in 10 ml EBSS and filtered through a 100 μm strainer. Cells were washed twice with hepatocyte culture medium (Table 2.5). Cells were counted and an appropriate cell number, depending on the respecitve growth area, was seeded on collagen coated culture plates (BD Biocoat). Culture medium was changed after 4 hours. Cells were kept in hepatocyte-medium for another 12 hours and then starved in hepatocyte-fasting-medium for 4 hours. Hepatocytes were stimulated with 50 ng/ml IL-6 in hepatocyte-fasting-medium for the indicated timepoints.

Isolation of non-parenchymal liver cells

Mice were sacrificed and their liver perfused with HBSS via vena cava. Liv-

ers were incubated in 5 ml liver dissociation buffer (150 mM NaCl, 5.6 mM KCl, 5.5 mM Glucose, 20.1 mM HEPES, 25 mM NaHCO$_3$, 2 mM CaCl$_2$, 2 mM MgCl$_2$, 500 U/ml collagenase IV, 150 U/ml DNAse I, pH 7.4), disrupted with the gentleMACS™ dissociator (Miltenyi Biotech, Bergisch Gladbach, Germany) and further incubated at 37°C. Cells were filtered through a 100 μm strainer, and both the c-tube as well as the strainer washed with PEB (0.5% BSA, 2 mM EDTA in PBS). The filtrate was centrifuged at 50 xg, 4°C for 5 min and the supernatant, containing the NPC fraction, filtered through a 40 μm strainer. The hepatocyte pellet was resuspended in 30 ml PEB, again centrifuged and the supernatant also filtered through the 40 μm strainer. The filtrate was centrifuged at 350 xg, 4°C for 10 min and the NPC-pellet resuspended in PEB up to a volume of 5 ml.

The NPC solution was mixed with 5 ml 40% Histodenz [w/v PBS] and 5 ml each underlayed 5 ml PEB in a small falcon tube for gradient purification. The gradients were centrifuged at 1500 xg, 4°C for 20 min without brake and the NPCs collected from the interface. NPCs from both tubes were combined and diluted in PEB up to a volume of 50 ml. Cells were centrifuged at 350 xg, 4°C for 10 min and the NPC-pellet resuspended in FACS buffer (2% FCS, 2 mM EDTA in PBS).

2.5 Chemicals and Materials

Table 2.11: Chemicals

Chemical	Supplier
β-mercaptoethanol	Applichem, Darmstadt, Germany
Acrylamide	Roth, Karlsruhe, Germany
Agarose	Peqlab, Erlangen, Germany
Ammoniumpersulfat (APS)	Sigma-Aldrich, Seelze, Germany
Bacillol	Bode Chemie, Hamburg, Germany
Bovine serum albumin (BSA)	Sigma-Aldrich, Seelze, Germany
Bromphenol blue	Merck, Darmstadt, Germany
Desoxy-ribonucleotid-triphosphates (dNTPs)	Amersham, Freiburg, Germany
Developer G153	AGFA, Mortsel, Belgium
DEPC	Applichem, Darmstadt, Germany

Table 2.11 – continued from previous page

Chemical	Supplier
Dimethylsulfoxide (DMSO)	Merck, Darmstadt, Germany
Enhanced chemiluminescence (ECL) Kit	Perbio Science, Bonn, Germany
Ethanol, absolute	Applichem, Darmstadt, Germany
Ethidium bromide	Sigma-Aldrich, Seelze, Germany
Ethylendiamine tetraacetate (EDTA)	Applichem, Darmstadt, Germany
Fixer G354	AGFA, Mortsel, Belgium
Formamide	Applichem, Darmstadt, Germany
Glycerol	Serva, Heidelberg, Germany
Glycine	Applichem, Darmstadt, Germany
GolgiPlug™	BD Biosciences
HEPES	Applichem, Darmstadt, Germany
Hydrochloric acid (37%)	KMF Laborchemie, Lohmar, Germany
Isopropanol (2-propanol)	Roth, Karlsruhe, Germany
LB	Applichem
Magnesium chloride	Merck, Darmstadt, Germany
Methanol	Roth, Karlsruhe, Germany
Nitrogen (liquid)	Linde, Pullach, Germany
Paraformaldehyde (PFA)	Sigma-Aldrich, Seelze, Germany
Phenol/Chloroform/Isoamylalkohol	Roth, Karlsruhe, Germany
Phosphate buffered saline (PBS)	Gibco BRL, Eggenstein, Germany
Potassium chloride	Merck, Darmstadt, Germany
Potassium dihydrogenphosphat	Merck, Darmstadt, Germany
Potassium hydroxide	Merck, Darmstadt, Germany
Sodium acetate	Applichem, Darmstadt, Germany
Sodium chloride	Applichem, Darmstadt, Germany
Sodium citrate	Merck, Darmstadt, Germany
Sodium dodecyl sulfate	Applichem, Darmstadt, Germany
Sodium fluoride	Merck, Darmstadt, Germany
Sodium hydrogen phosphate	Merck, Darmstadt, Germany
Sodium hydroxide	Applichem, Darmstadt, Germany
Sodium orthovanadate	Sigma-Aldrich, Seelze, Germany
Sodium pyrophosphate	Sigma-Aldrich, Seelze, Germany
Tetramethylethylenediamine (TEMED)	Sigma-Aldrich, Seelze, Germany
Trishydroxymethylaminomethane (Tris)	Applichem, Darmstadt, Germany
Triton X-100	Applichem, Darmstadt, Germany
Trizol	Applichem, Darmstadt, Germany
Tween 20	Applichem, Darmstadt, Germany
Western Blocking Reagent	Roche, Mannheim, Germany

3 Results

Inflammatory signaling comprises a plethora of metabolic processes. Its main function lies in the defense against infections, but the immune system tries also to counteract non-infectious burdens on the organism. The development of cancer heavily depends on the infiltration of immune cells into the tumor microenvironment. In case of so called inflammation-driven cancers, the secreted immune factors, such as cytokines and chemokines, are even a prerequisite for the tumor development. A low grade chronic inflammation has also been observed under obese conditions, where white adipose tissue stress in turn attract immune cells to this site.

3.1 Generation of a universal reporter tool for inflammatory signaling

The suppressor of cytokine signaling 3 (SOCS3) gene is part of a negative feedback-loop for numerous intracellular pathways, most prominently the JAK/STAT pathway or NF-κB, and is strongly upregulated independent of the particular cause of inflammation. Therefore the SOCS3 locus has been chosen to drive the SOCS3-U allele, a reporter tool to visualize active inflammatory signaling.

3.1.1 Genetic features of SOCS3-U

The SOCS3 <u>U</u>niversal <u>T</u>umormicroenvironment <u>A</u>ctivation <u>M</u>easurement <u>A</u>llele (SOCS3-UnTAMAble / SOCS3-U) is a versatile reporter tool to measure inflammatory signaling *in vitro* and *in vivo*. The activity of the allele is controlled by a loxP-flanked neo-stop cassette and depends on Cre-mediated recombination,
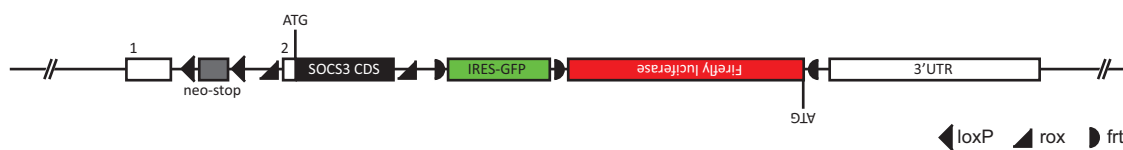
Figure 3.1: **SOCS3-U multi-recombinase reporter allele**
Activity of the SOCS3-U allele is controlled by a loxP-flanked neo-stop cassette. The rox-flanked endogenous SOCS3 CDS can be excised by Dre, and the IRES-GFP reporter can be switched to firefly luciferase expression by FLP-mediated recombination.

which not only terminated transcription, but also serves as a survival signal as it provides resistance against G418. Once active, the reporter allele utilizes the endogenous SOCS3 promoter to drive compound expression of SOCS3 and IRES-GFP. The SOCS3 coding sequence (CDS) is flanked by rox-sites and can be excised by Dre-mediated recombination, yielding a functional knock-out of SOCS3 in Dre-expressing tissues. After Dre-mediated recombination, the reporter allele can be modified by FLP-mediated recombination to switch from IRES-GFP to express firefly luciferase, enabling the visualization of SOCS3 activity *in vivo* in a non-invasive manner (Fig. 3.1).

3.1.2 SOCS3-U targeting vector generation

For the generation of the SOCS3-U targeting vector, existing genetic tools available in our lab could be used. The common Stop-eGFP-ROSA-CAGs [SERCA, Klisch, 2006] plasmid contains a loxp-flanked neo-stop cassette, followed by an IRES-GFP reporter cassette flanked by FRT sites in tandem orientation. In a first step, SOCS3 CDS was amplified by PCR from genomic DNA. Rox-sites for Dre-mediated recombination are small enough to be introduced into the PCR amplicon as primer overhangs. The rox-SOCS3-rox amplicon was digested with MluI restriction enzyme and ligated between the loxP-flanked stop cassette and the IRES-GFP reporter cassette into the AscI-digested SERCA plasmid. The complete loxP-neo/stop-loxP-rox-SOCS3-rox-frt-IRES-GFP-frt fragment was subsequently excised from the SERCA backbone with an NheI/EcoRV double digest and ligated into the GK12TK plasmid () backbone, cut with AvrII and PmeI. The left arm of homology

(LAH), necessary for targeting of the SOCS3 locus, was amplified by PCR from genomic DNA, digested with PvuI and PacI and inserted into the PacI restriction site in front of the loxP-flanked neo/stop cassette. The right arm of homology (RAH) for the SOCS3 was amplified by PCR from genomic DNA and the firefly luciferase CDS was amplified via PCR from the pTE-Luc plasmid (). The luciferase amplicon contained a FRT site at the 5′ end, introduced as a primer overhang, and was ligated as a reverse complement in front of the RAH into the pGEM-T-Easy cloning vector with AscI/SwaI double digest. The resulting luciferase-frt–RAH fragment was cut from the pGEM-T-Easy backbone via AgeI restriction digest and ligated at the 3′ end of targeting construct into the GK12TK plasmid.

The SOCS3-U allele was targeted into the SOCS3 locus, which consists of two exons. Exon 1 and the first 88 nucleotides of exon 2 form the 5′UTR. The coding sequence of SOCS3 is located within exon 2, followed by a 3′UTR (Fig. 3.2a). A targeting vector flanked by 5 kb homologous regions (LAH and RAH, respectively) was constructed, ensuring the correct targeting to the endogenous SOCS3 locus. To prevent random integration of the construct into the mouse genome, the targeting construct contains the negative selection marker herpes-simplex-virus thymidine kinase (HSV Tk) cassette besides the homologous regions (Fig. 3.2b). Upon random integration of HSK Tk, cells will also contain and express the viral thymidine kinase, which renders them susceptible to ganciclovir treatment. Correctly targeted cells only contain the region between the homologous regions and are therefore resistant to G418 and ganciclovir. Southern blot analysis can be performed to identify correctly targeted ES cells. Integration of the SOCS3-U allele introduces additional EcoRV restriction sites, yielding two smaller fragments (9 & 9.7 kb for probes LA1 and RA1 respectively) compared to the 17.9 kb wt fragment (Fig. 3.2c).

3.1.3 Successful targeting of the endogenous SOCS3 locus

10^7 Bruce4 C57BL/6 ES cells [Köntgen *et al.*, 1993] were transfected with 40 μg AsiSI-linearized SOCS3-U targeting construct and subsequently selected for G418
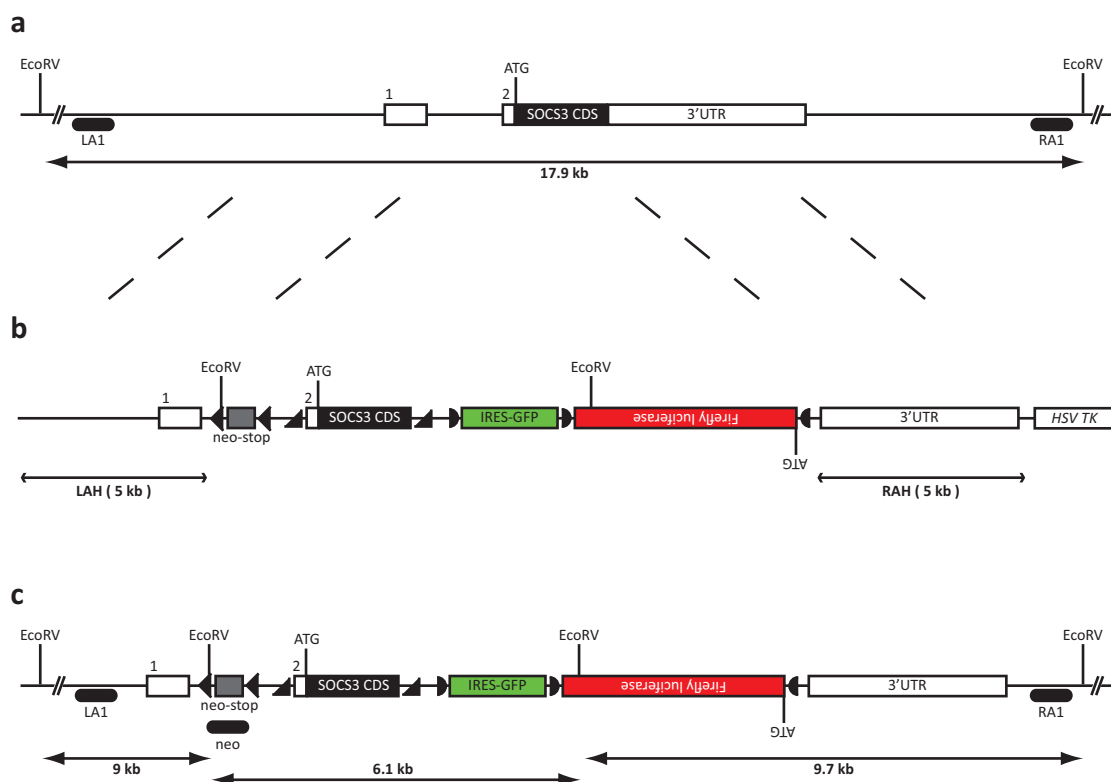
Figure 3.2: **SOCS3-U targeting construct is targeted to the murine SOCS3 locus**
(a) The murine SOCS3 locus comprises 2 exons, with exon 1 and the first 88 nucleotides of exon 2 forming the 5'UTR, and a 1.5 kb 3'UTR. The coding sequence, depicted in black, lies completely within exon 2. (b) Correct targeting of the targeting construct was assured by 5 kb homologous regions with the targeted locus (LAH and RAH respectively). The targeting construct contains a loxP flanked neo-stop cassette, the rox-flanked endogenous SOCS3 exon 2 and a FRT-flanked IRES-driven eGFP / firefly luciferase double reporter. Random, non-homologous recombination of the construct was inhibited by the HSV TK cassette outside the homologous regions of the targeting construct. (c) Integration of the targeting construct into the murine SOCS3 locus could be verified by Southern blot analysis. Integration of the targeting construct introduces additional EcoRV restriction sites, yielding two smaller fragments (9 & 9.7 kb for probes LA1 and RA1 respectively) compared to the 17.9 kb wt fragment, or a 6.1 kb fragment for the neo-probe, hybridizing with the neomycin resistance cassette.

resistance for 10 days. 800 ES cell clones were isolated, expanded and analyzed for correct integration of the SOCS3-U knock-in allele into the endogenous SOCS3 locus via Southern blot analysis. Southern-blot analyses of EcoRV-digested clonal DNA using both LA1 and RA1 probes on ES cell clones identified 3H2 and 8A10 as these clones showed the expected transgenic bands (9 & 9.7 kb for probes LA1 and RA1 respectively) besides the 17.9 kb wt band, confirming successful, heterozygous
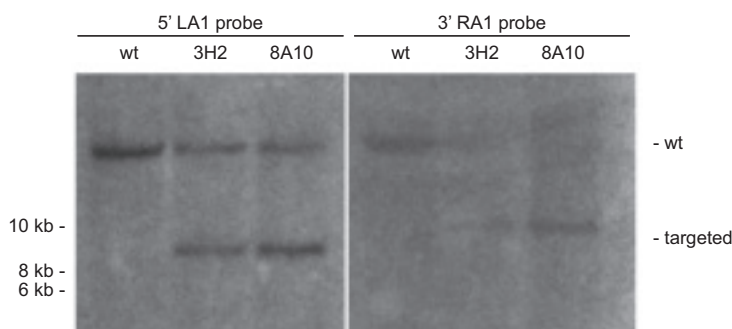
Figure 3.3: **Successful targeting of ES cells with SOCS3-U**
Southern blot analysis of transfected ES cells. Genomic DNA was isolated from ES cell clones and digested with EcoRV. ^{32}P radioactively labeled DNA probes, 5' LA1 probe and 3' RA1 probe respectively, were used to differentiate wt and targeted ES cells. Labeling of DNA from ES cell clones 3H2 and 8A10 gave rise both to the 17.9 kb wt band as well as the 9 kb and 9.7 kb targeted bands. (cf. Fig. 3.2)

targeting of ES cells with the SOCS3 U targeting construct (not shown). Correctly targeted 3H2 and 8A10 ES-cell clones were expanded and subjected to in depth Southern-Blot analysis, confirming that both clones show the expected, additional 9 & 9.7 kb bands (Fig. 3.3). ES cells from the 3H2 and 8A10 clones were injected into C.B20 blastocysts to obtain chimeras of *SOCS3-U*$^{fl;rox;frt-GFP/wt}$ mice. 3 chimeras were derived from the 3H2 clone, but displayed only very weak chimerism (5%, 5% and 20%), while 4 chimeras derived from the 8A10 clone exhibited higher chimerism (50%, 55%, 75% and 85%). Only the 75% chimera derived from the 8A10 clone transmitted the SOCS3-U allele through the germline, successfully establishing the SOCS3-U mouse line.

Collectively, we have successfully generated the SOCS3-U targeting vector, targeted ES-cells and SOCS3-U mice.

3.2 SOCS3-U variants to analyze inflammatory signaling

The SOCS3-U allele is present in three variants for analytic purposes. The parental *SOCS3-U*$^{fl;rox;frt-GFP}$ variant represents the inactivated state. This allele functions as a knock-out-first allele, since expression of the endogenous SOCS3 CDS is inhibited by the floxed neo-stop cassette (Fig. 3.4a). Since a whole-body
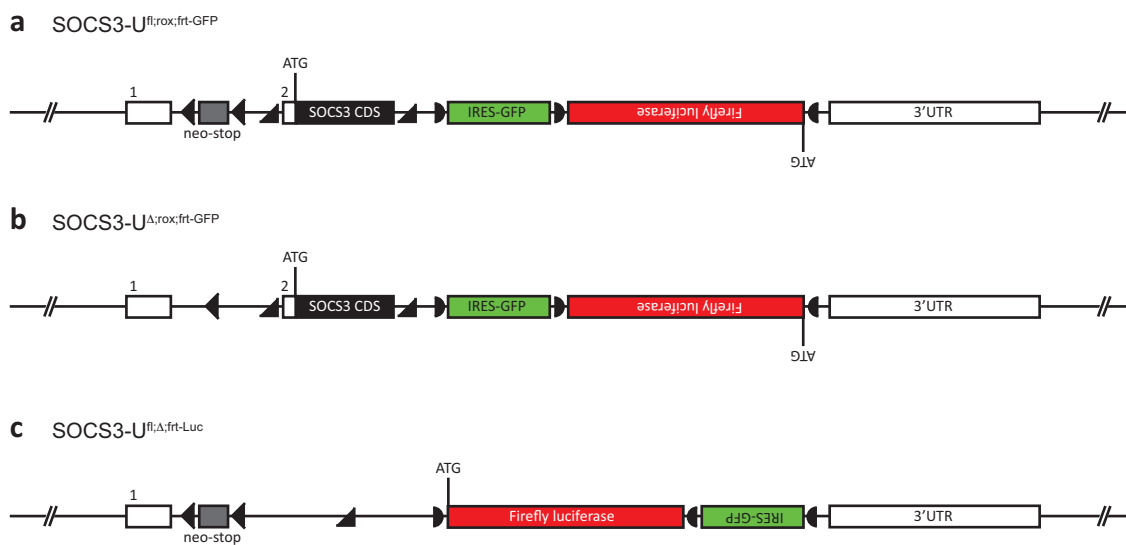
Figure 3.4: **SOCS3-U variants before and after site-specific recombination**
(a) The basic *SOCS3-U^{fl;rox;frt-GFP}* allele does neither express SOCS3, nor any of the reporter genes. (b) After Cre-mediated recombination, *SOCS3-U^{Δ;rox;frt-GFP}* expresses SOCS3 and an IRES driven GFP in the given target tissues. (c) Via Dre- and FLP-mediated recombination, the *SOCS3-U^{fl;Δ;frt-Luc}* allele does no longer express SOCS3, but utilizes the SOCS3 promoter to drive expression of firefly luciferase. The allele still has to be activated by Cre-mediated recombination.

SOCS3 ablation is embryonic lethal [Roberts *et al.*, 2001], the basic allele can only be kept heterozygous in *SOCS3-U^{fl;rox;frt-GFP/wt}* mice. Cre-mediated recombination will yield the *SOCS3-U^{Δ;rox;frt-GFP}* variant and re-enable the expression of SOCS3, as well as of IRES-GFP (Fig. 3.4b). Homozygous *SOCS3-U^{Δ;rox;frt-GFP/Δ;rox;frt-GFP}* mice can therefore be crossed to Dre-driver lines, thus generating tissue-specific SOCS3 knock-outs. For non-invasive *in vivo* imaging, FLP-mediated recombination can be used on Dre-deleted *SOCS3-U^{fl;Δ;FRT-GFP}* allele to generate the *SOCS3-U^{fl;Δ;frt-Luc}* variant (Fig. 3.4c). After subsequent Cre-mediated activation, firefly luciferase can be expressed from the endogenous SOCS3 promoter. D-luciferin can be injected *i.p.* and will be oxidized by luciferase in an ATP-dependent manner. The invested energy is released as bioluminescence upon decay of the formerly oxidized product. Thus, these SOCS3-U variants will help to characterize inflammatory signaling in the tumor microenvironment in different ways.

3.3 SOCS3-U can successfully be utilized *in vivo*

With generation of SOCS3-U mice, the ability to be activated *in vivo* and an exclusion of a potential phenotype of unactivated *SOCS3-U$^{fl;rox;frt-GFP/wt}$* mice had to be investigated.

3.3.1 Cre-activated SOCS3-U cells express GFP upon stimulation

In order to assess the ability of SOCS3-U to express GFP upon stimulation of SOCS3, SOCS3-U 8A10 ES cells were transfected with pPGK-Cre-bpA plasmid [Kurt Fellenberg, University of Cologne]. 200 clones were picked and successful Cre-mediated excision of the loxP-flanked stop cassette was assessed by Southern blot analyses. ES cell clone H2 contained the Cre-excised SOCS3-U allele (Fig. 3.5b). H2 cells were expanded and stimulated with LIF, LPS, or IL-6 for 24h. FACS quantification of stimulated SOCS3-U ES cells confirmed SOCS3 dependent GFP activity upon stimulation, though to a low extent (Fig. 3.5c).

To verify whether SOCS3-U can be activated by Cre-mediated recombination *in vivo*, *SOCS3-U$^{fl;rox;frt-GFP/wt}$* mice were crossed to Cre-deleter mice [Schwenk *et al.*, 1995] in order to activate SOCS3-U in the whole body (*SOCS3-U$^{\Delta;rox;FRT-GFP/wt}$*). Peritoneal macrophages and splenocytes were isolated and stimulated *ex vivo* with LPS, IL-6, IL-11 or TNFα for 24h. Stimulated macrophages exhibit increasing GFP fluorescence with IL-6, IL-11 and TNFα compared to LPS-stimulated cells or unstimulated macrophages (Fig. 3.6a). In contrast, splenocytes display similar levels of enhanced GFP fluorescence upon stimulation with LPS, IL-11, TNFα and IL-6 when compared to unstimulated splenocytes (Fig. 3.6b).

Taken together, these experiments demonstrates that the SOCS3-U allele works *in vitro* and *ex vivo*, though to minor effect under these conditions *in vivo*.

3.3.2 Wild-type like inflammation in SOCS3-U$^{fl;rox;frt-GFP/wt}$ mice

The SOCS3-U allele is conditionally activated to utilize the GFP or luciferase reporter as specifically as possible, i.e. either with spatial or temporal con-
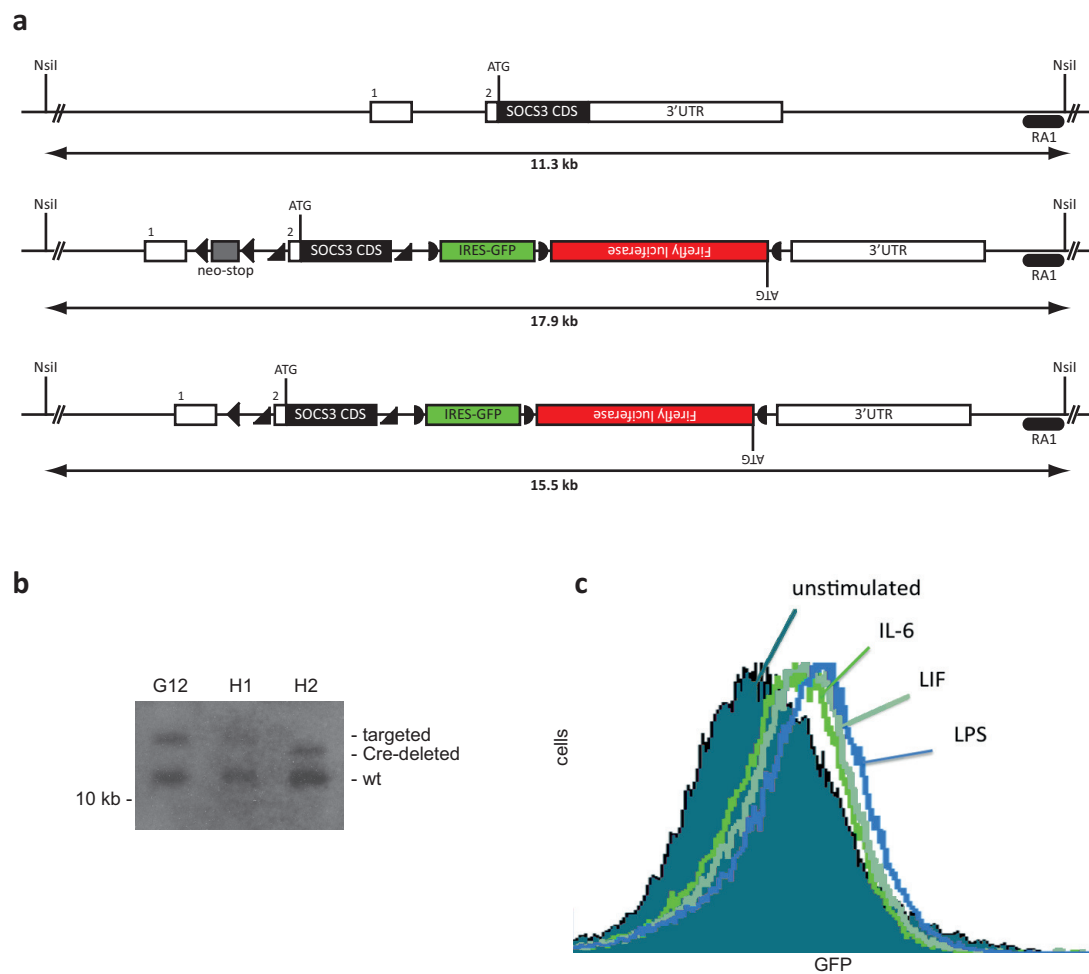
Figure 3.5: **GFP fluorescence of SOCS3-U ES cells after Cre activation**
(a) Genomic DNA of transfected 8A10 ES cells was isolated and digested with NsiI and analyzed with the RA1 probe, yielding an 11.3 kb fragment for the wt SOCS3 allele, a 17.9 kb fragment for the targeted SOCS3-U allele and an 15.5 kb fragment after Cre-mediated activation. (b) ES cell clone H2 shows the correct 15.5 kb band for Cre-mediated active SOCS3-U. (c) Stimulation with LIF [4×10^4 U], LPS [500 ng/ml] and IL-6 [30 ng/ml] upregulated GFP expression compared to unstimulated SOCS3-U control cells.

trol or a combination of both. Hence, off-target tissues will retain the basic *SOCS3-U$^{fl;rox;frt-GFP}$* allele, rendering them heterozygous SOCS3 knock-outs. In order to address, whether a heterozygous SOCS3 knock-out affects the duration or severity or inflammatory signaling, primary hepatocytes from either wt or *SOCS3-U$^{fl;rox;frt-GFP/wt}$* mice were isolated and 2×10^5 stimulated *in vitro* with 50 ng/ml IL-6 for 0, 15, 30, 60 or 120 min. IL-6 signaling both in wt and *SOCS3-U$^{fl;rox;frt-GFP/wt}$* mice leads to phosphorylation of STAT3 (pSTAT3) already after 15 min (Fig. 3.7a). SOCS3 protein levels begin to increase 30 min after IL-6
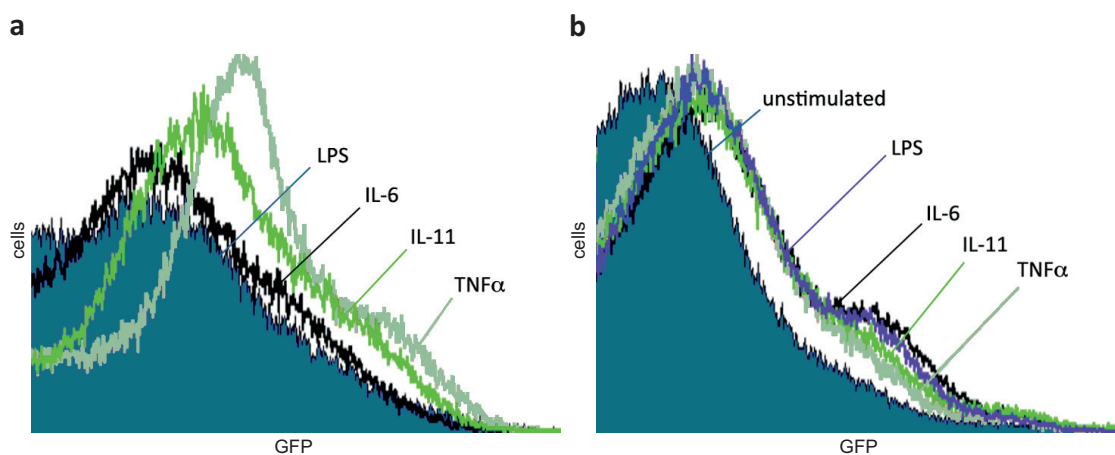
Figure 3.6: **Isolated cells from SOCS3-U mice express GFP upon stimulation**
(a) Peritoneal macrophages and (b) splenocytes from *SOCS3-U$^{\Delta;rox;FRT-GFP/wt}$* mice were isolated and stimulated *ex vivo* with LPS [500 ng/ml], IL-6 [100 ng/ml], IL-11 [100 ng/ml] or TNFα [20 ng/ml]. GFP fluorescence was analyzed by FACS quantification.

stimulation, where also the highest pSTAT3 levels are detected. SOCS3 activity subsequently blocks IL-6 downstream signaling, consistently decreasing pSTAT3 levels 60 and 120 min after stimulation. Furthermore, Analyzation of SOCS3 mRNA expression 0, 15 and 120 min after IL-6 stimulation from isolated control as well as *SOCS3-U$^{fl;rox;frt-GFP}$* primary hepatocyte RNA showed no differences in SOCS3 mRNA upregulation between wt and *SOCS3-U$^{fl;rox;frt-GFP}$* primary hepatocytes (Fig. 3.7b).

Importantly, a heterozygous SOCS3 knock-out in primary hepatocytes from *SOCS3-U$^{fl;rox;frt-GFP/wt}$* mice has no effect on the dynamics of IL-6 signaling *in vitro*. Thus, utilization of *SOCS3-U$^{fl;rox;frt-GFP/wt}$* mice in combination with tissue-specific Cre-driver lines to active SOCS3-U has no detrimental effect on inflammatory signaling, at least in hepatocytes, and can be used as GFP or luciferase reporters. However, no *SOCS3-U$^{fl;\Delta;frt-Luc/wt}$* animals to analzyse SOCS3-U driven luciferase expression could be obtained so far.

3.4 Contribution of macrophages to AOM/DSS induced CRC

Colorectal cancer (CRC) formation is a classic case of inflammation associated
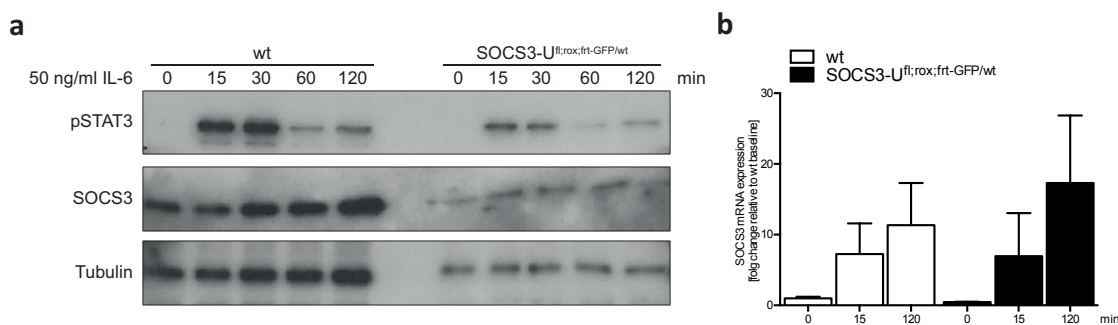
Figure 3.7: **Unaltered SOCS3 expression in SOCS3-U$^{fl;rox;frt-GFP/wt}$ hepatocyes**
(a) Western-blot analyses of primary hepatocytes isolated from wt or *SOCS3-U$^{fl;rox;frt-GFP/wt}$* mice using pSTAT3, Tubulin and SOCS3 antibodies. Primary hepatocytes were stimulated with 50 ng/ml IL-6 for 0, 15, 30, 60 or 120 min. (b) RNA was isolated from *wt* or *SOCS3-U$^{fl;rox;frt-GFP/wt}$* primary hepaotcytes stimulated with 50 ng/ml IL-6 for 0, 15 or 120 min and SOCS3 mRNA expression of was analyzed by qPCR. Displayed are means ± SEM, n=3.

cancerogenesis, where inflammatory bowel disease severely increases the risk of tumorigenesis. A persistent colitis increases the inflammatory tone in the colon, promoting the uncontrolled growth of intestinal epithelial cells to form polyps which can eventually transform into colorectal cancer. While the initial cause for the increased inflammation may have numerous reasons, the succession of immune cells infiltrating the inflamed tissue and their contribution to colorectal cancer formation remains to be elucidated.

3.4.1 IL-6 mediated colorectal cancer formation

Previous data from our lab indicate that IL-6Rα ablation has a protective effect on colorectal cancer formation, in that IL-6Rα deficient mice (*IL-6Rα$^{\Delta/\Delta}$*) exhibit reduced AOM/DSS induced tumors [Claudia Wunderlich, University of Cologne]. A microarray analyses of these IL-6Rα deficient vs. proficient tumors revealed decreased levels of CCL20 (chemokine ligand 20), CCR6 (chemokine receptor 6) and various lymphocyte markers in IL-6Rα$^{\Delta/\Delta}$ tumors. CCL20 is a lymphocyte attracting chemokine [Hieshima *et al.*, 1997] and signals via CCR6 on target cells [Baba *et al.*, 1997]. This observation suggests an IL-6 dependent mechanism of CCL20 expression, attracting lymphocytes to the colon to promote colorectal cancer

formation.

Abrogation of IL-6 signaling in myeloid cells severely diminishes their capability of differentiating into alternatively activated towards M2 macrophages [Mauer *et al.*, 2014]. As *IL-6Rα*$^{Δ/Δ}$ mice exhibit no M2 macrophages and reduced CCL20 expression, this led to the hypothesis that M2 macrophages during colitis attract lymphocytes to the colon, thereby promoting colorectal cancer formation. In order to shed light on the macrophage subpopulations and their contribution to colorectal cancerogenesis, *SOCS3-U*$^{fl;rox;frt-GFP/wt}$ mice were crossed to *LysM-Cre*$^{tg/wt}$ mice [Clausen *et al.*, 1999]. Furthermore, double-positives were subsequently crossed to*R26-fl-tdTomato*$^{fl/fl}$ mice [Madisen *et al.*, 2010] to control for Cre-mediated recombination by red fluorescence. The resulting *SOCS3-U*$^{fl;rox;frt-GFP/wt}$*;R26-fl-tdTomato*$^{fl/wt}$*;LysM-Cre*$^{tg/wt}$ mice were subjected to AOM/DSS treatment to recapitulate the early stage of acute colitis as a driving force for CRC development. *SOCS3-U*$^{fl;rox;frt-GFP/wt}$*;R26-fl-tdTomato*$^{fl/wt}$*;LysM-Cre*$^{tg/wt}$ mice will express the red fluorescent tdTomato protein in all myeloid lineage derived cells, and express GFP in a SOCS3 dependent manner.

3.4.2 SOCS3^{low} M2 macrophages express CCL20 and IL-17RA

After AOM injection, 5 days of DSS treatment and 3 days recovery phase, macrophages were isolated from the colon and subjected to fluorescence activated cell sorting. Untreated control animals exhibit a small cohort of red fluorescent tdTomato^{high};GFP^{low} macrophages, and virtually no tdTomato^{high};GFP^{high} macrophages (Fig. 3.8a). AOM/DSS treatment strongly increases the amount of macrophages in the colon, both of the tdTomato^{high};GFP^{low} type as well as tdTomato^{high};GFP^{high} macrophages (Fig. 3.8b). To investigate which if those macrophages express CCL20, RNA from sorted macrophages was isolated and the expression level of CCL20 mRNA was analyzed by qPCR (Fig. 3.8c). Expression of CCL20 in tdTomato^{high};GFP^{low} macrophages upon AOM/DSS treatment is significantly upregulated 6-fold compared to untreated tdTomato^{high};GFP^{low}
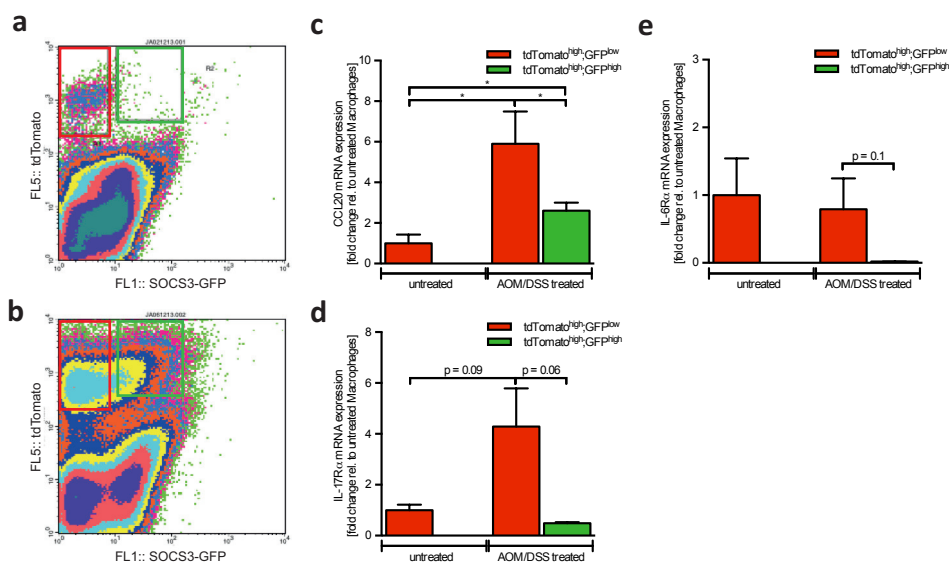
Figure 3.8: **SOCS3^{low} M2 macrophages express CCL20 upon AOM/DSS treatment**
Representative FACS blots of macrophages isolated from colons of *SOCS3-U$^{fl;rox;frt-GFP/wt}$;R26-fl-tdTomato$^{fl/wt}$;LysM-Cre$^{tg/wt}$* mice either (a) untreated or (b) treated with AOM/DSS for 5 days. Macrophages were sorted for tdTomato^{high};GFP^{low} (red square) and tdTomato^{high};GFP^{high} (green square) sub-populations. RNA from sorted cells was isolated and the expression level of (c) CCL20, (d) IL-17RA and (e) IL-6Rα mRNA was analyzed by qPCR. Displayed are means ± SEM, n=4. * p $\leqq$ 0.05

macrophages. Moreover, CCL20 expression is also significantly higher than in tdTomato^{high};GFP^{high} macrophages, which exhibit only a 2.5 fold upregulation from the untreated controls. Furthermore, tdTomato^{high};GFP^{low} macrophages have 4-fold upregulated IL-17 receptor (IL-17RA) expression compared to untreated macrophages (Fig. 3.8d). IL-17 producing T_H17 cells are known to massively infiltrate inflamed intestines [Gálvez, 2014]. Lastly, only tdTomato^{high};GFP^{low} macrophages express IL-6Rα and not tdTomato^{high};GFP^{high} macrophages (Fig. 3.8e). Cell numbers of untreated tdTomato^{high};GFP^{high} macrophages were too low to analyze mRNA expression.

Taken together, SOCS3^{low} M2-like tumor associated macrophages (TAMs) express significantly higher levels of CCL20 and IL-17RA upon AOM/DSS treatment than SOCS3^{high} M1-like macrophages. Additionally, SOCS3^{high} M1-like macrophages do not express IL-6Rα, consistent with the CCL20 expression profile upon IL-6Rα ablation. These date confirm a distinct influence of M2 TAMs on CRC de-

velopment and raise the possibility of an IL-17 mediated activity upon increased inflammation in the colon.

3.5 Investigating macrophage subpopulations in DEN-induced HCC

Hepatocellular carcinoma development is a classical inflammation associated cancer that can be experimentally elicited by injection of diethylnitrosamin (DEN) into 12-15 days old male mice [Vesselinovitch & Mihailovich, 1983]; DEN treated mice show hepatocellular carcinoma after 8 months.

The impact of Kupffer cell derived cytokines on tumor progression has been suggested but still remains to be proven [Naugler *et al.*, 2007]. *SOCS3-U$^{fl;rox;frt-GFP/wt}$;R26-fl-tdTomato$^{fl/wt}$;LysM-Cre$^{tg/wt}$* mice were subjected to the chronic DEN HCC model, in order to elucidate the contribution of the various macrophage subpopulations, namely liver resident Kupffer cells, classically activated M1 macrophages and alternatively activated M2 macrophages, to hepatocellular carcinogenesis. *SOCS3-U$^{fl;rox;frt-GFP/wt}$;R26-fl-tdTomato$^{fl/wt}$;LysM-Cre$^{tg/wt}$* mice will express the red fluorescent tdTomato protein in all myeloid lineage derived cells, and additionally express GFP in a SOCS3 dependent manner. Kupffer cells are not affected by LysM-Cre [Hume, 2011] and therefore express neither tdTomato nor GFP, but classic macrophage markers such as F4/80 [Austyn & Gordon, 1981].

SOCS3-U$^{fl;rox;frt-GFP/wt}$;R26-fl-tdTomato$^{fl/wt}$;LysM-Cre$^{tg/wt}$ mice were sacrificed after 8 months and non-parenchymal liver cells were isolated and labeled with an *α*-F4/80-PE/Cy7 antibody. Fluorescenctly labeled cells could be sorted into three distinct subpopulations, namely tdTomato^{low};F4/80^{high} Kupffer cells, tdTomato^{high};GFP^{low} alternatively activated macrophages and tdTomato^{high};GFP^{high} classically activated macrophages (Fig. 3.9a,b). Determination of the cell numbers revealed around 30% of all non-parenchymal liver cells to be tdTomato expressing macrophages and approximately 5% be-

a

b

c   **d**
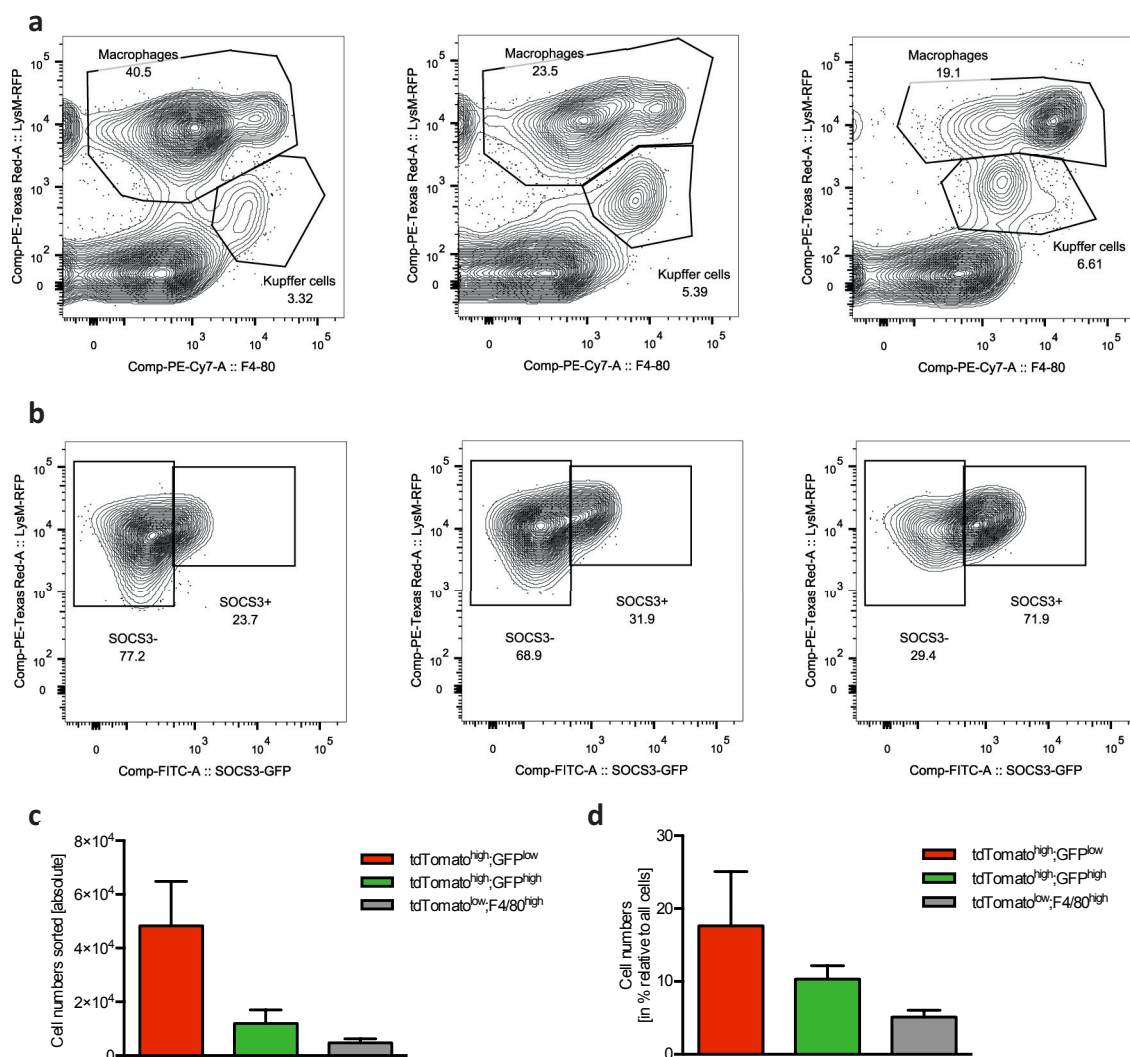
Figure 3.9: **SOCS3-U labels activated macrophages in DEN-induced HCC**

Representative FACS blots of non-parenchymal liver cells isolated from three *SOCS3-U$^{fl;rox;frt-GFP/wt}$;R26-fl-tdTomato$^{fl/wt}$;LysM-Cre$^{tg/wt}$* mice, labeled with an α-F4/80-PE/Cy7 antibody. (a) tdTomato^{low};F4/80^{high} cells were sorted from tdTomato^{high};F4/80^{high} cells. (b) Cells were further divided into SOCS3-U dependent GFP^{high} and GFP^{low} cells. Quantification of cell numbers for tdTomato^{high};GFP^{low}, tdTomato^{high};GFP^{high} and tdTomato^{low};F4/80^{high} cells in (c) absolute cell numbers sorted or as (d) relative cell counts of all non-parenchymal cells in percent. Displayed are means ± SEM, n=8 for (c) and n=3 for (d).

ing Kupffer cells (Fig. 3.9d). On average, around 4.8x10^4 of macrophages sorted were tdTomato^{high};GFP^{low} alternatively activated macrophages, 1.2x10^4 were tdTomato^{high};GFP^{high} classically activated macrophages and 5x10^3 were tdTomato^{low};F4/80^{high} Kupffer cells (Fig. 3.9c).

Collectively, application of *SOCS3-U$^{fl;rox;frt-GFP/wt}$;R26-fl-tdTomato$^{fl/wt}$;LysM-Cre$^{tg/wt}$*

mice in the DEN-induced HCC model enables the separation of infiltrating M1 macrophages from M2 macrophages as well as Kupffer cells. These respective macrophage subpopulations can then be subjected to further in depth analysis, e.g. transcriptome sequencing, to address their contribution to DEN-induced HCC development.

3.6 Activation of T-cells in the tumor microenvironment of HCC

Hepatocellular carcinoma is one of the most common cancers and has a very high mortality rate of around 95%. HCC develops predominantly from cirrhosis after hepatitis virus B or C infection, but it is also strongly driven by excessive alcohol consumption or non-alcoholic steatohepatitis (NASH). Similar to a hepatic viral infection, NASH causes enhanced inflammation in the liver, which is the common driver for HCC initiation. Consistently, infiltration and activation of immune cells into the steatotic liver could be observed in a mouse model of a choline deficient high fat diet (CD-HFD), recapitulating clinical observations of choline deficiency in NASH patients [Wolf *et al.*, 2014]. Furthermore, hepatic lipid uptake, and ultimately the transition from NASH to HCC, could be linked to LIGHT (TNFsf14, tumor necrosis factor ligand superfamily member 14) secretion from NK-T cells.

3.6.1 IL-6 dependent modification of LIGHT expression

Our previous data demonstrated that the protective effect of a whole body IL-6Rα deficiency (*IL-6R$\alpha^{\Delta/\Delta}$*) was abrogated under obese conditions [Gruber *et al.*, 2013]. Interestingly, IL-6Rα deficiency specifically in T-cells (*IL-6Rα^{T-KO}*) protects from HCC development in lean animals and even during obesity [Gruber, 2013]. Furthermore, IL-6Rα deficiency in hepatocytes showed unaltered HCC development, indicating that IL-6 signaling on T-cells is critical for HCC development. Together with the experiments by Wolf *et al.* we hypothesize that IL-6 induces LIGHT ex-

a

b
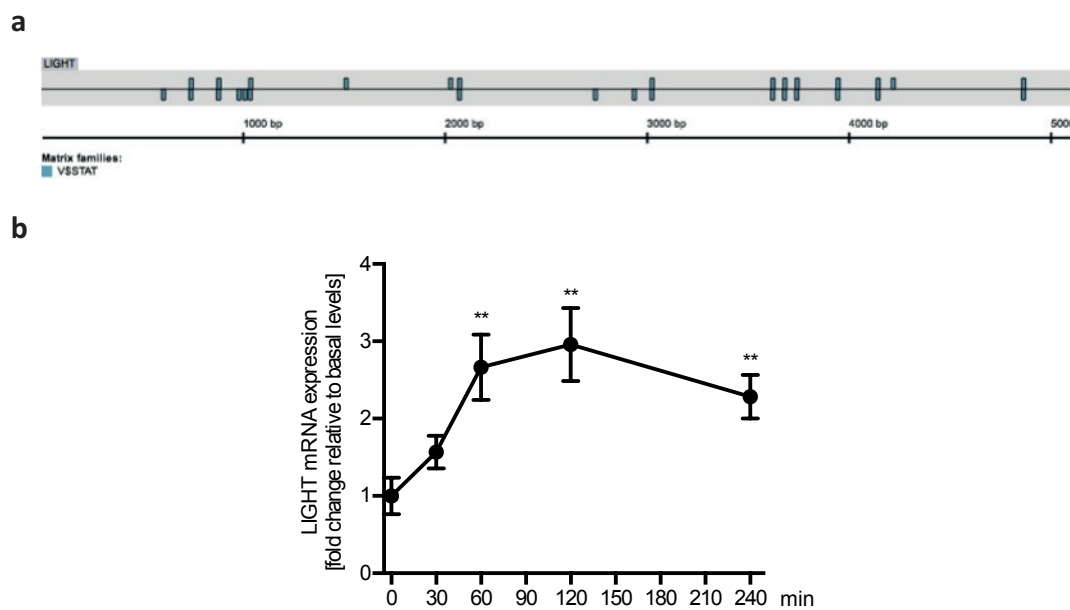
Figure 3.10: **IL-6 signaling induces hepatic LIGHT mRNA expression**
(a) 5000 bp LIGHT promoter analysis with STAT binding sites [MatInspector, Genomatix, Munich, Germany]. (b) LIGHT mRNA expression in the liver at indicated timepoints after IL-6 stimulation. Displayed are means ± SEM, n=8. ** $p \leqq 0.01$ [data produced with Peter Ströhle]

pression to promote hepatic lipid uptake and progression from NASH to HCC, corroborated by an analysis of the LIGHT promoter, revealing 30 STAT regulatory binding sites 5000 bp upstream of the transcription start (Fig. 3.10a). To investigate this, control mice were injected with IL-6 [50 ng/g] *i.p.* and hepatic LIGHT expression was analyzed after 30, 60, 120 and 240 minutes in order to address, whether expression of LIGHT is regulated by IL-6 signaling. Stimulation with IL-6 leads to a 1.5 fold induction of hepatic LIGHT mRNA expression already after 30 min, reaching significance after 60 min with a 2.5 fold induction and peaking with a 3-fold upregulation after 2h (Fig. 3.10b). This clearly demonstrates that LIGHT mRNA expression in the liver is affected by IL-6 signaling.

To shed light on the contribution of IL-6 signaling on hepatic LIGHT mRNA expression in the tumor initiating phase of DEN-induced HCC development, *IL-6Rα^{fl/fl}*, *IL-6Rα^{Δ/Δ}* and *IL-6Rα^{T-KO}* mice were subjected to the acute DEN model and LIGHT mRNA expression was analyzed after 1, 2, 3 and 10 days in whole-liver extracts by qPCR. It was already demonstrated that acute DEN treatment
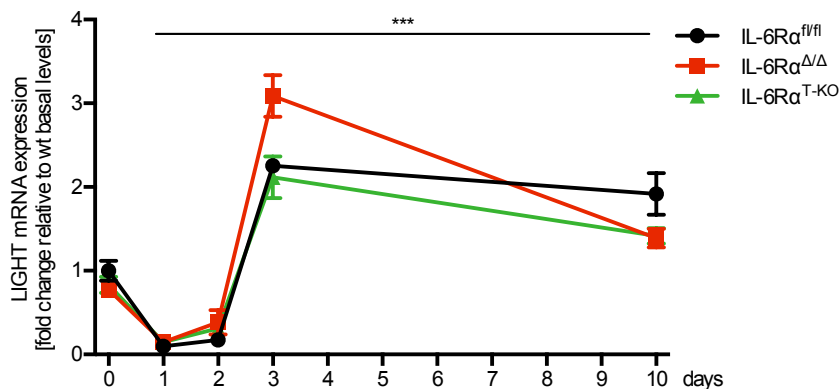
Figure 3.11: **Alteration of LIGHT mRNA expression upon DEN stimulation**
LIGHT mRNA expression in the liver of *IL-6Rα^{fl/fl}*, *IL-6Rα^{Δ/Δ}* and *IL-6Rα^{T-KO}* mice at indicated timepoints after DEN treatment. Displayed are means ± SEM, n=8. *** p ≤ 0.001 [data produced with Sabine Gruber]

stimulates IL-6 release into the blood stream, peaking after 8 hours with a 4 fold concentration and returning to baseline levels after 30 hours [Gruber *et al.*, 2013]. Acute DEN treatment leads to significant LIGHT mRNA downregulation after 24h both in *IL-6Rα^{fl/fl}* and *IL-6Rα^{Δ/Δ}* animals as well as *IL-6Rα^{T-KO}* mice, persisting until 48h after DEN injection (Fig. 3.11). Subsequently, LIGHT mRNA expression is significantly increased 72h after DEN treatment, with a 2 fold upregulation compared to the basal state in *IL-6Rα^{fl/fl}* and *IL-6Rα^{T-KO}* mice and up to 3 fold in *IL-6Rα^{Δ/Δ}* mice. LIGHT mRNA expression continues to be elevated and is still upregulated 1.5-2 fold in all genotypes after 10 days. Collectively, IL-6 signaling has an inhibitory effect on hepatic LIGHT mRNA expression in the first 48h after DEN injection, recapitulating the early, tumor initiating phase of hepatocellular carcinogenesis, followed by a significant induction of LIGHT mRNA expression.

Taken together, LIGHT expression is clearly affected by IL-6 signaling and altered upon high-dose DEN injection, but with minor differences between presence or absence of IL-6Rα, both in all cell types or only in T-cells. In line with these experiments, Wolf *et al.* show that LIGHT in CD-HFD induced HCC was derived from NK-T cells, which are a special T-cell subpopulation. Furthermore, we have demonstrated earlier that only a marginal population of NK-T cells (i.e. 2%), the source of LIGHT expression, do express IL-6Rα [Gruber, 2013]. However, with uti-
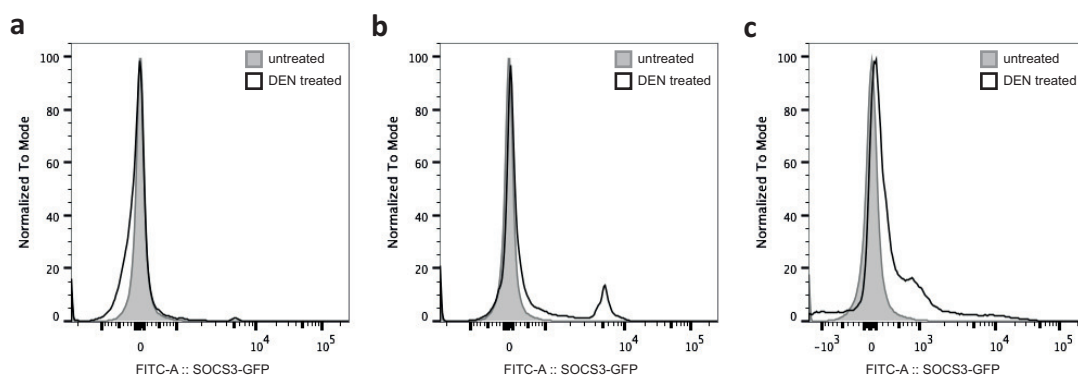
Figure 3.12: **Acute DEN elevates SOCS3-GFP expression**
GFP fluorescence histograms of non-parenchymal liver cells isolated from
$SOCS3\text{-}U^{fl;rox;frt\text{-}GFP/wt}$;$CD4\text{-}Cre^{tg/wt}$ mice. SOCS3-GFP intensity is displayed (a)
1 day after acute DEN treatment, (b) 2 days after treatment or (c) 3 days after
treatment compared to untreated control animals in gray.

lization of SOCS3-U reporter mice, active cell-type specific IL-6 signaling can be
visualized to gain further insight into the contribution of IL-6 signaling on NK-T
cells with respect to LIGHT mRNA expression.

3.6.2 Separation of NK-T cell subpopulations using SOCS3-U

In order to address, whether NK-T cells might be a driving force for hepatocel-
lular carcinoma initiation, $SOCS3\text{-}U^{fl;rox;frt\text{-}GFP/wt}$ mice were crossed to $CD4\text{-}Cre^{tg/wt}$
[Lee *et al.*, 2001] mice to express GFP in a SOCS3 dependent manner in all T-cell re-
ceptor α/β (TCRα/β) expressing T-cells. Acute DEN treatment for 1, 2 and 3 days
leads to an increasing GFP fluorescence intensity in isolated, non-parenchymal liver
cells (NPLCs) (Fig. 3.12). This demonstrates that $SOCS3\text{-}U^{fl;rox;frt\text{-}GFP/wt}$;$CD4\text{-}Cre^{tg/wt}$
mice can be utilized to identify lymphocyte subpopulations which are specifically
activated by IL-6 upon acute DEN treatment.

$SOCS3\text{-}U^{fl;rox;frt\text{-}GFP/wt}$;$CD4\text{-}Cre^{tg/wt}$ mice were subjected to the acute DEN model
and their non-parenchymal liver cells were isolated 60h after injection, to elu-
cidate which cell subpopulation exhibits the strong LIGHT mRNA upregula-
tion oberserved in the liver (Fig. 3.11). ⅞ of the isolated non-parenchymal cells
were labeled with α-CD90.2-PE and α-NK1.1-PE/Cy5 antibodies for FACS sort-
ing (Fig. 3.13), and the remaining ⅛ was used for quantitative flow cytometry via
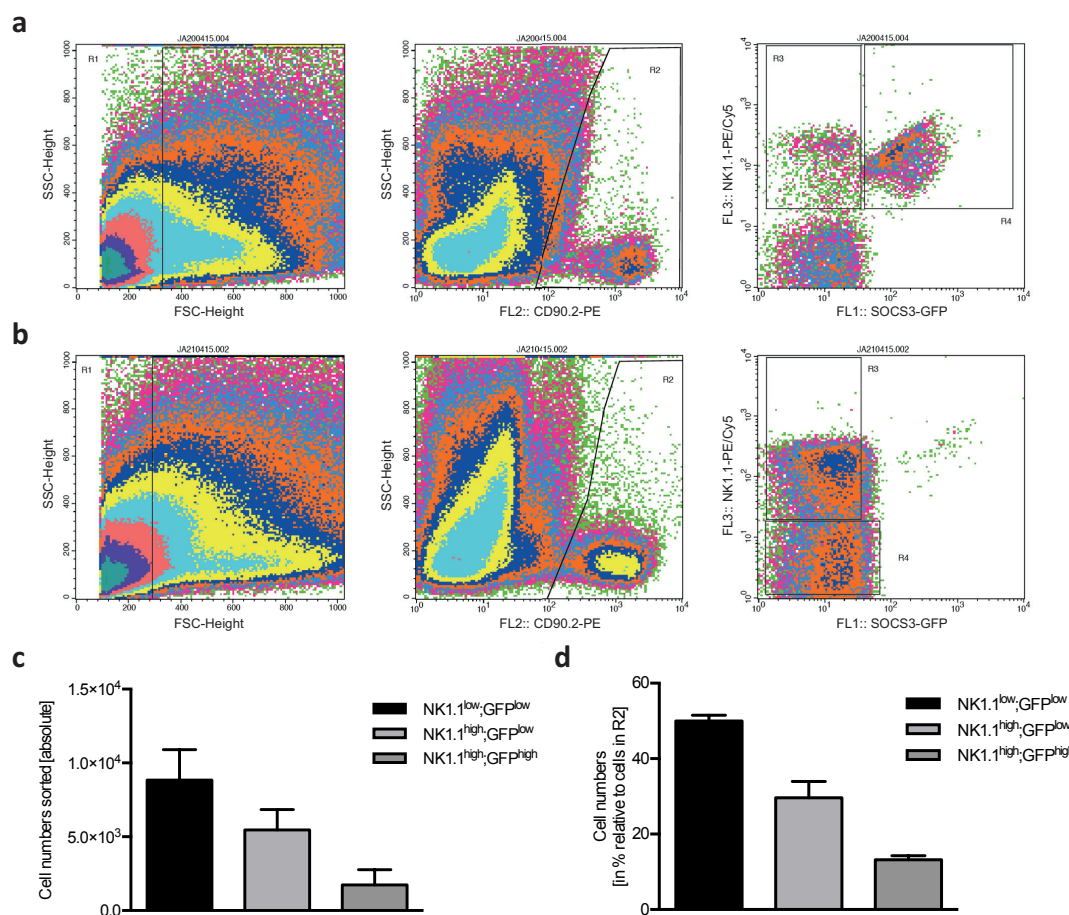
Figure 3.13: **Activation of NK-T cells in the liver upon 60h DEN treatment**
Representative FACS blots of non-parenchymal liver cells isolated from *SOCS3-U$^{fl;rox;frt-GFP/wt}$;CD4-Cre$^{tg/wt}$* mice, labeled with α-CD90.2-PE and α-NK1.1-PE/Cy5 antibodies. (a) Cells were gated in R1 for lymphocytes and in R2 for T-cells. Cells isolated 60h after treatment with DEN were gated in R3 for NK1.1^{high};GFP^{low} and R4 for NK1.1^{high};GFP^{high} cells. (b) Cells isolated from untreated controls were gated in R3 for NK1.1^{high};GFP^{low} and in R4 for NK1.1^{low};GFP^{low} cells. Quantification of cell numbers for NK1.1^{low};GFP^{low}, NK1.1^{high};GFP^{low} and NK1.1^{high};GFP^{high} cells in (c) absolute cell numbers sorted or as (d) relative cell counts of all cells in R2 in percent. Displayed are means $\pm$ SEM, n=5.

MACSQuant (cf. 3.6.4).

Labeled, non-parenchymal liver cells from DEN treated mice were gated for CD90.2^{high} T-cells and sorted into NK1.1^{high};GFP^{low} and NK1.1^{high};GFP^{high} cells (Fig. 3.13a). Isolated T-cells from untreated control animals showed almost no NK1.1^{high};GFP^{high} cells and were therefore sorted into NK1.1^{high};GFP^{low} and NK1.1^{low};GFP^{low} cells (Fig. 3.13b). Quantification of sorted cells reveales around 45% of all liver T-cells in DEN treated mice to be NK-T cells, with 65% of

them being GFP^{low} and 35% being GFP^{high} NK-T cells (Fig. 3.13d). On average, 1×10^4 NK1.1^{low};GFP^{low} T-cells, 5×10^3 NK1.1^{high};GFP^{low} NK-T cells and 2.5×10^3 NK1.1^{high};GFP^{high} NK-T cells were sorted and their RNA isolated for gene expression analysis.

3.6.3 IL-6 signaling in NK-T cells blocks LIGHT mRNA expression

Gene expression analysis via quantitative real-time PCR of NK1.1^{low};GFP^{low} cells, NK1.1^{high};GFP^{low} cells and NK1.1^{high};GFP^{high} cells reveals a highly significant downregulation of T-cell markers CD8 and CD4 in both NK1.1^{high};GFP^{low} and NK1.1^{high};GFP^{high} cells compared to NK1.1^{low};GFP^{low} cells, confirming that NK1.1^{low};GFP^{low} cells are T-cells and the two NK1.1^{high} populations are NK-T cells (Fig. 3.14). Furthermore, gene expression analysis of IL-6Rα demonstrates that, although only a very small subpopulation of NK-T cells express IL-6Rα in the basal state (cf. 3.6.1), NK1.1^{high};GFP^{high}, comprising around 35% of all NK-T cells (Fig. 3.13d), have IL-6Rα significantly upregulated compared to NK1.1^{high};GFP^{low} NK-T cells that show nearly undetectable levels of IL-6Rα expression. In contrast, NK1.1^{high};GFP^{low} NK-T cells exhibit a significant 2.5-fold LIGHT upregulation compared to NK1.1^{low};GFP^{low} T-cells, whereas NK1.1^{high};GFP^{high} NK-T cells express only marginal LIGHT mRNA levels (Fig. 3.14).

Taken together, acute DEN treatment leads to a significant IL-6Rα upregulation in about 35% of NK-T cells after 60h, while LIGHT mRNA expression is inhibited in this NK-T cell subpopulation.

3.6.4 NK-T cells upregulate IL-6Rα upon acute DEN treatment

In order to verify the IL-6Rα upregulation in NK-T cells upon acute DEN treatment, isolated, non-parenchymal liver cells from untreated and acute DEN treated *SOCS3-U$^{fl;rox;frt-GFP/wt}$;CD4-Cre$^{tg/wt}$* mice were labeled with α-CD3-VioBlue, α-IL-6Rα-PE and α-NK1.1-APC antibodies; dead cells were stained with the Aqua dead cell stain kit and excluded.
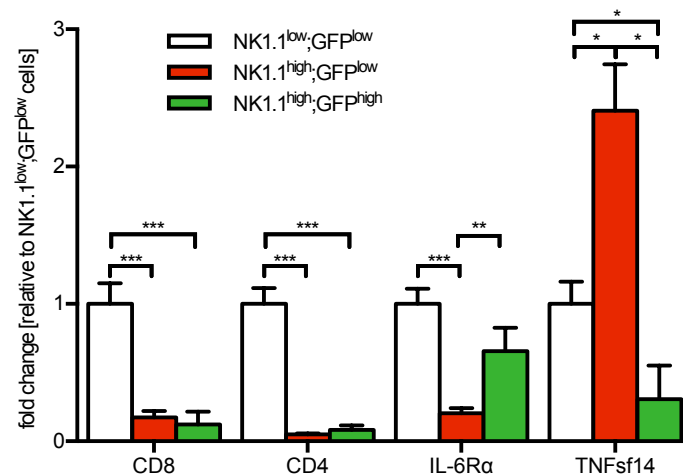
Figure 3.14: **LIGHT is mainly expressed by NK-T cells lacking IL-6Rα**
Quantitative real-time PCR analysis of sorted, non-parenchymal liver cells isolated from *SOCS3-U*$^{fl;rox;frt-GFP/wt}$*;CD4-Cre*$^{tg/wt}$ mice 60h after acute DEN treatment. Gene expression is displayed as fold change compared to NK1.1^{low};GFP^{low} cells as means $\pm$ SEM, n=5. *** p $\leqq$ 0.001, ** p $\leqq$ 0.01, * p $\leqq$ 0.05

NPLCs were gated for CD3^{high};Aqua^{low} alive T-cells (Fig. 3.15a,b), and no significant differences were observed between untreated and DEN treated animals. T-cells were subsequently analyzed for NK1.1 and IL-6Rα expression (Fig. 3.15c,d) as well as SOCS3-U-dependent GFP expression (Fig. 3.15e). Whereas 50% of hepatic T-cells in untreated mice are NK1.1^{+};IL-6Rα^{-} NK-T cells, acute DEN treatment induces IL-6Rα expression in around 35% of NK-T cells (Fig. 3.15f), consistent with appearance of GFP expression in these T-cells. Taken together, acute DEN treatment induces a significant shift of the hepatic NK-T cell population towards IL-6Rα expression and downstream signaling.

In a reverse assay, *IL-6Rα*$^{fl/fl}$, *IL-6Rα*$^{T-KO}$ and *IL-6Rα*$^{\Delta/\Delta}$ mice were subjected to the acute DEN model and NPLCs were isolated after 10 days. Isolated NPLCs were labeled with α-CD3-TexasRed, α-NK1.1-FITC, α-IL-6Rα-PE and α-TCRβ-PE/Cy7 antibodies; dead cells were stained with the Aqua dead cell stain kit.

NPLCs were gated for alive, single-cell T-lymphocytes and analyzed for T-cells and NK-T cells (Fig. 3.16a-c). *IL-6Rα*$^{fl/fl}$, *IL-6Rα*$^{T-KO}$ and *IL-6Rα*$^{\Delta/\Delta}$ mice show equal numbers of T-cells and NK-T cells, demonstrating that acute DEN treatment does not affect the distribution of T-cell and NK-T cell populations in an
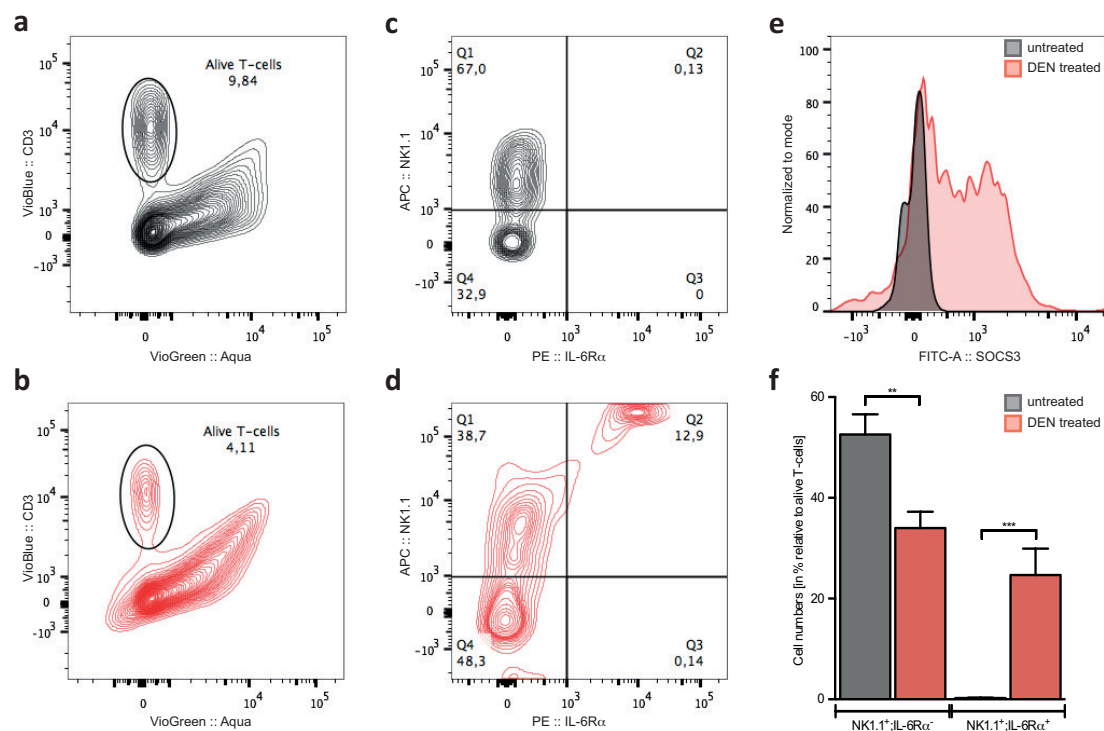
Figure 3.15: **NK-T cells upregulate IL-6Rα upon acute DEN treatment**
Representative FACS blots of non-parenchymal liver cells isolated from untreated (in black) and DEN treated (in red) *SOCS3-U$^{fl;rox;frt-GFP/wt}$;CD4-Cre$^{tg/wt}$* mice, labeled with α-CD3-VioBlue, α-IL-6Rα-PE, α-NK1.1-APC antibodies and the aqua dead cell stain kit. Contour blots show (a,b) alive T-cells, analyzed for (c,d) NK1.1 and IL-6Rα expression. (e) SOCS3-GFP intensity of alive T-cells is displayed as an histogram overlay analyses. (f) Quantification of NK1.1$^+$;IL-6Rα^- NK-T cells in Q1 and NK1.1$^+$;IL-6Rα^+ NK-T cells in Q2 is displayed as means $\pm$ SEM, n=5. *** p $\leqq$ 0.001, ** p $\leqq$ 0.01

IL-6Rα-dependent manner. IL-6Rα expression analyses of gated NK-T cells however confirms that a NK-T cell subpopulation from *IL-6R$\alpha^{fl/fl}$* mice expresses IL-6Rα, which is not present in both in the whole body or T-cell specific IL-6Rα knock-outs (Fig. 3.16d).

Collectively, while direct, *i.p.* injection of IL-6 induces acute, hepatic LIGHT mRNA expression, acute DEN treatment first leads to downregulation of hepatic LIGHT mRNA expression for 48 hours after injection, followed by a strong LIGHT upregulation. Concomitantly, acute DEN treatment stimulates IL-6Rα expression in an NK-T cell subpopulation. Interestingly, LIGHT expression is specifically upregulated in the remaining IL-6Rα^- subpopulation, but downregulated in IL-6Rα^+ cells. However, the exact connection between LIGHT inhibition and IL-6Rα upreg-
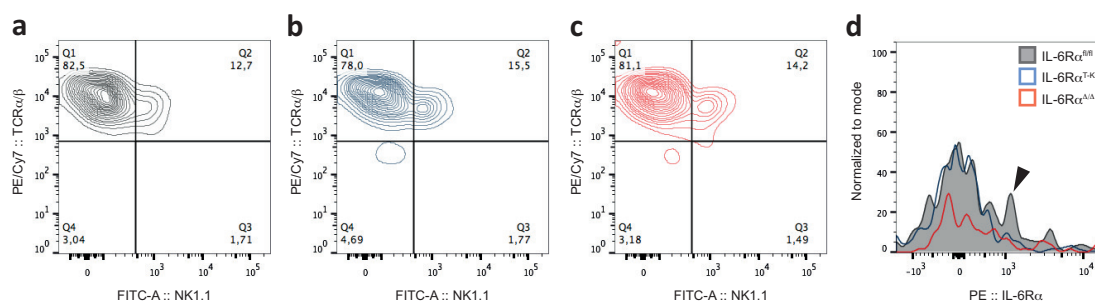
Figure 3.16: **Lack of NK1.1⁺;IL-6Rα⁺ NK-T cells in IL-6Rα deficient mice**
Representative FACS blots of non-parenchymal liver cells isolated from
IL-6Rα^{fl/fl}, *IL-6Rα^{T-KO}* and *IL-6Rα^{Δ/Δ}* mice, labeled with α-CD3-TexasRed,
α-NK1.1-FITC, α-IL-6Rα-PE and α-TCRβ-PE/Cy7 antibodies. Contour blots
show T-cells in Q1 and NK-T cells in Q2 from (a) *IL-6Rα^{fl/fl}*, (b) *IL-6Rα^{T-KO}* and
(c) *IL-6Rα^{Δ/Δ}* mice. (d) IL-6Rα expression from Q2 NK-T cells is displayed as
an histogram overlay analyses, with the IL-6Rα positive subpopulation marked
by an arrowhead.

ulation still remains to be elucidated.

Moreover, our experiments also demonstrated that the protective effect of IL-6Rα
deficiencies on DEN-induced HCC can be pinpointed to NK-T cells. Only 35%
of those cells react to IL-6, as evidenced by IL-6Rα expression and subsequent
SOCS3-U-GFP expression. This specific NK-T cell subpopulation is of critical im-
portance for HCC development, and understanding the molecular mechanisms
how these cells promote HCC progression might lead to novel therapeutic ap-
proaches. Whether LIGHT is the effector molecule of this population remains elu-
sive.

3.7 Dre-mediated recombination in hepatocytes using AlbDre
mice

The SOCS3-U construct allows for the Dre-mediated excision of the SOCS3 CDS
from the activated *SOCS3-U^{Δ;rox;frt-GFP}* allele, in order to generate tissue specific
SOCS3 knock-outs. In order to analyze the function of SOCS3 in the liver, a hepato-
cyte specific Dre driver mouse line under control of the murine albumin promoter,
termed AlbDre, was generated. The albumin promoter has already been utilized
in generating the hepatocyte specific Cre driver line AlbCre [Postic *et al.*, 1999].
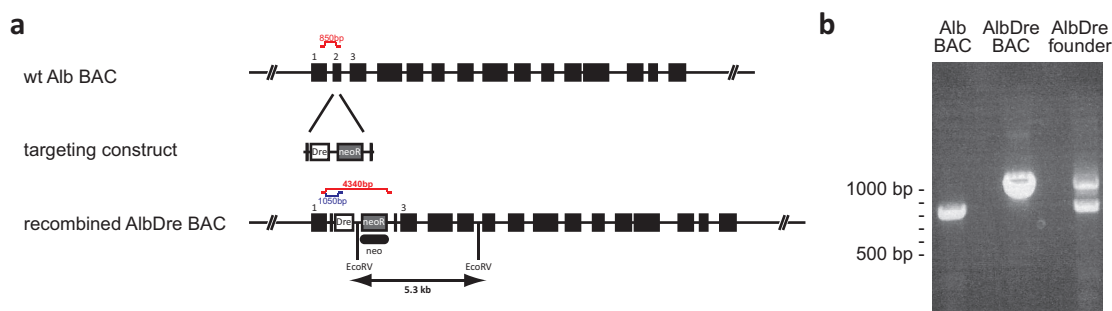
Figure 3.17: **Alb BAC recombination to generate AlbDre mice**
(a) Dre CDS and neomycin / kanamycin resistance cassette were amplified by PCR, containing 50 bp homology arms to exon 2 of the albumin BAC. Successful Red/ET recombination integrates the Dre CDS into exon 2, yielding a 1050 bp PCR fragment opposed to the 850 bp wt fragment. EcoRV digest for Southern-Blot analysis using the neo-probe hybridizing with the neomycin resistance cassette gives rise to a 5.3 kb fragment. (b) PCR analysis to identify positive AlbDre constructs, displaying unmodified Alb BAC, recombined AlbDre BAC and an AlbDre founder animal.

To generate transgenic AlbDre mice via BAC recombineering, a strategy was developed to integrate the Dre CDS and kanamycin resistance cassette into the BAC RP23-301A23, containing the albumin ORF. To this end, the pBAD vector, carrying the viral Redα and Redβ genes, was transformed into RP23-301A23 containing *E. coli*. Subsequently, Dre CDS and kanamycin resistance cassette were amplified by PCR from the pTE-Dre-neo/kana plasmid [provided by Tim Klöckener, University of Cologne], flanked by 50 bp 5' and 3' homologous regions to exon 2 of the Alb gene, and the PCR product transformed into the *E. coli* carrying the albumin BAC as well as pBAD plasmid. Successful homologous recombination with the albumin BAC integrates the Dre CDS into exon 2 of the albumin BAC (Fig. 3.17a). DNA from *E. coli* resistant to chloramphenicol (conveyed by the albumin BAC) and kanamycin (conveyed by the kanamycin resistance cassette introduced by successful recombineering) was isolated and subjected to PCR analysis to identify the wt BAC by an 850 bp band or AlbDre BAC by a 1050 bp band (Fig. 3.17b). Correct AlbDre BAC was purified, sequenced, linearized with PI-SceI and injected into the male pronucleus of a fertilized oocyte to produce AlbDre founder animals. AlbDre founder mice were crossed to *SOCS3-U$^{fl;rox;frt-GFP/wt}$* mice and their recombination efficiency was determined by PCR and Southern-blot analyses.

3.7.1 AlbDre recombines rox-sites specifically in hepatocytes

In order to address the functionality and tissue specificity of the albumin driven Dre line, its ability to recombine the SOCS3-U allele was assessed. To this end, *SOCS3-U$^{fl;rox;frt-GFP/wt}$* mice were crossed to *AlbDre$^{tg/wt}$* mice, with *SOCS3-U$^{fl;rox;frt-GFP/wt}$* as controls. 12w old animals were sacrificed and genomic DNA was extracted from numerous tissues to analyze Dre-mediated DNA recombination by PCR in the designated target tissue as well as off-target tissues (Fig. 3.18a). Further genomic DNA was digested with EcoRV and subjected to Southern-blot analysis. The rox-flanked SOCS3 coding sequence creates a 6.1 kb fragment, also harboring the neomycin resistance cassette and the IRES-GFP (Fig. 3.2c). Dre-mediated recombination excises SOCS3 CDS and decreases the detectable DNA fragment size to 5 kb. DNA fragments were labeled with a DNA probe specific for the neomycin resistance cassette, which also detects the neomycin/kanamycin resistance cassette in the AlbDre construct, where EcoRV digest creates a 5.3 kb fragment (Fig. 3.17a). Dre-mediated recombination of SOCS3-U was detected in hepatocytes with very high efficiency, whereas no recombination occurred in other tissues such as brain, white adipose tissue and skeletal muscle or in hepatocytes without Dre expression (Fig. 3.18b).

This confirms not only that the Dre recombinase is functional and exclusively active in hepatocytes, but also that the SOCS3-U allele can be used with AlbDre to produce a hepatocyte-specific SOCS3 knock-out mice.

3.7.2 Generating homozygous SOCS3^{L-KO} mice using AlbDre

To produce hepatocyte-specific, homozygous SOCS3 knock-out (*SOCS3^{L-KO}*) mice, *SOCS3-U$^{\Delta;rox;frt-GFP/wt}$* mice were crossed to *SOCS3-U$^{\Delta;rox;frt-GFP/wt}$;AlbDre$^{tg/wt}$* mice. To assess Dre-recombination efficiency, primary hepatocytes were isolated from *SOCS3-U$^{\Delta;rox;frt-GFP/\Delta;rox;frt-GFP}$* and *SOCS3-U$^{\Delta;rox;frt-GFP/\Delta;rox;frt-GFP}$;AlbDre$^{tg/wt}$* mice and 2×10^5 were stimulated *in vitro* with 50 ng/ml IL-6 for 0, 15, 30, 60 or 120 min.
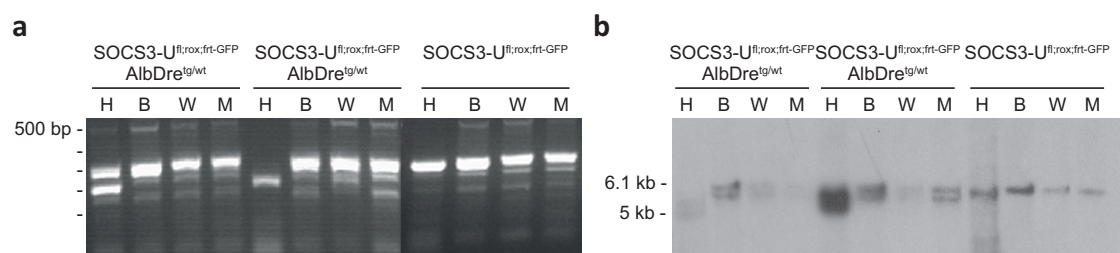
Figure 3.18: **AlbDre is exclusively active in hepatocytes**
(a) PCR analysis of isolated DNA from hepatocytes (H), brain (B), white adipose tissue (W) and muscle (M) of either $SOCS3\text{-}U^{fl;rox;frt\text{-}GFP/wt};AlbDre^{tg/wt}$ or $SOCS3\text{-}U^{fl;rox;frt\text{-}GFP/wt}$ mice. Dre-mediated recombination decreases the fragment size from 300 bp to 230 bp. (b) Southern-blot analysis of isolated DNA to verify PCR genotyping. Isolated DNA was digested with EcoRV and hybridized with the neo^{R} probe. EcoRV digest of the SOCS3-U allele gives rise to a 6.1 kb fragment (Fig. 3.2c). Dre-mediated recombination decreases the fragment size to 5 kb. The 5 kb fragment only appears in hepatocytes of $SOCS3\text{-}U^{fl;rox;frt\text{-}GFP/wt}$ / $AlbDre^{tg/wt}$ mice, neither in off-target tissues nor in hepatocytes in the absence of AlbDre. The band between 6.1 kb and 5 kb is derived from the AlbDre neomcin/kanamycin cassette, which also hybridizes with the neomycin probe.

IL-6 stimulation leads to phosphorylation of STAT3 after 15 min both in hepatocytes from $SOCS3\text{-}U^{\Delta;rox;frt\text{-}GFP/\Delta;rox;frt\text{-}GFP}$ as well as from $SOCS3\text{-}U^{\Delta;rox;frt\text{-}GFP/\Delta;rox;frt\text{-}GFP};AlbDre^{tg/wt}$ mice (Fig. 3.19a). $SOCS3\text{-}U^{\Delta;rox;frt\text{-}GFP/\Delta;rox;frt\text{-}GFP};AlbDre^{tg/wt}$ hepatocytes display even higher pSTAT3 levels throughout the course of stimulation, indicating the absence of negative feedback inhibition by SOCS3 in these hepatocytes. Furthermore, though progression of pSTAT3 and SOCS3 levels decrease over time in $SOCS3\text{-}U^{\Delta;rox;frt\text{-}GFP/\Delta;rox;frt\text{-}GFP}$ hepatocytes, phosphorylation of STAT3 in $SOCS3\text{-}U^{\Delta;rox;frt\text{-}GFP/\Delta;rox;frt\text{-}GFP};AlbDre^{tg/wt}$ hepatocytes is persistently elevated even after 120 min. Consistently, SOCS3 protein levels are reduced in $SOCS3\text{-}U^{\Delta;rox;frt\text{-}GFP/\Delta;rox;frt\text{-}GFP};AlbDre^{tg/wt}$ hepatocytes at all timepoints investigated. Moreover, analyzation of SOCS3 mRNA expression 0, 15 and 120 min after IL-6 stimulation from isolated wt as well as $SOCS3\text{-}U^{\Delta;rox;frt\text{-}GFP/\Delta;rox;frt\text{-}GFP};AlbDre^{tg/wt}$ primary hepatocyte RNA demonstrates a similar trend, but has to be repeated for several timepoints (Fig. 3.19b).

Taken together, recombination of rox-flanked SOCS3-U by AlbDre is occurring at a high efficiency, as evident by the strong decrease of SOCS3 protein levels upon
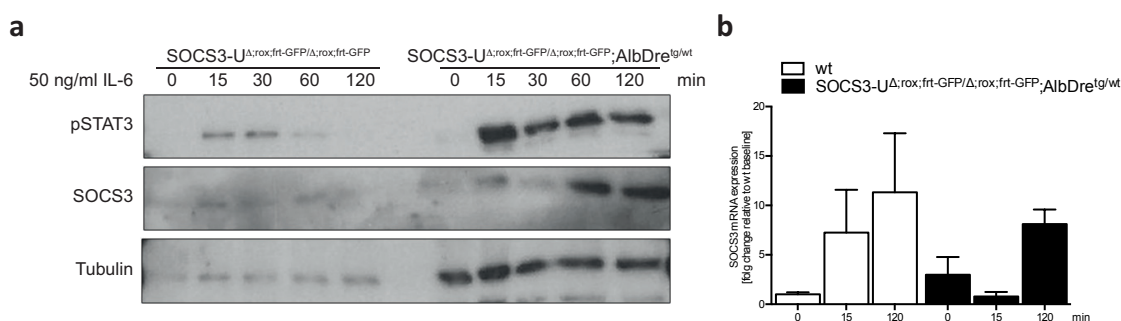
Figure 3.19: **Prolonged pSTAT3 activity in SOCS3$^{\text{L-KO}}$ mice**
(a) Western-blot analyses of primary hepatocytes isolated from *SOCS3-U$^{\Delta;rox;frt-GFP/\Delta;rox;frt-GFP}$* or *SOCS3-U$^{\Delta;rox;frt-GFP/\Delta;rox;frt-GFP}$;AlbDre$^{tg/wt}$* mice using pSTAT3, Tubulin and SOCS3 antibodies. Primary hepatocytes were stimulated with 50 ng/ml IL-6 for 0, 15, 30, 60 or 120 min. (b) RNA was isolated from *wt* or *SOCS3-U$^{\Delta;rox;frt-GFP/\Delta;rox;frt-GFP}$;AlbDre$^{tg/wt}$* primary hepaotcytes stimulated with 50 ng/ml IL-6 for 0, 15 or 120 min and SOCS3 mRNA expression of was analyzed by qPCR. Displayed are means ± SEM, n=3.

IL-6 stimulation in *SOCS3-U$^{\Delta;rox;frt-GFP/\Delta;rox;frt-GFP}$;AlbDre$^{tg/wt}$* hepatocytes. Consequently, STAT3 phosphorylation upon IL-6 stimulation is increased and prolonged in the absence of SOCS3 in hepatocytes. In conclusion, combination of AlbDre and *SOCS3-U$^{\Delta;rox;frt-GFP/\Delta;rox;frt-GFP}$* is suited to generate *SOCS3^{L-KO}* mice with a tissue-specific, functional SOCS3 knock-out exclusively in hepatocytes.

4 Discussion

Since the 1950's, dramatic changes in the global population structure led to the aggravation of existing and the emergence of novel health burdens world wide, a continous trend that has great impact on health both in industrialized as well as developing regions. The average life expectancy has increased from about 50 years in 1950 to around 70 today and will approach 80 in 2050 [UN Dept. of Economic and Social Affairs, 2002]. This development of an ageing population goes hand in hand with a global drop in fertility rate from 5 in 1950 to 2 in 2050. Consequently, a larger portion of the global population will be of advanced age, namely 20% will be above 60 years of age in 2050. A second trend is the ever increasing number of overweight and even obese individuals [Wang *et al.*, 2008], which is ironically the reason why the increase in life expectancy is expected to plateau in around 20 years. Since both ageing and obesity are known risk factors for cancer development, it is tempting to speculate that future populations will on average be older, heavier and suffer from a higher incidence of cancer. The underlying cellular and molecular mechanisms for ageing, obesity and cancer are numerous and so far only partially understood. Basic research uses animal models to investigate connections between different diseases, and increased inflammation lies at the heart of many pathologies, including obesity, cancer and even ageing. The novel inflammatory reporter mouse line SOCS3-U presented in this thesis can help unraveling hitherto unknown mechanisms in inflammation associated diseases. Moreover, SOCS3-U allows for the generation of conditional SOCS3 knock-outs by Dre-mediated recombination.

4.1 The SOCS3-U allele as a novel reporter tool

Cancer research in the last decades has profoundly deepened our understanding of tumor formation and shifted the paradigm of prerequisites towards a broader selection of hallmarks [Hanahan & Weinberg, 2011]. The pro-tumorigenic effect of the tumor microenvironment, encompassing endothelial, epithelial and mesenchymal cells in the near vicinity of cancer cells, as well as immune cells infiltrating the tumor site and the cytokines secreted by these immune cells, have more and more been focussed by recent research efforts.

Inflammatory signaling is largely carried out by secretion of cytokines, a broad category of proteins including interferons, interleukins, colony stimulating factors and chemokines. Immune cells release these factors into the developing tumor to induce apoptosis in cancerous cells and drive proliferation and differentiation in neighboring cells to compensate for the increased cell death. This continuous inflammation however will eventually have detrimental effects on the tumor sites, since deleterious byproducts like reactive oxygen species accumulate and/or because the increased proliferation leads to transformations of hitherto healthy cells [Bisgaard & Thorgeirsson, 1996; Maeda & Akaike, 1998]. Misguided actions of the immune system have therefore been recognized as a key player in cancerogenesis.

Although it is now known that inflammatory signaling by immune cells contributes to cancer formation, the various cancer entities differ immensely in respect to the exact inflammatory mediator, the source of this mediator and the target cell of the mediator. Thus, our understanding of the signaling machinery responsible for cancer formation in general is still very limited. This thesis therefore aimed at developing a reporter mouse line, which, through conditional gene targeting, should be universally applicable in a large variety of cancer models. The resulting SOCS3-U reporter mouse can visualize inflammatory signaling both *in vivo* and *in vitro* with high specificity.

4.1.1 Successful generation of SOCS3-U mice

The SOCS3-U reporter allele couples expression of either an IRES-driven eGFP or the firefly luciferase to expression of SOCS3, a negative feedback regulator of the JAK/STAT pathway in inflammatory signaling. SOCS3-U is targeted to the endogenous SOCS3 locus, to ensure that all regulatory elements of the SOCS3 promoter are applied to expression of SOCS3-U. Correct genomic targeting of the SOCS3-U allele was addressed by Southern-blot analyses, and could be confirmed for two ES-cell clones.

Genetically, SOCS3-U is designed as a knock-out first allele, and activity of SOCS3-U is dependent on Cre-mediated recombination. Upon activation, SOCS3 and an IRES-driven eGFP will be expressed from the SOCS3-U allele under the control of the endogenous SOCS3 promoter. Cre-mediated activation of SOCS3-U and resulting GFP activity after cytokine-stimulation of targeted ES-cells was analyzed with transfection of a Cre-expressing plasmid *in vitro* prior to injection of ES-cells into blastocysts. SOCS3-U ES-cells demonstrated reproducible but an overall weak GFP fluorescence upon cytokine stimulation. ES-cells in culture are kept pluripotent by addition of leukemia inhibitory factor (LIF), an IL-6-type cytokine inhibiting cell differentiation [Suman *et al.*, 2013]. LIF signals through a heterodimer of one LIF-Receptor β-chain and the common gp130 β-chain, activating the JAK/STAT pathway. The constant exposure of SOCS3-U ES-cells to LIF signaling results in high, basal levels of SOCS3 [Naka *et al.*, 1997], thereby compromising the SOCS3-GFP induction by cytokine stimulation and resulting in the rather low shift in GFP fluorescence.

4.1.2 *SOCS-U$^{fl;rox;frt-GFP/wt}$* mice show wt inflammation response

The precondition of Cre-mediated recombination to activate SOCS3-U and concomitantly expression of SOCS3 from the SOCS3-U allele necessitates that the off-target tissues are functionally SOCS3 haploinsufficient. In order to ensure that presence of the non activated *SOCS-U$^{fl;rox;frt-GFP}$* allele does not cause sig-

nificant aberrations in the inflammation response, primary hepatocytes from *SOCS-U*$^{fl;rox;frt-GFP/wt}$ mice were isolated and their response to IL-6 stimulation was compared to wild-type hepatocytes. IL-6 stimulation led to comparable phosphorylation of STAT3 and the resulting SOCS3 upregulation showed an equal capability to inhibit further pSTAT3 activity after induction of SOCS3. Thus, one SOCS3 allele can inhibit the JAK/STAT pathway as efficient as two alleles.

4.1.3 SOCS3-U visualizes inflammation in a Cre-dependent manner

Taken together, the novel SOCS3-U reporter mouse line allows for the visualization of numerous inflammatory processes *in vitro* and *in vivo*. SOCS3, and concomitantly also the eGFP or luciferase reporter respectively, is upregulated not only by IL-6 type cytokines or TNFα via NF-κB as classical inflammatory mediators, but also by leptin and insulin, opening up versatile possibilities to monitor metabolic processes. It is however noteworthy that whole-body SOCS3 haploinsufficiency conveys a certain level of protection from diet-induced obesity via an increased leptin sensitivity [Howard *et al.*, 2004].

Since the activity of SOCS3-U is conditionally controlled by Cre-mediated recombination, utilization of SOCS3-U can take full advantage of the wide array of available Cre-driver lines. Accordingly, SOCS3-U can be activated specifically in defined immune cell populations, neuronal cells or parenchymal tissues. Additionally, AAV-delivered Cre-recombinase or inducible Cre driver can activate SOCS3-U even in adult animals in a defined manner.

4.2 M2 TAMs attract T-cells to the colon upon AOM/DSS treatment

Colorectal cancer constitutes a major health burden worldwide, especially in industrialized countries, and predominantly develops as a consequence of chronic inflammation in the bowel. Chronic inflammation can be caused by chronic in-

fections, tobacco smoking or other pollutants, or dietary factors such as obesity. Patients already suffering from inflammatory bowel diseases, such as Crohn's disease or ulcerative colitis, have a strongly increased risk of developing colorectal cancer. Progression of colorectal cancer as a classic case of colitis associated cancerogenesis is recapitulated in the AOM/DSS mouse model [Tanaka *et al.*, 2003]. Injection of the pro-carcinogen AOM is coupled to supplementation of the drinking water with DSS, which is a strong inducer of colitis.

The cancer promoting effect of the AOM/DSS model can be abrogated in genetic mouse models, in which inflammatory signaling is disturbed. Deletion of IKKβ in cells of the myeloid lineage reduces the inflammatory tone and alleviates the tumor burden after AOM/DSS treatment [Greten *et al.*, 2004]. Experiments from our own lab demonstrate that abrogation of IL-6 signaling in IL-6Rα deficient mice (*IL-6R$\alpha^{\Delta/\Delta}$*) reduces colorectal tumor formation in the AOM/DSS model [Claudia Wunderlich, University of Cologne]. Furthermore, transcriptome analysis of *IL-6R$\alpha^{\Delta/\Delta}$* tumors revealed significant differences compared to IL-6Rα proficient tumors, such as an overall reduction in lymphocyte markers as well as decreased CCL20 and CCR6 expression. Additional data showed that loss of IL-6Rα on myeloid cells abrogates alternative macrophage activation towards the M2 subtype [Mauer *et al.*, 2014]. Collectively, these observations prompted the hypothesis that IL-6 signaling driven M2 macrophages, upon increased inflammation in the colon, express CCL20, which attract CCR6 expressing lymphocytes [Baba *et al.*, 1997; Hieshima *et al.*, 1997], promoting colorectal cancer development.

Utilization of *SOCS3-U$^{fl;rox;frt-GFP/wt}$;R26-fl-tdTomato$^{fl/wt}$;LysM-Cre$^{tg/wt}$* mice in the AOM/DSS model enabled the identification of M1 and M2 macrophages in order to elucidate the contribution of the respective subpopulations to colorectal cancer formation. Expression of tdTomato in LysM-Cre expressing myeloid cells resulted in red fluorescence both in M1 and M2 macrophages, whereas expression of eGFP from the SOCS3-U allele in LysM-Cre expressing myeloid cells however was dependent on stimulation of SOCS3. Hence, fluorescence activated cell sorting allowed

for the separation of tdTomato^{high};GFP^{low} M2-like and tdTomato^{high};GFP^{high} M1-like macrophages for in depth analysis.

SOCS3 is highly expressed in infiltrating macrophages [Liu *et al.*, 2008] and shows a strong correlation with M1 macrophages [Arnold *et al.*, 2014]. Data from this study now could demonstrate the absence of IL-6Rα expression in tdTomato^{high};GFP^{high} M1-like macrophages and a concomitant, unaltered IL-6Rα expression in tdTomato^{high};GFP^{low} M2-like macrophages, corroborating a polarized IL-6Rα expression in M2 macrophages and lack of IL-6Rα expression in M1 macrophages. Interestingly, CCL20 mRNA expression exhibited a similar pattern towards M2 macrophages, substantiating our initial hypothesis of M2 macrophages predominantly expressing CCL20 upon AOM/DSS treatment.

In addition to the converse CCL20 and IL-6Rα expression in M1- and M2-like macrophages, tdTomato^{high};GFP^{low} M2-like macrophages exhibited a strikingly elevated IL-17RA expression. Our initial hypothesis was that IL-6 drives CCL20 expression in macrophages. However, stimulation of BMDMs and qPCR of CCL20 led to undetectable CCL20 levels upon stimulation, thereby excluding IL-6 as an activator of CCL20 expression. Thus, we proposed that macrophage polarization towards M2 as already described leads to the susceptibility to express CCL20, by uprgulation of IL-17RA. IL-17RA is one of five IL-17 receptor subunits and forms heterodimers with IL-17RC, transducing signaling evoked by IL-17A and IL-17F, two of the six IL-17 cytokines, ligand binding [Gaffen, 2009]. IL-17A and IL-17F play a crucial role in recruitment and activation of immune cells, inducing the expression of pro-inflammatory cytokines and chemokines, including CCL20 [Iwakura *et al.*, 2011].

Thus, our current hypothesis is that IL-17 produced by T-cells activates CCL20 expression in IL-17RA expressing M2 macrophages and thereby creates a vicious cycle of inflammation that drives CRC development. Additionally, IL-17 can signal directly on intestinal epithelial cells, promoting cell growth and survival. It is intriguing to speculate that T$_H$17 and $\gamma\delta$T-cells release IL-17 cytokines with differ-

ent target cells, both acting in concert and driving colorectal cancer development. Further investigation of this hypothesis will lead to novel therapeutic strategies to combat the continuing spread of colorectal cancer in the coming years.

4.3 Activation of the tumor microenvironment in DEN induced HCC

Hepatocellular carcinoma account for 85-90% of primary liver cancers, representing a large global health burden, particularly in males of less developed countries [El-Serag, 2011]. HCC usually develops gradually from chronic hepatitis, through either dietary or alcoholically induced, steatotic liver into liver fibrosis, to liver cirrhosis and ultimately to HCC. Common to all the initial causes for HCC development is increased inflammation, marking HCC as an inflammation associated cancer. Persistent liver inflammation causes hepatocyte death, inducing a compensating hyperproliferation of neighboring hepatocytes, a driving force for cancerogenesis [Bisgaard & Thorgeirsson, 1996]. HCC development can be recapitulated in a mouse model of DEN injection into 12-15 days old, male mice, which develop tumors after 8 months [Vesselinovitch & Mihailovich, 1983]. Furthermore, 8 week old male mice can be injected with an acute dose of DEN, mimicking the increased inflammation occurring in the tumor initiation phase.

Abrogation of inflammatory signaling protects against DEN-induced HCC

Numerous observations implicate immune cell action and inflammatory signaling in HCC development. Abrogation of IL-6 signaling was demonstrated to protect from DEN-induced HCC formation, either in whole-body IL-6 knock-out [Park *et al.*, 2010] or by IL-6Rα deficiency (*IL-6Rα$^{\Delta/\Delta}$*) [Gruber *et al.*, 2013]. Kupffer cell derived IL-6 after hepatocyte death has been shown to aggravate HCC development, indicating a contribution of Kupffer cells to liver tumor formation [Naugler *et al.*, 2007]. Interestingly, contribution of IL-6 signaling to HCC formation does not

occur directly on hepatocytes, as IL-6Rα deficiency specifically in hepatocytes does not protect form DEN-induced HCC development; however, the protective effect of whole-body IL-6Rα deficiency is recapitulated in a T-cell specific IL-6Rα ablation model [Gruber, 2013]. Despite these observations of the influence of Kupffer cells as well as lymphocytes on hepatocellular carcinoma development, the exact contribution and interplay between the respective immune cell populations remains to be elucidated.

4.3.1 Unraveling macrophage subpopulations in DEN induced HCC using SOCS3-U

Tumor associated macrophages are important mediators of cancer-related inflammation and comprise a large part of infiltrating immune cells [Solinas *et al.*, 2009]. Consistently, signaling by macrophages has been implicated on numerous occasions with HCC development [Capece *et al.*, 2013]. IL-6 represents a critical inflammatory mediator of TAM signaling, in that TAM derived IL-6 promotes T_H17 expansion, which suppresses cytotoxic T-cell activity [Kuang *et al.*, 2010; Zhao *et al.*, 2011]. In addition to M1 and M2 macrophages, inflammatory signaling by liver resident Kupffer cells affects HCC formation. Interestingly, IL-6 signaling neither in infiltrating M1 nor in M2 macrophages contributes to DEN-induced HCC formation, as demonstrated by unaltered tumor formation in *IL-6Rα$^{fl/fl}$;LysM-Cre$^{tg/wt}$* mice, but might impact Kupffer cells, as they are not affected by LysM-Cre mediated recombination [Hume, 2011].

Although Kupffer cells are not affected by LysM-Cre expression, they still express classic marcophage markers such as F4/80 [Austyn & Gordon, 1981]. Isolation of non-parenchymal liver cells from *SOCS3-U$^{fl;rox;frt-GFP/wt}$;R26-fl-tdTomato$^{fl/wt}$;LysM-Cre$^{tg/wt}$* mice subjected to the chronic DEN model and subsequent labeling with an F4/80 antibody therefore allowed for the identification of tdTomato^{high};GFP^{high} M1 macrophages, tdTomato^{high};GFP^{low} M2 macrophages and tdTomato^{low};F4/80^{high} Kupffer cells.

Parallel transcriptome analysis of all three macrophage subpopulation after chronic DEN treatment should give novel insight into the crosstalk between myeloid cells, epithelial cells and lymphocytes in hepatocellular carcinomas. This task is still under investigation.

4.3.2 Acute DEN treatment induces IL-6Rα proficient NK-T cells

Previous data from our lab already demonstrated a central role for lymphocytes in HCC development in an IL-6 dependent manner, in that IL-6Rα deficiency on T-cells protects from DEN-induced HCC development [Gruber, 2013]. Increased liver steatosis upon CD-HFD feeding, mimicking a tumor development promoting environment, increases hepatic T-cell numbers, including NK-T cells as well as T_{reg}s, and drives elevated expression of IL-1, IL-17 and LIGHT [Wolf *et al.*, 2014]. NK-T cell secreted LIGHT has been demonstrated to be pivotal for hepatic lipid uptake in this context, ultimately constituting a driving force for HCC development.

Data from this study revealed additional molecular mechanisms linking active and NK-T cell function to DEN-induced HCC development. mRNA expression analysis of NPLCs isolated from *SOCS3-U$^{fl;rox;frt-GFP/wt}$;CD4-Cre$^{tg/wt}$* mice subjected to the acute DEN model demonstrated that approximately 35% of NK-T cells upregulate IL-6Rα upon DEN treatment, whereas non activated NK-T cells do not express IL-6Rα. In line with this experiment, analysis of NPLCs isolated from control and IL-6Rα deficient mice after acute DEN treatment substantiated an emergence of an IL-6Rα$^+$ NK-T cell subpopulation. Unexpectedly, LIGHT mRNA expression was significantly higher in the remaining IL-6Rα$^-$ NK-T cells subpopulation. It is however reasonable to assume that the alteration of LIGHT mRNA expression upon acute DEN treatment follows a similar mechanism, since increased IL-6 levels were previously demonstrated to be delayed after acute DEN injection [Gruber *et al.*, 2013].

Collectively, acute DEN injection separates hepatic NK-T cells into two subpop-

ulations, one IL-6Rα deficient population expressing LIGHT, and one IL-6Rα proficient population with an elusive function that promotes HCC development. It is intriguing to speculate that both populations function in concert with active effector T-cells to drive hepatocellular carcinoma initiation. Increased levels of IL-1 and IL-17 in the CD-HFD model indicate a possible role for T$_H$17 cells to be the respective effector T-cell population, corroborated by a TAM-derived IL-6 mediated T$_H$17 cell increase. Continuing analysis of the hitherto unidentified IL-6Rα expressing NK-T cell subpopulation, the upstream mediator of LIGHT expression by IL-6Rα deficient NK-T cells and additional hepatocellular target genes will give further insights into the intricate network of lymphocyte interaction in HCC development.

4.4 AlbDre is a new tissue-specific Dre-driver line

Genetic mouse models represent a cornerstone of basic research in the 21st century and are a constant source of discoveries with implications for applied research, pharmaceutical sciences and clinical trials. Efficient genetic analyses relies on specific genetic tools, to modify genes and study their impact on development, pathologies or maintenance of a functional orgnanism.

Conditional gene targeting, that is genetic modification using site specific recombinases, enables a wide array of possible gene modifications, including gene disruption, activation or overexpression [Rajewsky *et al.*, 1996]. Site specific recombination requires the modification of the target gene with recombinase target sites, depending on the desired effect after recombination. The two most common applications for site specific recombination are conditional gene knock-outs, where usually several exons are flanked by recombinase target sites and will be excised after recombination, or conditional knock-ins, where expression of the gene of interest is inhibited by a target site flanked transcriptional stop cassette until recombination activates gene expression. The Cre recombinase from bacteriophage P1 and the corresponding loxP recombination target sites have emerged as the primary site specific recombination system in the last two decades, combining high efficiency

with high versatility.

More sophisticated approaches in conditional gene targeting might need a second site specific recombination system with similar requirements concerning versatility and efficiency. A distinct recombination system can e.g. be used to simultaneously modify two different target alleles in one mouse, or to enhance the specificity of a construct by tandem application of both recombination systems. The Dre/rox site specific recombination system from bacteriophage D6 matches these criteria and can be utilized in parallel or in concert with Cre/loxP [Sauer & McDermott, 2004; Anastassiadis *et al.*, 2009]. This study aimed at creating a tissue-specific Dre-driver line, expressing the Dre-recombinase specifically in hepatocytes using the albumin (Alb) promoter.

The Alb promoter was chosen to express Dre-recombinase specifically in hepatocytes, as it has been already successfully applied to express Cre-recombinase [Postic *et al.*, 1999]. Alb encodes for serum albumin, a protein produced exclusively in the liver and secreted into the blood stream. Expression of the albumin promoter starts at embryonic day 9.5 (E9.5), and is increasing with full development of the liver [Kellendonk *et al.*, 2000]. Recombination efficiency in the liver of albumin-driven Cre-recombinase has been found to be 80%, with no recombination in any other tissue analyzed, while a closer analysis of target protein levels exclusively in hepatocytes after Alb-Cre mediated recombination revealed even a reduction by 95% [Postic *et al.*, 1999].

A BAC containing the albumin ORF and the complete promoter including all regulatory elements was used to generate the transgenic mouse line by recombineering in *E. coli* [Zhang *et al.*, 1998]. To this end, the Dre-recombinase CDS was amplified by PCR and introduced into the Alb-BAC by homologous recombination, mediated by the recombination system Redα and Redβ transformed into the BAC carrying bacteria. Successful integration of the Dre-recombinase CDS into exon 2 of the Alb ORF was verified by PCR and sequencing and the recombined AlbDre BAC injected into the male pronucleus of fertilized oocytes. Integration of

the recombined BAC occurs randomly and potentially multiple times, so that every positive founder mouse constitutes a separate transgenic mouse line, and recombination efficiency has to be determined both for the target tissue as well as off-target tissues.

The ability of AlbDre to recombine DNA *in vivo* was addressed in *SOCS3-U*$^{fl;rox;frt\text{-}GFP/wt}$*;AlbDre*$^{tg/wt}$ mice by Southern-Blot analysis. Genomic DNA was isolated from hepatocytes, brain tissue, white adipose tissue and muscle tissue, and recombined DNA was exclusively detected in hepatocellular DNA. The Southern-Blot analysis revealed a very high recombination efficiency for AlbDre, with at least 95% of the DNA being successfully recombined.

To use the AlbDre mouse to conditionally inactivate SOCS3 in hepatocytes, the *SOCS3-U*$^{fl;rox;frt\text{-}GFP}$ allele had to be activated, in order to determine the recombination efficiency of AlbDre on the protein level. Hence, hepatocytes from *SOCS3-U*$^{\Delta;rox;frt\text{-}GFP/\Delta;rox;frt\text{-}GFP}$ and *SOCS3-U*$^{\Delta;rox;frt\text{-}GFP/\Delta;rox;frt\text{-}GFP}$*;AlbDre*$^{tg/wt}$ (*SOCS3*$^{L\text{-}KO}$) mice were isolated and stimulated *ex vivo* with IL-6 to drive SOCS3 expression. *SOCS3*$^{L\text{-}KO}$-hepatocytes exhibited a significantly delayed upregulation of SOCS3 upon IL-6 stimulation, confirming a high recombination efficiency for AlbDre. Consistently, STAT3 phosphorylation was significantly prolonged in *SOCS3*$^{L\text{-}KO}$-hepatocytes. The eventual expression of SOCS3 even in *SOCS3*$^{L\text{-}KO}$-hepatocytes can be attributed to remaining hepatocytes, that have escaped Dre mediated recombination.

Taken together, a hepatocyte specific SOCS3 knock-out can be generated using *SOCS3-U*$^{\Delta;rox;frt\text{-}GFP/\Delta;rox;frt\text{-}GFP}$ and *AlbDre*$^{tg/wt}$ mice, which can be combined with an additional Cre-dependent knock-out of any gene of interest in another cell type.

5 Bibliography

AGGARWAL, SUDEEPTA, GHILARDI, NICO, XIE, MING-HONG, DE SAUVAGE, FREDERIC J, & GURNEY, AUSTIN L. 2003. Interleukin-23 promotes a distinct CD4 T cell activation state characterized by the production of interleukin-17. *Journal of biological chemistry*, **278**(3), 1910–1914. [16]

ALLAVENA, P, SICA, A, VECCHI, A, LOCATI, M, SOZZANI, S, & MANTOVANI, A. 2000. The chemokine receptor switch paradigm and dendritic cell migration: its significance in tumor tissues. *Immunological reviews*, **177**(Oct.), 141–149. [4]

ANASTASSIADIS, K, FU, J, PATSCH, C, HU, S, WEIDLICH, S, DUERSCHKE, K, BUCHHOLZ, F, EDENHOFER, FRANK, & STEWART, A F. 2009. Dre recombinase, like Cre, is a highly efficient site-specific recombinase in E. coli, mammalian cells and mice. *Disease models & mechanisms*, **2**(9-10), 508–515. [25, 26, 87]

ANDREWS, B J, PROTEAU, G A, BEATTY, L G, & SADOWSKI, P D. 1985. The FLP recombinase of the 2 micron circle DNA of yeast: interaction with its target sequences. *Cell*, **40**(4), 795–803. [23]

ARNOLD, CHRISTINA E, WHYTE, CLAIRE S, GORDON, PETER, BARKER, ROBERT N, REES, ANDREW J, & WILSON, HEATHER M. 2014. A critical role for suppressor of cytokine signalling 3 in promoting M1 macrophage activation and function in vitro and in vivo. *Immunology*, **141**(1), 96–110. [17, 82]

AUERNHAMMER, C J, BOUSQUET, C, & MELMED, S. 1999. Autoregulation of pituitary corticotroph SOCS-3 expression: characterization of the murine SOCS-3 promoter. *Proceedings of the national academy of sciences of the united states of america*, **96**(12), 6964–6969. [12]

AUSTIN, S, ZIESE, M, & STERNBERG, N. 1981. A novel role for site-specific recombination in maintenance of bacterial replicons. *Cell*, **25**(3), 729–736. [25]

AUSTYN, J M, & GORDON, S. 1981. F4/80, a monoclonal antibody directed specifically against the mouse macrophage. *European journal of immunology*, **11**(10), 805–815. [61, 84]

BABA, M, IMAI, T, NISHIMURA, M, KAKIZAKI, M, TAKAGI, S, HIESHIMA, K, NOMIYAMA, H, & YOSHIE, O. 1997. Identification of CCR6, the specific receptor for a novel lymphocyte-directed CC chemokine LARC. *Journal of biological chemistry*, **272**(23), 14893–14898. [58, 81]

BABON, JEFFREY J, & NICOLA, NICOS A. 2012. The biology and mechanism of action of suppressor of cytokine signaling 3. *Growth factors (chur, switzerland)*, **30**(4), 207–219. [12]

BABON, JEFFREY J, YAO, SHENGGEN, DESOUZA, DAVID P, HARRISON, CHRISTOPHER F, FABRI, LOUIS J, LIEPINSH, EDVARDS, SCROFANI, SERGIO D, BACA, MANUEL, & NORTON, RAYMOND S. 2005. Secondary structure assignment of mouse SOCS3 by NMR defines the domain boundaries and identifies an unstructured insertion in the SH2 domain. *The febs journal*, **272**(23), 6120–6130. [13]

BABON, JEFFREY J, SABO, JENNIFER K, ZHANG, JIAN-GUO, NICOLA, NICOS A, & NORTON, RAYMOND S. 2009. The SOCS box encodes a hierarchy of affinities for Cullin5: implications for ubiquitin ligase formation and cytokine signalling suppression. *Journal of molecular biology*, **387**(1), 162–174. [11]

BAO, LIDAO, FU, XUDONG, SI, MINGWEN, WANG, YI, MA, RUILIAN, REN, XIANHUA, & LV, HAIJUN. 2015. MicroRNA-185 Targets SOCS3 to Inhibit Beta-Cell Dysfunction in Diabetes. *Plos one*, **10**(2), e0116067. [14]

BELCHEVA, ANTOANETA, IRRAZABAL, THERGIORY, ROBERTSON, SUSAN J, STREUTKER, CATHERINE, MAUGHAN, HEATHER, RUBINO, STEPHEN, MORIYAMA, EDUARDO H, COPELAND, JULIA K, KUMAR, SACHIN, GREEN, BLERTA, GEDDES, KAORU, PEZO, ROSSANNA C, NAVARRE, WILLIAM W, MILOSE-VIC, MICHAEL, WILSON, BRIAN C, GIRARDIN, STEPHEN E, WOLEVER, THOMAS M S, EDELMANN, WINFRIED, GUTTMAN, DAVID S, PHILPOTT, DANA J, & MARTIN, ALBERTO. 2014. Gut microbial metabolism drives transformation of MSH2-deficient colon epithelial cells. *Cell*, **158**(2), 288–299. [9]

BELTEKI, GUSZTAV, GERTSENSTEIN, MARINA, OW, DAVID W, & NAGY, ANDRAS. 2003. Site-specific cassette exchange and germline transmission with mouse ES cells expressing φC31 integrase. *Nature biotechnology*, **21**(3), 321–324. [25]

BISGAARD, H C, & THORGEIRSSON, S S. 1996. Hepatic regeneration. The role of regeneration in pathogenesis of chronic liver diseases. *Clinics in laboratory medicine*, **16**(2), 325–339. [5, 78, 83]

BJØRBAEK, CHRISTIAN, ELMQUIST, J K, FRANTZ, J D, SHOELSON, S E, & FLIER, J S. 1998. Identification of SOCS-3 as a potential mediator of central leptin resistance. *Molecular cell*, **1**(4), 619–625. [12]

BJØRBAEK, CHRISTIAN, ELMQUIST, J K, EL-HASCHIMI, K, KELLY, J, AHIMA, R S, HILEMAN, S, & FLIER, J S. 1999. Activation of SOCS-3 messenger ribonucleic acid in the hypothalamus by ciliary neu-rotrophic factor. *Endocrinology*, **140**(5), 2035–2043. [12]

BOOSANI, CHANDRA S, & AGRAWAL, DEVENDRA K. 2015. Methylation and microRNA-mediated epigenetic regulation of SOCS3. *Molecular biology reports*, Feb., 1–20. [13]

BRANDA, CATHERINE S, & DYMECKI, SUSAN M. 2004. Talking about a revolution: The impact of site-specific recombinases on genetic analyses in mice. *Developmental cell*, **6**(1), 7–28. [23]

BRENDER, C, TANNAHILL, G M, JENKINS, B J, FLETCHER, J, COLUMBUS, R, SARIS, C J M, ERNST, M, NICOLA, N A, HILTON, D J, ALEXANDER, W S, & STARR, R. 2007. Suppressor of cytokine signaling 3 regulates CD8 T-cell proliferation by inhibition of interleukins 6 and 27. *Blood*, **110**(7), 2528–2536. [15]

BUCHHOLZ, F, RINGROSE, L, ANGRAND, P O, ROSSI, F, & STEWART, A F. 1996. Different thermostabil-ities of FLP and Cre recombinases: implications for applied site-specific recombination. *Nucleic acids research*, **24**(21), 4256–4262. [25]

BUCHHOLZ, F, ANGRAND, P O, & STEWART, A F. 1998. Improved properties of FLP recombinase evolved by cycling mutagenesis. *Nature biotechnology*, **16**(7), 657–662. [25]

CALLE, EUGENIA E, RODRIGUEZ, CARMEN, WALKER-THURMOND, KIMBERLY, & THUN, MICHAEL J. 2003. Overweight, obesity, and mortality from cancer in a prospectively studied cohort of U.S. adults. *The new england journal of medicine*, **348**(17), 1625–1638. [6]

CAO, WEI, YANG, YIQING, WANG, ZHENGYI, LIU, AILIAN, FANG, LEI, WU, FENGLAN, HONG, JIAN, SHI, YUFANG, LEUNG, STEWART, DONG, CHEN, & ZHANG, JINGWU Z. 2011. Leukemia Inhibitory Factor Inhibits T Helper 17 Cell Differentiation and Confers Treatment Effects of Neural Progenitor Cell Therapy in Autoimmune Disease. *Immunity*, **35**(2), 273–284. [16]

CAPECCHI, MARIO R. 2005. Essay: Gene targeting in mice: functional analysis of the mammalian genome for the twenty-first century. *Nature reviews genetics*, **6**(6), 507–512. [22]

CAPECE, DARIA, FISCHIETTI, MARIAFAUSTA, VERZELLA, DANIELA, GAGGIANO, AGATA, CICCIARELLI, GERMANA, TESSITORE, ALESSANDRA, ZAZZERONI, FRANCESCA, & ALESSE, EDOARDO. 2013. The inflammatory microenvironment in hepatocellular carcinoma: a pivotal role for tumor-associated macrophages. *Biomed research international*, **2013**(1), 187204–15. [84]

CHANG, PAMELA V, HAO, LIMING, OFFERMANNS, STEFAN, & MEDZHITOV, RUSLAN. 2014. The microbial metabolite butyrate regulates intestinal macrophage function via histone deacetylase inhibition. *Proceedings of the national academy of sciences of the united states of america*, **111**(6), 2247–2252. [9]

CHEN, Z, LAURENCE, A, KANNO, Y, PACHER-ZAVISIN, M, ZHU, B M, TATO, C, YOSHIMURA, A, HENNIGHAUSEN, L, & O'SHEA, J J. 2006. Selective regulatory function of Socs3 in the formation of IL-17-secreting T cells. *Proceedings of the national academy of sciences*, **103**(21), 8137–8142. [16]

CLAUSEN, B E, BURKHARDT, C, REITH, W, RENKAWITZ, R, & FÖRSTER, I. 1999. Conditional gene targeting in macrophages and granulocytes using LysMcre mice. *Transgenic research*, **8**(4), 265–277. [59]

COUSSENS, LISA M, & WERB, ZENA. 2002. Inflammation and cancer. *Nature*, **420**(6917), 860–867. [4]

CROKER, BEN A, KREBS, DANIELLE L, ZHANG, JIAN-GUO, WORMALD, SAM, WILLSON, TRACY A, STANLEY, EDOUARD G, ROBB, LORRAINE, GREENHALGH, CHRISTOPHER J, FÖRSTER, IRMGARD, CLAUSEN, BJÖRN E, NICOLA, NICOS A, METCALF, DONALD, HILTON, DOUGLAS J, ROBERTS, ANDREW W, & ALEXANDER, WARREN S. 2003. SOCS3 negatively regulates IL-6 signaling in vivo. *Nature immunology*, **4**(6), 540–545. [11]

DANESE, SILVIO, MALESCI, ALBERTO, & VETRANO, STEFANIA. 2011. Colitis-associated cancer: the dark side of inflammatory bowel disease. *Gut*, **60**(12), 1609–1610. [8]

DOGANCI, AYSEFA, EIGENBROD, TATJANA, KRUG, NORBERT, DE SANCTIS, GEORGE T, HAUSDING, MICHAEL, ERPENBECK, VEIT J, HADDAD, EL-BDAOUI, LEHR, HANS A, SCHMITT, EDGAR, BOPP, TOBIAS, KALLEN, KARL-J, HERZ, UDO, SCHMITT, STEFFEN, LUFT, CORNELIA, HECHT, OLAF, HOHLFELD, JENS M, ITO, HIROAKI, NISHIMOTO, NORIHIRO, YOSHIZAKI, KAZUYUKI, KISHIMOTO, TADAMITSU, ROSE-JOHN, STEFAN, RENZ, HARALD, NEURATH, MARKUS F, GALLE, PETER R, & FINOTTO, SUSETTA. 2005. The IL-6R alpha chain controls lung CD4+CD25+ Treg development and function during allergic airway inflammation in vivo. *The journal of clinical investigation*, **115**(2), 313–325. [16]

DONATO, F, TAGGER, A, GELATTI, U, PARRINELLO, G, BOFFETTA, P, ALBERTINI, A, DECARLI, A, TREVISI, P, RIBERO, M L, MARTELLI, C, PORRU, S, & NARDI, G. 2002. Alcohol and hepatocellular carcinoma: the effect of lifetime intake and hepatitis virus infections in men and women. *American journal of epidemiology*, **155**(4), 323–331. [4]

DVORAK, H F. 1986. Tumors: wounds that do not heal. Similarities between tumor stroma generation and wound healing. *The new england journal of medicine*, **315**(26), 1650–1659. [3]

EGWUAGU, CHARLES E, YU, CHENG-RONG, ZHANG, MEIFEN, MAHDI, RASHID M, KIM, STEPHEN J, & GERY, IGAL. 2002. Suppressors of cytokine signaling proteins are differentially expressed in Th1 and Th2 cells: implications for Th cell lineage commitment and maintenance. *Journal of immunology (baltimore, md : 1950)*, **168**(7), 3181–3187. [15]

EL-SERAG, HASHEM B. 2011. Hepatocellular carcinoma. *The new england journal of medicine*, **365**(12), 1118–1127. [4, 83]

EMANUELLI, B, PERALDI, P, FILLOUX, C, SAWKA-VERHELLE, D, HILTON, D, & VAN OBBERGHEN, E. 2000. SOCS-3 is an insulin-induced negative regulator of insulin signaling. *The journal of biological chemistry*, **275**(21), 15985–15991. [12]

EMANUELLI, B, PERALDI, P, FILLOUX, C, CHAVEY, C, FREIDINGER, K, HILTON, D J, HOTAMISLIGIL, G S, & VAN OBBERGHEN, E. 2001. SOCS-3 inhibits insulin signaling and is up-regulated in response to tumor necrosis factor-alpha in the adipose tissue of obese mice. *The journal of biological chemistry*, **276**(51), 47944–47949. [12, 20]

ENDO, HIROKI, HOSONO, KUNIHIRO, UCHIYAMA, TAKASHI, SAKAI, EIJI, SUGIYAMA, MICHIKO, TAKAHASHI, HIROKAZU, NAKAJIMA, NORIKO, WADA, KOICHIRO, TAKEDA, KIYOSHI, NAKAGAMA, HITOSHI, & NAKAJIMA, ATSUSHI. 2011. Leptin acts as a growth factor for colorectal tumours at stages subsequent to tumour initiation in murine colon carcinogenesis. *Gut*, **60**(10), 1363–1371. [21]

ENDO, T A, MASUHARA, M, YOKOUCHI, M, SUZUKI, R, SAKAMOTO, H, MITSUI, K, MATSUMOTO, A, TANIMURA, S, OHTSUBO, M, MISAWA, H, MIYAZAKI, T, LEONOR, N, TANIGUCHI, T, FUJITA, T, KANAKURA, Y, KOMIYA, S, & YOSHIMURA, A. 1997. A new protein containing an SH2 domain that inhibits JAK kinases. *Nature*, **387**(6636), 921–924. [10]

ERWIG, L P, KLUTH, D C, WALSH, G M, & REES, A J. 1998. Initial cytokine exposure determines function of macrophages and renders them unresponsive to other cytokines. *The journal of immunology*, **161**(4), 1983–1988. [17]

FAUSTO, N. 2000. Liver regeneration. *Journal of hepatology*, **32**(1 Suppl), 19–31. [5]

FELDMAN, DOUGLAS EDMUND, CHEN, CHIALIN, PUNJ, VASU, TSUKAMOTO, HIDEKAZU, & MACHIDA, KEIGO. 2012. Pluripotency factor-mediated expression of the leptin receptor (OB-R) links obesity to oncogenesis through tumor-initiating stem cells. *Proceedings of the national academy of sciences of the united states of america*, **109**(3), 829–834. [22]

FERLAY, JACQUES, SOERJOMATARAM, ISABELLE, DIKSHIT, RAJESH, ESER, SULTAN, MATHERS, COLIN, REBELO, MARISE, PARKIN, DONALD MAXWELL, FORMAN, DAVID, & BRAY, FREDDIE. 2015. Cancer incidence and mortality worldwide: sources, methods and major patterns in GLOBOCAN 2012. *International journal of cancer*, **136**(5), E359–86. [1, 2]

FONTENOT, JASON D, RASMUSSEN, JEFFREY P, GAVIN, MARC A, & RUDENSKY, ALEXANDER Y. 2005. A function for interleukin 2 in Foxp3-expressing regulatory T cells. *Nature immunology*, **6**(11), 1142–1151. [17]

FRIEDMAN, JEFFREY. 2014. 20 years of leptin: leptin at 20: an overview. *The journal of endocrinology*, **223**(1), T1–8. [19]

GAFFEN, SARAH L. 2009. Structure and signalling in the IL-17 receptor family. *Nature reviews immunology*, **9**(8), 556–567. [82]

GALIC, SANDRA, SACHITHANANDAN, NIRUPA, KAY, THOMAS W, & STEINBERG, GREGORY R. 2014. Suppressor of cytokine signalling (SOCS) proteins as guardians of inflammatory responses critical for regulating insulin sensitivity. *The biochemical journal*, **461**(2), 177–188. [11]

GÁLVEZ, JULIO. 2014. Role of Th17 Cells in the Pathogenesis of Human IBD. *Isrn inflammation*, **2014**(4), 928461–14. [60]

GAO, DONGNI, ZHAI, AIXIA, QIAN, JUN, LI, AIMEI, LI, YUJUN, SONG, WUQI, ZHAO, HONG, YU, XIN, WU, JING, ZHANG, QINGMENG, KAO, WENPING, WEI, LANLAN, ZHANG, FENGMIN, & ZHONG, ZHAOHUA. 2015. Down-regulation of suppressor of cytokine signaling 3 by miR-122 enhances interferon-mediated suppression of hepatitis B virus. *Antiviral research*, Mar. [13]

GARRETT, WENDY S. 2015. Cancer and the microbiota. *Science (new york, ny)*, **348**(6230), 80–86. [9]

GERMANO, GIOVANNI, ALLAVENA, PAOLA, & MANTOVANI, ALBERTO. 2008. Cytokines as a key component of cancer-related inflammation. *Cytokine*, **43**(3), 374–379. [4]

GOCHEVA, VASILENA, WANG, HAO-WEI, GADEA, BEDRICK B, SHREE, TANAYA, HUNTER, KAREN E, GARFALL, ALFRED L, BERMAN, TARA, & JOYCE, JOHANNA A. 2010. IL-4 induces cathepsin protease activity in tumor-associated macrophages to promote cancer growth and invasion. *Genes & development*, **24**(3), 241–255. [3]

GREEN, MICHAEL R, & SAMBROOK, JOSEPH. 2012. *Molecular Cloning: A Laboratory Manual*. 4th edn. Cold Spring Harbor Laboratory Press. [29]

GRETEN, FLORIAN R, ECKMANN, LARS, GRETEN, TIM F, PARK, JIN MO, LI, ZHI-WEI, EGAN, LAURENCE J, KAGNOFF, MARTIN F, & KARIN, MICHAEL. 2004. IKKbeta links inflammation and tumorigenesis in a mouse model of colitis-associated cancer. *Cell*, **118**(3), 285–296. [8, 81]

GRIVENNIKOV, SERGEI I, WANG, KEPENG, MUCIDA, DANIEL, STEWART, C ANDREW, SCHNABL, BERND, JAUCH, DOMINIK, TANIGUCHI, KOJI, YU, GUANN-YI, OSTERREICHER, CHRISTOPH H, HUNG, KENNETH E, DATZ, CHRISTIAN, FENG, YING, FEARON, ERIC R, OUKKA, MOHAMED, TESSAROLLO, LINO, COPPOLA, VINCENZO, YAROVINSKY, FELIX, CHEROUTRE, HILDE, ECKMANN, LARS, TRINCHIERI, GIORGIO, & KARIN, MICHAEL. 2012. Adenoma-linked barrier defects and microbial products drive IL-23/IL-17-mediated tumour growth. *Nature*, **491**(7423), 254–258. [9]

GRUBER, SABINE. 2013 (Nov.). *The Role of Interleukin 6 and Obesity in the Development of Hepatocellular Carcinoma*. Ph.D. thesis, University of Cologne. [7, 63, 65, 84, 85]

GRUBER, SABINE, STRAUB, BEATE K, ACKERMANN, P JUSTUS, WUNDERLICH, CLAUDIA M, MAUER, JAN, SEEGER, JENS M, BÜNING, HILDEGARD, HEUKAMP, LUKAS, KASHKAR, HAMID, SCHIRMACHER, PETER, BRÜNING, JENS C, & WUNDERLICH, F THOMAS. 2013. Obesity promotes liver carcinogenesis via Mcl-1 stabilization independent of IL-6Rα signaling. *Cell reports*, **4**(4), 669–680. [7, 63, 65, 83, 85]

HAAN, SERGE, FERGUSON, PAUL, SOMMER, ULRIKE, HIREMATH, MEENA, MCVICAR, DANIEL W, HEINRICH, PETER C, JOHNSTON, JAMES A, & CACALANO, NICHOLAS A. 2003. Tyrosine phosphorylation disrupts elongin interaction and accelerates SOCS3 degradation. *The journal of biological chemistry*, **278**(34), 31972–31979. [13]

HAGEMANN, THORSTEN, LAWRENCE, TOBY, MCNEISH, IAIN, CHARLES, KELLIE A, KULBE, HAGEN, THOMPSON, RICHARD G, ROBINSON, STEPHEN C, & BALKWILL, FRANCES R. 2008. "Re-educating"tumor-associated macrophages by targeting NF-kappaB. *The journal of experimental medicine*, **205**(6), 1261–1268. [4]

HAJDU, STEVEN I. 2011. A note from history: landmarks in history of cancer, part 1. *Cancer*, **117**(5), 1097–1102. [1]

HANAHAN, DOUGLAS, & WEINBERG, ROBERT A. 2011. Hallmarks of cancer: the next generation. *Cell*, **144**(5), 646–674. [1, 78]

HARRINGTON, LAURIE E, HATTON, ROBIN D, MANGAN, PAUL R, TURNER, HENRIETTA, MURPHY, THERESA L, MURPHY, KENNETH M, & WEAVER, CASEY T. 2005. Interleukin 17-producing CD4+ effector T cells develop via a lineage distinct from the T helper type 1 and 2 lineages. *Nature immunology*, **6**(11), 1123–1132. [16]

HATTING, M, SPANNBAUER, M, PENG, J, AL MASAOUDI, M, SELLGE, G, NEVZOROVA, Y A, GASSLER, N, LIEDTKE, C, CUBERO, F J, & TRAUTWEIN, C. 2015. Lack of gp130 expression in hepatocytes attenuates tumor progression in the DEN model. *Cell death and disease*, **6**(3), e1667. [21]

HE, BIAO, YOU, LIANG, UEMATSU, KAZUTSUGU, ZANG, KELING, XU, ZHIDONG, LEE, AMIE Y, COSTELLO, JOSEPH F, MCCORMICK, FRANK, & JABLONS, DAVID M. 2003. SOCS-3 is frequently silenced by hypermethylation and suppresses cell growth in human lung cancer. *Proceedings of the national academy of sciences of the united states of america*, **100**(24), 14133–14138. [14]

HENNIGHAUSEN, L, WALL, R J, TILLMANN, U, LI, M, & FURTH, P A. 1995. Conditional gene expression in secretory tissues and skin of transgenic mice using the MMTV-LTR and the tetracycline responsive system. *Journal of cellular biochemistry*, **59**(4), 463–472. [16]

HIESHIMA, K, IMAI, T, OPDENAKKER, G, VAN DAMME, J, KUSUDA, J, TEI, H, SAKAKI, Y, TAKATSUKI, K, MIURA, R, YOSHIE, O, & NOMIYAMA, H. 1997. Molecular cloning of a novel human CC chemokine liver and activation-regulated chemokine (LARC) expressed in liver. Chemotactic activity for lymphocytes and gene localization on chromosome 2. *Journal of biological chemistry*, **272**(9), 5846–5853. [58, 81]

HILTON, D J, RICHARDSON, R T, ALEXANDER, W S, VINEY, E M, WILLSON, T A, SPRIGG, N S, STARR, R, NICHOLSON, S E, METCALF, D, & NICOLA, N A. 1998. Twenty proteins containing a C-terminal SOCS box form five structural classes. *Proceedings of the national academy of sciences of the united states of america*, **95**(1), 114–119. [10]

HOTAMISLIGIL, G S, SHARGILL, N S, & SPIEGELMAN, B M. 1993. Adipose expression of tumor necrosis factor-alpha: direct role in obesity-linked insulin resistance. *Science (new york, ny)*, **259**(5091), 87–91. [4, 20]

HOWARD, JANE K, CAVE, BELINDA J, OKSANEN, LAURA J, TZAMELI, IPHIGENIA, BJØRBAEK, CHRISTIAN, & FLIER, JEFFREY S. 2004. Enhanced leptin sensitivity and attenuation of diet-induced obesity in mice with haploinsufficiency of Socs3. *Nature medicine*, **10**(7), 734–738. [20, 80]

HUME, DAVID A. 2011. Applications of myeloid-specific promoters in transgenic mice support in vivo imaging and functional genomics but do not support the concept of distinct macrophage and dendritic cell lineages or roles in immunity. *Journal of leukocyte biology*, **89**(4), 525–538. [61, 84]

IMAM, J S, BUDDAVARAPU, K, LEE-CHANG, J S, GANAPATHY, S, CAMOSY, C, CHEN, Y, & RAO, M K. 2010. MicroRNA-185 suppresses tumor growth and progression by targeting the Six1 oncogene in human cancers. *Oncogene*, **29**(35), 4971–4979. [14]

INAGAKI-OHARA, K, MAYUZUMI, H, KATO, S, MINOKOSHI, Y, OTSUBO, T, KAWAMURA, Y I, DOHI, T, MATSUZAKI, G, & YOSHIMURA, A. 2014. Enhancement of leptin receptor signaling by SOCS3 deficiency induces development of gastric tumors in mice. *Oncogene*, **33**(1), 74–84. [22]

ISLAM, K B M SAIFUL, FUKIYA, SATORU, HAGIO, MASAHITO, FUJII, NOBUYUKI, ISHIZUKA, SATOSHI, OOKA, TADASUKE, OGURA, YOSHITOSHI, HAYASHI, TETSUYA, & YOKOTA, ATSUSHI. 2011. Bile acid is a host factor that regulates the composition of the cecal microbiota in rats. *Gastroenterology*, **141**(5), 1773–1781. [9]

IWAKURA, YOICHIRO, ISHIGAME, HARUMICHI, SAIJO, SHINOBU, & NAKAE, SUSUMU. 2011. Functional specialization of interleukin-17 family members. *Immunity*, **34**(2), 149–162. [82]

JESS, TINE, GAMBORG, MICHAEL, MATZEN, PETER, MUNKHOLM, PIA, & SØRENSEN, THORKILD I A. 2005. Increased risk of intestinal cancer in Crohn's disease: a meta-analysis of population-based cohort studies. *The american journal of gastroenterology*, **100**(12), 2724–2729. [8]

JIANG, RUNQIU, XIA, YONGXIANG, LI, JUN, DENG, LEI, ZHAO, LIANG, SHI, JIAN, WANG, XUEHAO, & SUN, BEICHENG. 2010. High expression levels of IKKalpha and IKKbeta are necessary for the malignant properties of liver cancer. *International journal of cancer*, **126**(5), 1263–1274. [5]

JORDAN, SABINE D, KRÜGER, MARKUS, WILLMES, DIANA M, REDEMANN, NORA, WUNDERLICH, F THOMAS, BRÖNNEKE, HELLA S, MERKWIRTH, CARSTEN, KASHKAR, HAMID, OLKKONEN, VESA M, BÖTTGER, THOMAS, BRAUN, THOMAS, SEIBLER, JOST, & BRÜNING, JENS C. 2011. Obesity-induced overexpression of miRNA-143 inhibits insulin-stimulated AKT activation and impairs glucose metabolism. *Nature cell biology*, **13**(4), 434–446. [32]

JORGENSEN, S B, O'NEILL, H M, SYLOW, L, HONEYMAN, J, HEWITT, K A, PALANIVEL, R, FULLERTON, M D, OBERG, L, BALENDRAN, A, GALIC, S, VAN DER POEL, C, TROUNCE, I A, LYNCH, G S, SCHERTZER, J D, & STEINBERG, G R. 2012. Deletion of Skeletal Muscle SOCS3 Prevents Insulin Resistance in Obesity. *Diabetes*, **62**(1), 56–64. [20]

KAKUMU, S, SHINAGAWA, T, ISHIKAWA, T, YOSHIOKA, K, WAKITA, T, ITO, Y, TAKAYANAGI, M, & IDA, N. 1991. Serum interleukin 6 levels in patients with chronic hepatitis B. *The american journal of gastroenterology*, **86**(12), 1804–1808. [4]

KAMURA, TAKUMI, MAENAKA, KATSUMI, KOTOSHIBA, SHUHEI, MATSUMOTO, MASAKI, KOHDA, DAISUKE, CONAWAY, RONALD C, CONAWAY, JOAN WELIKY, & NAKAYAMA, KEIICHI I. 2004. VHL-box and SOCS-box domains determine binding specificity for Cul2-Rbx1 and Cul5-Rbx2 modules of ubiquitin ligases. *Genes & development*, **18**(24), 3055–3065. [10]

KARATSOREOS, ILIA N, THALER, JOSHUA P, BORGLAND, STEPHANIE L, CHAMPAGNE, FRANCES A, HURD, YASMIN L, & HILL, MATTHEW N. 2013. Food for thought: hormonal, experiential, and neural influences on feeding and obesity. *The journal of neuroscience : the official journal of the society for neuroscience*, **33**(45), 17610–17616. [19]

KELLENDONK, C, OPHERK, C, ANLAG, K, SCHÜTZ, G, & TRONCHE, F. 2000. Hepatocyte-specific expression of Cre recombinase. *Genesis (new york, ny : 2000)*, **26**(2), 151–153. [87]

Kershaw, Nadia J, Murphy, James M, Liau, Nicholas P D, Varghese, Leila N, Laktyushin, Artem, Whitlock, Eden L, Lucet, Isabelle S, Nicola, Nicos A, & Babon, Jeffrey J. 2013. SOCS3 binds specific receptor-JAK complexes to control cytokine signaling by direct kinase inhibition. *Nature structural & molecular biology*, **20**(4), 469–476. [12]

Khoruts, A, Stahnke, L, McClain, C J, Logan, G, & Allen, J I. 1991. Circulating tumor necrosis factor, interleukin-1 and interleukin-6 concentrations in chronic alcoholic patients. *Hepatology (baltimore, md.)*, **13**(2), 267–276. [4]

Kievit, Paul, Howard, Jane K, Badman, Michael K, Balthasar, Nina, Coppari, Roberto, Mori, Hiroyuki, Lee, Charlotte E, Elmquist, Joel K, Yoshimura, Akihiko, & Flier, Jeffrey S. 2006. Enhanced leptin sensitivity and improved glucose homeostasis in mice lacking suppressor of cytokine signaling-3 in POMC-expressing cells. *Cell metabolism*, **4**(2), 123–132. [19]

Kinjyo, I. 2006. Loss of SOCS3 in T helper cells resulted in reduced immune responses and hyperproduction of interleukin 10 and transforming growth factor- 1. *Journal of experimental medicine*, **203**(4), 1021–1031. [16]

Klisch, Bruno. 2006. Generierung Cre-aktivierbarer Transgene zur konditionalen Expression in der Maus. M.Phil. thesis, University of Cologne. [32, 50, II]

Köntgen, F, & Stewart, C L. 1993. Simple screening procedure to detect gene targeting events in embryonic stem cells. *Methods in enzymology*, **225**, 878–890. [34]

Köntgen, F, Süss, G, Stewart, C, Steinmetz, M, & Bluethmann, H. 1993. Targeted disruption of the MHC class II Aa gene in C57BL/6 mice. *International immunology*, **5**(8), 957–964. [51]

Kornfeld, Jan-Wilhelm, Baitzel, Catherina, Könner, A Christine, Nicholls, Hayley T, Vogt, Merly C, Herrmanns, Karolin, Scheja, Ludger, Haumaitre, Cécile, Wolf, Anna M, Knippschild, Uwe, Seibler, Jost, Cereghini, Silvia, Heeren, Joerg, Stoffel, Markus, & Brüning, Jens C. 2013. Obesity-induced overexpression of miR-802 impairs glucose metabolism through silencing of Hnf1b. *Nature*, **494**(7435), 115. [14]

Kortylewski, Marcin, Xin, Hong, Kujawski, Maciej, Lee, Heehyoung, Liu, Yong, Harris, Timothy, Drake, Charles, Pardoll, Drew, & Yu, Hua. 2009. Regulation of the IL-23 and IL-12 balance by Stat3 signaling in the tumor microenvironment. *Cancer cell*, **15**(2), 114–123. [4]

Kuang, Dong-Ming, Peng, Chen, Zhao, Qiyi, Wu, Yan, Chen, Min-Shan, & Zheng, Limin. 2010. Activated monocytes in peritumoral stroma of hepatocellular carcinoma promote expansion of memory T helper 17 cells. *Hepatology (baltimore, md.)*, **51**(1), 154–164. [84]

Kühn, R, Schwenk, F, Aguet, M, & Rajewsky, K. 1995. Inducible gene targeting in mice. *Science (new york, ny)*, **269**(5229), 1427–1429. [22]

Lang, Roland, Pauleau, Anne-Laure, Parganas, Evan, Takahashi, Yutaka, Mages, Jörg, Ihle, James N, Rutschman, Robert, & Murray, Peter J. 2003. SOCS3 regulates the plasticity of gp130 signaling. *Nature immunology*, **4**(6), 546–550. [12]

Lee, P P, Fitzpatrick, D R, Beard, C, Jessup, H K, Lehar, S, Makar, K W, Pérez-Melgosa, M, Sweetser, M T, Schlissel, M S, Nguyen, S, Cherry, S R, Tsai, J H, Tucker, S M, Weaver, W M, Kelso, A, Jaenisch, R, & Wilson, C B. 2001. A critical role for Dnmt1 and DNA methylation in T cell development, function, and survival. *Immunity*, **15**(5), 763–774. [66]

Li, Q, Wang, J-X, He, Y-Q, Feng, C, Zhang, X-J, Sheng, J-Q, & Li, P-F. 2014. MicroRNA-185 regulates chemotherapeutic sensitivity in gastric cancer by targeting apoptosis repressor with caspase recruitment domain. *Cell death and disease*, **5**(4), e1197. [14]

Li, Yi, Deuring, Jasper, Peppelenbosch, Maikel P, Kuipers, Ernst J, de Haar, Colin, & van der Woude, C Janneke. 2012. IL-6-induced DNMT1 activity mediates SOCS3 promoter hypermethylation in ulcerative colitis-related colorectal cancer. *Carcinogenesis*, **33**(10), 1889–1896. [13]

Liu, Ming, Lang, Nan, Chen, Xiangzhen, Tang, Qiulin, Liu, Surui, Huang, Juan, Zheng, Yi, & Bi, Feng. 2011. miR-185 targets RhoA and Cdc42 expression and inhibits the proliferation potential of human colorectal cells. *Cancer letters*, **301**(2), 151–160. [14]

Liu, Wen-bin, Ao, Lin, Zhou, Zi-yuan, Cui, Zhi-hong, Zhou, Yan-hong, Yuan, Xiao-yan, Xiang, Yun-long, Cao, Jia, & Liu, Jin-yi. 2010. CpG island hypermethylation of multiple tumor suppressor genes associated with loss of their protein expression during rat lung carcinogenesis induced by 3-methylcholanthrene and diethylnitrosamine. *Biochemical and biophysical research communications*, **402**(3), 507–514. [14]

Liu, Yu, Stewart, Keith N, Bishop, Eileen, Marek, Carylyn J, Kluth, David C, Rees, Andrew J, & Wilson, Heather M. 2008. Unique expression of suppressor of cytokine signaling 3 is essential for classical macrophage activation in rodents in vitro and in vivo. *Journal of immunology (baltimore, md : 1950)*, **180**(9), 6270–6278. [17, 82]

Livak, K J, & Schmittgen, T D. 2001. Analysis of relative gene expression data using real-time quantitative PCR and the 2(-Delta Delta C(T)) Method. *Methods (san diego, calif)*, **25**(4), 402–408. [41]

Louis, Petra, Hold, Georgina L, & Flint, Harry J. 2014. The gut microbiota, bacterial metabolites and colorectal cancer. *Nature reviews microbiology*, **12**(10), 661–672. [8]

Luedde, Tom, Beraza, Naiara, Kotsikoris, Vasileios, van Loo, Geert, Nenci, Arianna, De Vos, Rita, Roskams, Tania, Trautwein, Christian, & Pasparakis, Manolis. 2007. Deletion of NEMO/IKKgamma in liver parenchymal cells causes steatohepatitis and hepatocellular carcinoma. *Cancer cell*, **11**(2), 119–132. [5]

Ma, Ning, Wang, Xidi, Qiao, Yu, Li, Fuyuan, Hui, Yang, Zou, Chaoxia, Jin, Jianfeng, Lv, Guixiang, Peng, Yahui, Wang, Lujing, Huang, Hui, Zhou, Lingyun, Zheng, Xiaofei, & Gao, Xu. 2011. Coexpression of an intronic microRNA and its host gene reveals a potential role for miR-483-5p as an IGF2 partner. *Molecular and cellular endocrinology*, **333**(1), 96–101. [14]

Madisen, Linda, Zwingman, Theresa A, Sunkin, Susan M, Oh, Seung Wook, Zariwala, Hatim A, Gu, Hong, Ng, Lydia L, Palmiter, Richard D, Hawrylycz, Michael J, Jones, Allan R, Lein, Ed S, & Zeng, Hongkui. 2010. A robust and high-throughput Cre reporting and characterization system for the whole mouse brain. *Nature neuroscience*, **13**(1), 133–140. [59]

Maeda, H, & Akaike, T. 1998. Nitric oxide and oxygen radicals in infection, inflammation, and cancer. *Biochemistry*, **63**(7), 854–865. [3, 78]

Maeda, Shin, Kamata, Hideaki, Luo, Jun-Li, Leffert, Hyam, & Karin, Michael. 2005. IKKβ Couples Hepatocyte Death to Cytokine-Driven Compensatory Proliferation that Promotes Chemical Hepatocarcinogenesis. *Cell*, **121**(7), 977–990. [5]

MALAGUARNERA, M, DI FAZIO, I, LAURINO, A, FERLITO, L, ROMANO, M, & TROVATO, B A. 1997. Serum interleukin 6 concentrations in chronic hepatitis C patients before and after interferon-alpha treatment. *International journal of clinical pharmacology and therapeutics*, **35**(9), 385–388. [4]

MANTOVANI, ALBERTO. 2007. Cancer: an infernal triangle. *Nature*, **448**(7153), 547–548. [5]

MANTOVANI, ALBERTO, SOZZANI, SILVANO, LOCATI, MASSIMO, ALLAVENA, PAOLA, & SICA, ANTONIO. 2002. Macrophage polarization: tumor-associated macrophages as a paradigm for polarized M2 mononuclear phagocytes. *Trends in immunology*, **23**(11), 549–555. [4]

MANTOVANI, ALBERTO, ALLAVENA, PAOLA, SOZZANI, SILVANO, VECCHI, ANNUNCIATA, LOCATI, MASSIMO, & SICA, ANTONIO. 2004. Chemokines in the recruitment and shaping of the leukocyte infiltrate of tumors. *Seminars in cancer biology*, **14**(3), 155–160. [3]

MAO, X, FUJIWARA, Y, & ORKIN, S H. 1999. Improved reporter strain for monitoring Cre recombinase-mediated DNA excisions in mice. *Proceedings of the national academy of sciences of the united states of america*, **96**(9), 5037–5042. [38]

MATSUMOTO, AKIRA, SEKI, YOH-ICHI, WATANABE, RYOSUKE, HAYASHI, KATSUHIKO, JOHNSTON, JAMES A, HARADA, YOHSUKE, ABE, RYO, YOSHIMURA, AKIHIKO, & KUBO, MASATO. 2003. A role of suppressor of cytokine signaling 3 (SOCS3/CIS3/SSI3) in CD28-mediated interleukin 2 production. *Journal of experimental medicine*, **197**(4), 425–436. [15]

MATSUMURA, YUMIKO, KOBAYASHI, TAKASHI, ICHIYAMA, KENJI, YOSHIDA, RYOKO, HASHIMOTO, MASAYUKI, TAKIMOTO, TOMOHITO, TANAKA, KENTARO, CHINEN, TAKATOSHI, SHICHITA, TAKASHI, WYSS-CORAY, TONY, SATO, KATSUAKI, & YOSHIMURA, AKIHIKO. 2007. Selective expansion of foxp3-positive regulatory T cells and immunosuppression by suppressors of cytokine signaling 3-deficient dendritic cells. *Journal of immunology (baltimore, md : 1950)*, **179**(4), 2170–2179. [17]

MAUER, JAN, CHAURASIA, BHAGIRATH, GOLDAU, JULIA, VOGT, MERLY C, RUUD, JOHAN, NGUYEN, KHOA D, THEURICH, SEBASTIAN, HAUSEN, A CHRISTINE, SCHMITZ, JOEL, BRÖNNEKE, HELLA S, ESTEVEZ, EMMA, ALLEN, TAMARA L, MESAROS, ANDREA, PARTRIDGE, LINDA, FEBBRAIO, MARK A, CHAWLA, AJAY, WUNDERLICH, F THOMAS, & BRÜNING, JENS C. 2014. Signaling by IL-6 promotes alternative activation of macrophages to limit endotoxemia and obesity-associated resistance to insulin. *Nature immunology*, **15**(5), 423–430. [59, 81]

MORI, HIROYUKI, HANADA, REIKO, HANADA, TOSHIKATSU, AKI, DAISUKE, MASHIMA, RYUICHI, NISHINAKAMURA, HITOMI, TORISU, TAKEHIRO, CHIEN, KENNETH R, YASUKAWA, HIDEO, & YOSHIMURA, AKIHIKO. 2004. Socs3 deficiency in the brain elevates leptin sensitivity and confers resistance to diet-induced obesity. *Nature medicine*, **10**(7), 739–743. [19]

MORIWAKI, ATSUSHI, INOUE, HIROMASA, NAKANO, TAKAKO, MATSUNAGA, YUKO, MATSUNO, YUKIKO, MATSUMOTO, TAKAFUMI, FUKUYAMA, SATORU, KAN-O, KEIKO, MATSUMOTO, KOICHIRO, TSUDA-EGUCHI, MIYUKI, NAGAKUBO, DAISUKE, YOSHIE, OSAMU, YOSHIMURA, AKIHIKO, KUBO, MASATO, & NAKANISHI, YOICHI. 2011. T cell treatment with small interfering RNA for suppressor of cytokine signaling 3 modulates allergic airway responses in a murine model of asthma. *American journal of respiratory cell and molecular biology*, **44**(4), 448–455. [16]

MOSSER, DAVID M, & EDWARDS, JUSTIN P. 2008. Exploring the full spectrum of macrophage activation. *Nature reviews immunology*, **8**(12), 958–969. [17]

Mouse Genome Sequencing Consortium, Waterston, Robert H, Lindblad-Toh, Kerstin, Birney, Ewan, Rogers, Jane, Abril, Josep F, Agarwal, Pankaj, Agarwala, Richa, Ainscough, Rachel, Alexandersson, Marina, An, Peter, Antonarakis, Stylianos E, Attwood, John, Baertsch, Robert, Bailey, Jonathon, Barlow, Karen, Beck, Stephan, Berry, Eric, Birren, Bruce, Bloom, Toby, Bork, Peer, Botcherby, Marc, Bray, Nicolas, Brent, Michael R, Brown, Daniel G, Brown, Stephen D, Bult, Carol, Burton, John, Butler, Jonathan, Campbell, Robert D, Carninci, Piero, Cawley, Simon, Chiaromonte, Francesca, Chinwalla, Asif T, Church, Deanna M, Clamp, Michele, Clee, Christopher, Collins, Francis S, Cook, Lisa L, Copley, Richard R, Coulson, Alan, Couronne, Olivier, Cuff, James, Curwen, Val, Cutts, Tim, Daly, Mark, David, Robert, Davies, Joy, Delehaunty, Kimberly D, Deri, Justin, Dermitzakis, Emmanouil T, Dewey, Colin, Dickens, Nicholas J, Diekhans, Mark, Dodge, Sheila, Dubchak, Inna, Dunn, Diane M, Eddy, Sean R, Elnitski, Laura, Emes, Richard D, Eswara, Pallavi, Eyras, Eduardo, Felsenfeld, Adam, Fewell, Ginger A, Flicek, Paul, Foley, Karen, Frankel, Wayne N, Fulton, Lucinda A, Fulton, Robert S, Furey, Terrence S, Gage, Diane, Gibbs, Richard A, Glusman, Gustavo, Gnerre, Sante, Goldman, Nick, Goodstadt, Leo, Grafham, Darren, Graves, Tina A, Green, Eric D, Gregory, Simon, Guigó, Roderic, Guyer, Mark, Hardison, Ross C, Haussler, David, Hayashizaki, Yoshihide, Hillier, LaDeana W, Hinrichs, Angela, Hlavina, Wratko, Holzer, Timothy, Hsu, Fan, Hua, Axin, Hubbard, Tim, Hunt, Adrienne, Jackson, Ian, Jaffe, David B, Johnson, L Steven, Jones, Matthew, Jones, Thomas A, Joy, Ann, Kamal, Michael, Karlsson, Elinor K, Karolchik, Donna, Kasprzyk, Arkadiusz, Kawai, Jun, Keibler, Evan, Kells, Cristyn, Kent, W James, Kirby, Andrew, Kolbe, Diana L, Korf, Ian, Kucherlapati, Raju S, Kulbokas, Edward J, Kulp, David, Landers, Tom, Leger, J P, Leonard, Steven, Letunic, Ivica, Levine, Rosie, Li, Jia, Li, Ming, Lloyd, Christine, Lucas, Susan, Ma, Bin, Maglott, Donna R, Mardis, Elaine R, Matthews, Lucy, Mauceli, Evan, Mayer, John H, McCarthy, Megan, McCombie, W Richard, McLaren, Stuart, McLay, Kirsten, McPherson, John D, Meldrim, Jim, Meredith, Beverley, Mesirov, Jill P, Miller, Webb, Miner, Tracie L, Mongin, Emmanuel, Montgomery, Kate T, Morgan, Michael, Mott, Richard, Mullikin, James C, Muzny, Donna M, Nash, William E, Nelson, Joanne O, Nhan, Michael N, Nicol, Robert, Ning, Zemin, Nusbaum, Chad, O'Connor, Michael J, Okazaki, Yasushi, Oliver, Karen, Overton-Larty, Emma, Pachter, Lior, Parra, Genís, Pepin, Kymberlie H, Peterson, Jane, Pevzner, Pavel, Plumb, Robert, Pohl, Craig S, Poliakov, Alex, Ponce, Tracy C, Ponting, Chris P, Potter, Simon, Quail, Michael, Reymond, Alexandre, Roe, Bruce A, Roskin, Krishna M, Rubin, Edward M, Rust, Alistair G, Santos, Ralph, Sapojnikov, Victor, Schultz, Brian, Schultz, Jörg, Schwartz, Matthias S, Schwartz, Scott, Scott, Carol, Seaman, Steven, Searle, Steve, Sharpe, Ted, Sheridan, Andrew, Shownkeen, Ratna, Sims, Sarah, Singer, Jonathan B, Slater, Guy, Smit, Arian, Smith, Douglas R, Spencer, Brian, Stabenau, Arne, Stange-Thomann, Nicole, Sugnet, Charles, Suyama, Mikita, Tesler, Glenn, Thompson, Johanna, Torrents, David, Trevaskis, Evanne, Tromp, John, Ucla, Catherine, Ureta-Vidal, Abel, Vinson, Jade P, Von Niederhausern, Andrew C, Wade, Claire M, Wall, Melanie, Weber, Ryan J, Weiss, Robert B, Wendl, Michael C, West, Anthony P, Wetterstrand, Kris, Wheeler, Raymond, Whelan, Simon, Wierzbowski, Jamey, Willey, David, Williams, Sophie, Wilson, Richard K, Winter, Eitan, Worley, Kim C, Wyman, Dudley, Yang, Shan, Yang, Shiaw-Pyng, Zdobnov, Evgeny M, Zody, Michael C, & Lander, Eric S. 2002. Initial sequencing and comparative analysis of the mouse genome. *Nature*, **420**(6915), 520–562. [22]

Muyrers, J P, Zhang, Y, Testa, G, & Stewart, A F. 1999. Rapid modification of bacterial artificial

chromosomes by ET-recombination. *Nucleic acids research*, **27**(6), 1555–1557. [27, 33]

NAKA, T, NARAZAKI, M, HIRATA, M, MATSUMOTO, T, MINAMOTO, S, AONO, A, NISHIMOTO, N, KAJITA, T, TAGA, T, YOSHIZAKI, K, AKIRA, S, & KISHIMOTO, T. 1997. Structure and function of a new STAT-induced STAT inhibitor. *Nature*, **387**(6636), 924–929. [10, 79]

NAKAYA, M, HASHIMOTO, M, NAKAGAWA, R, WAKABAYASHI, Y, ISHIZAKI, T, TAKADA, I, KOMAI, K, YOSHIDA, H, & YOSHIMURA, A. 2009. SOCS3 in T and NKT Cells Negatively Regulates Cytokine Production and Ameliorates ConA-Induced Hepatitis. *The journal of immunology*, **183**(11), 7047–7053. [18]

NAUGLER, WILLSCOTT E, SAKURAI, TOSHIHARU, KIM, SUNHWA, MAEDA, SHIN, KIM, KYOUNGHYUN, ELSHARKAWY, AHMED M, & KARIN, MICHAEL. 2007. Gender disparity in liver cancer due to sex differences in MyD88-dependent IL-6 production. *Science (new york, ny)*, **317**(5834), 121–124. [5, 61, 83]

NICHOLSON, S E, DE SOUZA, D, FABRI, L J, CORBIN, J, WILLSON, T A, ZHANG, J G, SILVA, A, ASIMAKIS, M, FARLEY, A, NASH, A D, METCALF, D, HILTON, D J, NICOLA, N A, & BACA, M. 2000. Suppressor of cytokine signaling-3 preferentially binds to the SHP-2-binding site on the shared cytokine receptor subunit gp130. *Proceedings of the national academy of sciences of the united states of america*, **97**(12), 6493–6498. [11]

NIEMAND, CLAUDIA, NIMMESGERN, ARIANE, HAAN, SERGE, FISCHER, PATRICK, SCHAPER, FRED, ROSSAINT, ROLF, HEINRICH, PETER C, & MÜLLER-NEWEN, GERHARD. 2003. Activation of STAT3 by IL-6 and IL-10 in primary human macrophages is differentially modulated by suppressor of cytokine signaling 3. *The journal of immunology*, **170**(6), 3263–3272. [12]

NISH, SIMONE A, SCHENTEN, DOMINIK, WUNDERLICH, F THOMAS, POPE, SCOTT D, GAO, YAN, HOSHI, NAMIKO, YU, SHUANG, YAN, XITING, LEE, HEUNG KYU, PASMAN, LESLEY, BRODSKY, IGOR, YORDY, BRIAN, ZHAO, HONGYU, BRÜNING, JENS, & MEDZHITOV, RUSLAN. 2014. T cell-intrinsic role of IL-6 signaling in primary and memory responses. *elife*, **3**, e01949. [7]

NIWA, YASUHARU, KANDA, HIROAKI, SHIKAUCHI, YUKO, SAIURA, AKIO, MATSUBARA, KENICHI, KITAGAWA, TOMOYUKI, YAMAMOTO, JUNJI, KUBO, TAKAHIKO, & YOSHIKAWA, HIROHIDE. 2005. Methylation silencing of SOCS-3 promotes cell growth and migration by enhancing JAK/STAT and FAK signalings in human hepatocellular carcinoma. *Oncogene*, **24**(42), 6406–6417. [14]

O'CONNOR, JASON C, SHERRY, CHRISTINA L, GUEST, CHRISTOPHER B, & FREUND, GREGORY G. 2007. Type 2 diabetes impairs insulin receptor substrate-2-mediated phosphatidylinositol 3-kinase activity in primary macrophages to induce a state of cytokine resistance to IL-4 in association with overexpression of suppressor of cytokine signaling-3. *The journal of immunology*, **178**(11), 6886–6893. [18]

OGATA, H, CHINEN, T, YOSHIDA, T, KINJYO, I, TAKAESU, G, SHIRAISHI, H, IIDA, M, KOBAYASHI, T, & YOSHIMURA, A. 2006a. Loss of SOCS3 in the liver promotes fibrosis by enhancing STAT3-mediated TGF-beta1 production. *Oncogene*, **25**(17), 2520–2530. [21]

OGATA, HISANOBU, KOBAYASHI, TAKASHI, CHINEN, TAKATOSHI, TAKAKI, HIROMI, SANADA, TAKAHITO, MINODA, YASUMASA, KOGA, KEIKO, TAKAESU, GIICHI, MAEHARA, YOSHIHIKO, IIDA, MITSUO, & YOSHIMURA, AKIHIKO. 2006b. Deletion of the SOCS3 gene in liver parenchymal cells promotes hepatitis-induced hepatocarcinogenesis. *Gastroenterology*, **131**(1), 179–193. [18, 20]

PALANIVEL, R, FULLERTON, M D, GALIC, S, HONEYMAN, J, HEWITT, K A, JORGENSEN, S B, & STEINBERG, G R. 2012. Reduced Socs3 expression in adipose tissue protects female mice against obesity-induced insulin resistance. *Diabetologia*, **55**(11), 3083–3093. [20]

PARK, EEK JOONG, LEE, JUN HEE, YU, GUANN-YI, HE, GUOBIN, ALI, SYED RAZA, HOLZER, RYAN G, OSTERREICHER, CHRISTOPH H, TAKAHASHI, HIROYUKI, & KARIN, MICHAEL. 2010. Dietary and Genetic Obesity Promote Liver Inflammation and Tumorigenesis by Enhancing IL-6 and TNF Expression. *Cell*, **140**(2), 197–208. [7, 83]

PARK, HEON, LI, ZHAOXIA, YANG, XUEXIAN O, CHANG, SEON HEE, NURIEVA, ROZA, WANG, YI-HONG, WANG, YING, HOOD, LEROY, ZHU, ZHOU, TIAN, QIANG, & DONG, CHEN. 2005. A distinct lineage of CD4 T cells regulates tissue inflammation by producing interleukin 17. *Nature immunology*, **6**(11), 1133–1141. [16]

PEITZ, MICHAEL, PFANNKUCHE, KURT, RAJEWSKY, KLAUS, & EDENHOFER, FRANK. 2002. Ability of the hydrophobic FGF and basic TAT peptides to promote cellular uptake of recombinant Cre recombinase: a tool for efficient genetic engineering of mammalian genomes. *Proceedings of the national academy of sciences*, **99**(7), 4489–4494. [36]

PIKARSKY, ELI, PORAT, RINNAT M, STEIN, ILAN, ABRAMOVITCH, RINAT, AMIT, SHARON, KASEM, SHAFIKA, GUTKOVICH-PYEST, ELENA, URIELI-SHOVAL, SIMCHA, GALUN, EITHAN, & BEN-NERIAH, YINON. 2004. NF-kappaB functions as a tumour promoter in inflammation-associated cancer. *Nature*, **431**(7007), 461–466. [5]

PILLEMER, BRENDAN B L, XU, HUI, ORISS, TIMOTHY B, QI, ZENGBIAO, & RAY, ANURADHA. 2007. Deficient SOCS3 expression in CD4+CD25+FoxP3+ regulatory T cells and SOCS3-mediated suppression of Treg function. *European journal of immunology*, **37**(8), 2082–2089. [16]

POSTIC, C, SHIOTA, M, NISWENDER, K D, JETTON, T L, CHEN, Y, MOATES, J M, SHELTON, K D, LINDNER, J, CHERRINGTON, A D, & MAGNUSON, M A. 1999. Dual roles for glucokinase in glucose homeostasis as determined by liver and pancreatic beta cell-specific gene knock-outs using Cre recombinase. *Journal of biological chemistry*, **274**(1), 305–315. [71, 87]

QIN, HONGWEI, WANG, LANFANG, FENG, TING, ELSON, CHARLES O, NIYONGERE, SANDRINE A, LEE, SUN JUNG, REYNOLDS, STEPHANIE L, WEAVER, CASEY T, ROARTY, KEVIN, SERRA, ROSA, BENVENISTE, ETTY N, & CONG, YINGZI. 2009. TGF-beta promotes Th17 cell development through inhibition of SOCS3. *Journal of immunology (baltimore, md : 1950)*, **183**(1), 105. [16]

QIN, HONGWEI, HOLDBROOKS, ANDREW T, LIU, YUDONG, REYNOLDS, STEPHANIE L, YANAGISAWA, LORA L, & BENVENISTE, ETTY N. 2012. SOCS3 deficiency promotes M1 macrophage polarization and inflammation. *Journal of immunology (baltimore, md : 1950)*, **189**(7), 3439–3448. [18]

RAJEWSKY, K, GU, H, KÜHN, R, BETZ, U A, MÜLLER, W, ROES, J, & SCHWENK, F. 1996. Conditional gene targeting. *The journal of clinical investigation*, **98**(3), 600–603. [22, 86]

RAYMOND, CHRISTOPHER S, & SORIANO, PHILIPPE. 2007. High-Efficiency FLP and ΦC31 Site-Specific Recombination in Mammalian Cells. *Plos one*, **2**(1), e162. [25]

RENEHAN, ANDREW G, TYSON, MARGARET, EGGER, MATTHIAS, HELLER, RICHARD F, & ZWAHLEN, MARCEL. 2008. Body-mass index and incidence of cancer: a systematic review and meta-analysis of prospective observational studies. *Lancet*, **371**(9612), 569–578. [21]

RIGBY, R J, SIMMONS, J G, GREENHALGH, C J, ALEXANDER, W S, & LUND, P K. 2007. Suppressor of cytokine signaling 3 (SOCS3) limits damage-induced crypt hyper-proliferation and inflammation-associated tumorigenesis in the colon. *Oncogene*, **26**(33), 4833–4841. [21]

ROBERTS, A W, ROBB, L, RAKAR, S, HARTLEY, L, CLUSE, L, NICOLA, N A, METCALF, D, HILTON, D J, & ALEXANDER, W S. 2001. Placental defects and embryonic lethality in mice lacking suppressor of cytokine signaling 3. *Proceedings of the national academy of sciences*, **98**(16), 9324–9329. [14, 54]

ROEDIGER, W E, MOORE, J, & BABIDGE, W. 1997. Colonic sulfide in pathogenesis and treatment of ulcerative colitis. *Digestive diseases and sciences*, **42**(8), 1571–1579. [9]

ROGERS, S, WELLS, R, & RECHSTEINER, M. 1986. Amino acid sequences common to rapidly degraded proteins: the PEST hypothesis. *Science (new york, ny)*, **234**(4774), 364–368. [13]

ROMAIN, MÉLISSA, TALEB, SORAYA, DALLOZ, MARION, PONNUSWAMY, PADMAPRIYA, ESPOSITO, BRUNO, PÉREZ, NICOLAS, WANG, YU, YOSHIMURA, AKIHIKO, TEDGUI, ALAIN, & MALLAT, ZIAD. 2013. Over-expression of SOCS3 in T lymphocytes leads to impaired interleukin-17 production and severe aortic aneurysm formation in mice–brief report. *Arteriosclerosis, thrombosis, and vascular biology*, **33**(3), 581–584. [16]

RU, PENG, STEELE, ROBERT, HSUEH, EDDY C, & RAY, RATNA B. 2011. Anti-miR-203 Upregulates SOCS3 Expression in Breast Cancer Cells and Enhances Cisplatin Chemosensitivity. *Genes & cancer*, **2**(7), 720–727. [14]

SACHITHANANDAN, NIRUPA, FAM, BARBARA C, FYNCH, STACEY, DZAMKO, NICOLAS, WATT, MATTHEW J, WORMALD, SAM, HONEYMAN, JANE, GALIC, SANDRA, PROIETTO, JOSEPH, ANDRIKOPOU-LOS, SOFIANOS, HEVENER, ANDREA L, KAY, THOMAS W H, & STEINBERG, GREGORY R. 2010. Liver-specific suppressor of cytokine signaling-3 deletion in mice enhances hepatic insulin sensitivity and lipogenesis resulting in fatty liver and obesity1. *Hepatology (baltimore, md.)*, **52**(5), 1632–1642. [20]

SAKURAI, TOSHIHARU, HE, GUOBIN, MATSUZAWA, ATSUSHI, YU, GUANN-YI, MAEDA, SHIN, HARDIMAN, GARY, & KARIN, MICHAEL. 2008. Hepatocyte necrosis induced by oxidative stress and IL-1 alpha release mediate carcinogen-induced compensatory proliferation and liver tumorigenesis. *Cancer cell*, **14**(2), 156–165. [5]

SASAKI, ATSUO, INAGAKI-OHARA, KYOKO, YOSHIDA, TAKAFUMI, YAMANAKA, ATSUSHI, SASAKI, MIKA, YASUKAWA, HIDEO, KOROMILAS, ANTONIS E, & YOSHIMURA, AKIHIKO. 2003. The N-terminal trun-cated isoform of SOCS3 translated from an alternative initiation AUG codon under stress con-ditions is stable due to the lack of a major ubiquitination site, Lys-6. *The journal of biological chemistry*, **278**(4), 2432–2436. [13]

SAUER, BRIAN, & MCDERMOTT, JEFFREY. 2004. DNA recombination with a heterospecific Cre ho-molog identified from comparison of the pac-c1 regions of P1-related phages. *Nucleic acids re-search*, **32**(20), 6086–6095. [25, 87]

SCHENTEN, DOMINIK, NISH, SIMONE A, YU, SHUANG, YAN, XITING, LEE, HEUNG KYU, BRODSKY, IGOR, PASMAN, LESLEY, YORDY, BRIAN, WUNDERLICH, F THOMAS, BRÜNING, JENS C, ZHAO, HONGYU, & MEDZHITOV, RUSLAN. 2014. Signaling through the adaptor molecule MyD88 in CD4+ T cells is required to overcome suppression by regulatory T cells. *Immunity*, **40**(1), 78–90. [7]

SCHOPPMANN, SEBASTIAN F, BIRNER, PETER, STÖCKL, JOHANNES, KALT, ROMANA, ULLRICH, ROBERT, CAUCIG, CAROLA, KRIEHUBER, ERNST, NAGY, KATALIN, ALITALO, KARI, & KERJASCHKI, DONTSCHO. 2002. Tumor-associated macrophages express lymphatic endothelial growth factors and are related to peritumoral lymphangiogenesis. *The american journal of pathology*, **161**(3), 947–956. [4]

SCHWENK, F, BARON, U, & RAJEWSKY, K. 1995. A cre-transgenic mouse strain for the ubiquitous deletion of loxP-flanked gene segments including deletion in germ cells. *Nucleic acids research*, **23**(24), 5080–5081. [55]

SEKI, YOH-ICHI, INOUE, HIROMASA, NAGATA, NAOKO, HAYASHI, KATSUHIKO, FUKUYAMA, SATORU, MATSUMOTO, KOICHIRO, KOMINE, OKIRU, HAMANO, SHINJIRO, HIMENO, KUNISUKE, INAGAKI-OHARA, KYOKO, CACALANO, NICHOLAS, O'GARRA, ANNE, OSHIDA, TADAHILO, SAITO, HIROHISA, JOHNSTON, JAMES A, YOSHIMURA, AKIHIKO, & KUBO, MASATO. 2003. SOCS-3 regulates onset and maintenance of T(H)2-mediated allergic responses. *Nature medicine*, **9**(8), 1047–1054. [15]

SENN, J J, KLOVER, P J, NOWAK, I A, ZIMMERS, T A, KONIARIS, L G, FURLANETTO, R W, & MOONEY, R A. 2003. Suppressor of Cytokine Signaling-3 (SOCS-3), a Potential Mediator of Interleukin-6-dependent Insulin Resistance in Hepatocytes. *Journal of biological chemistry*, **278**(16), 13740–13746. [20]

SHERMAN, MORRIS. 2005. Hepatocellular carcinoma: epidemiology, risk factors, and screening. *Seminars in liver disease*, **25**(2), 143–154. [4]

SMITH, PATRICK M, HOWITT, MICHAEL R, PANIKOV, NICOLAI, MICHAUD, MONIA, GALLINI, CAREY ANN, BOHLOOLY-Y, MOHAMMAD, GLICKMAN, JONATHAN N, & GARRETT, WENDY S. 2013. The microbial metabolites, short-chain fatty acids, regulate colonic Treg cell homeostasis. *Science (new york, ny)*, **341**(6145), 569–573. [9]

SOLINAS, G, GERMANO, G, MANTOVANI, A, & ALLAVENA, P. 2009. Tumor-associated macrophages (TAM) as major players of the cancer-related inflammation. *Journal of leukocyte biology*, **86**(5), 1065–1073. [84]

STARR, R, WILLSON, T A, VINEY, E M, MURRAY, L J, RAYNER, J R, JENKINS, B J, GONDA, T J, ALEXANDER, W S, METCALF, D, NICOLA, N A, & HILTON, D J. 1997. A family of cytokine-inducible inhibitors of signalling. *Nature*, **387**(6636), 917–921. [10, 12]

STEPPAN, CLAIRE M, WANG, JUAN, WHITEMAN, EILEEN L, BIRNBAUM, MORRIS J, & LAZAR, MITCHELL A. 2005. Activation of SOCS-3 by resistin. *Molecular and cellular biology*, **25**(4), 1569–1575. [12]

STERNBERG, N, & HAMILTON, D. 1981. Bacteriophage P1 site-specific recombination. I. Recombination between loxP sites. *Journal of molecular biology*, **150**(4), 467–486. [23]

STRÖHLE, PETER. 2012 (Jan.). *The role of inflammatory mediators in the development of insulin resistance and hepatocellular carcinoma*. Ph.D. thesis, University of Cologne. [5]

SUMAN, PANKAJ, MALHOTRA, SUDHA SARYU, & GUPTA, SATISH KUMAR. 2013. LIF-STAT signaling and trophoblast biology. *Jak-stat*, **2**(4), e25155. [79]

TAKAHASHI, YUKARI, FORREST, ALISTAIR R R, MAENO, EMI, HASHIMOTO, TAKEHIRO, DAUB, CARSTEN O, & YASUDA, JUN. 2009. MiR-107 and MiR-185 can induce cell cycle arrest in human non small cell lung cancer cell lines. *Plos one*, **4**(8), e6677. [14]

TANAKA, TAKUJI, KOHNO, HIROYUKI, SUZUKI, RIKAKO, YAMADA, YASUHIRO, SUGIE, SHIGEYUKI, & MORI, HIDEKI. 2003. A novel inflammation-related mouse colon carcinogenesis model induced by azoxymethane and dextran sodium sulfate. *Cancer science*, **94**(11), 965–973. [8, 81]

THANGARAJU, MUTHUSAMY, CRESCI, GAIL A, LIU, KEBIN, ANANTH, SUDHA, GNANAPRAKASAM, JAYA P, BROWNING, DARREN D, MELLINGER, JOHN D, SMITH, SYLVIA B, DIGBY, GREGORY J, LAMBERT, NEVIN A, PRASAD, PUTTUR D, & GANAPATHY, VADIVEL. 2009. GPR109A is a G-protein-coupled receptor for the bacterial fermentation product butyrate and functions as a tumor suppressor in colon. *Cancer research*, **69**(7), 2826–2832. [9]

TORISU, TAKEHIRO, SATO, NAOICHI, YOSHIGA, DAIGO, KOBAYASHI, TAKASHI, YOSHIOKA, TOMOKO, MORI, HIROYUKI, IIDA, MITSUO, & YOSHIMURA, AKIHIKO. 2007. The dual function of hepatic SOCS3 in insulin resistance in vivo. *Genes to cells : devoted to molecular & cellular mechanisms*, **12**(2), 143–154. [20]

UEKI, K, KONDO, T, TSENG, Y H, & KAHN, C R. 2004a. Central role of suppressors of cytokine signaling proteins in hepatic steatosis, insulin resistance, and the metabolic syndrome in the mouse. *Proceedings of the national academy of sciences*, **101**(28), 10422–10427. [20]

UEKI, KOHJIRO, KONDO, TATSUYA, & KAHN, C RONALD. 2004b. Suppressor of cytokine signaling 1 (SOCS-1) and SOCS-3 cause insulin resistance through inhibition of tyrosine phosphorylation of insulin receptor substrate proteins by discrete mechanisms. *Molecular and cellular biology*, **24**(12), 5434–5446. [20]

UN DEPT. OF ECONOMIC AND SOCIAL AFFAIRS. 2002. *World Population Ageing, 1950-2050*. United Nations Publications. [77]

VAJDIC, CLAIRE M, & VAN LEEUWEN, MARINA T. 2009. Cancer incidence and risk factors after solid organ transplantation. *International journal of cancer*, **125**(8), 1747–1754. [3]

VAN DER FLIER, LAURENS G, & CLEVERS, HANS. 2009. Stem cells, self-renewal, and differentiation in the intestinal epithelium. *Annual review of physiology*, **71**(1), 241–260. [8]

VESSELINOVITCH, S D, & MIHAILOVICH, N. 1983. Kinetics of diethylnitrosamine hepatocarcinogenesis in the infant mouse. *Cancer research*, **43**(9), 4253–4259. [61, 83]

WANG, YAN, AUSMAN, LYNNE M, GREENBERG, ANDREW S, RUSSELL, ROBERT M, & WANG, XIANG-DONG. 2009. Nonalcoholic steatohepatitis induced by a high-fat diet promotes diethylnitrosamine-initiated early hepatocarcinogenesis in rats. *International journal of cancer*, **124**(3), 540–546. [6]

WANG, YOUFA, BEYDOUN, MAY A, LIANG, LAN, CABALLERO, BENJAMIN, & KUMANYIKA, SHIRIKI K. 2008. Will all Americans become overweight or obese? estimating the progression and cost of the US obesity epidemic. *Obesity (silver spring, md.)*, **16**(10), 2323–2330. [77]

WHYTE, CLAIRE S, BISHOP, EILEEN T, RUCKERL, DOMINIK, GASPAR-PEREIRA, SILVIA, BARKER, ROBERT N, ALLEN, JUDITH E, REES, ANDREW J, & WILSON, HEATHER M. 2011. Suppressor of cytokine signaling (SOCS)1 is a key determinant of differential macrophage activation and function. *Journal of leukocyte biology*, **90**(5), 845–854. [18]

WILLIAMS, JAMIE J L, & PALMER, TIMOTHY M. 2012. Unbiased identification of substrates for the Epac1-inducible E3 ubiquitin ligase component SOCS-3. *Biochemical society transactions*, **40**(1), 215–218. [10]

WOLF, MONIKA JULIA, ADILI, ARLIND, PIOTROWITZ, KIRA, ABDULLAH, ZEINAB, BOEGE, YANNICK, STEMMER, KERSTIN, RINGELHAN, MARC, SIMONAVICIUS, NICOLE, EGGER, MICHÈLE, WOHLLEBER, DIRK, LORENTZEN, ANNA, EINER, CLAUDIA, SCHULZ, SABINE, CLAVEL, THOMAS, PROTZER, ULRIKE, THIELE, CHRISTOPH, ZISCHKA, HANS, MOCH, HOLGER, TSCHÖP, MATTHIAS, TUMANOV, ALEXEI V, HALLER, DIRK, UNGER, KRISTIAN, KARIN, MICHAEL, KOPF, MANFRED, KNOLLE, PERCY, WEBER, ACHIM, & HEIKENWALDER, MATHIAS. 2014. Metabolic activation of intrahepatic CD8+ T cells and NKT cells causes nonalcoholic steatohepatitis and liver cancer via cross-talk with hepatocytes. *Cancer cell*, **26**(4), 549–564. [7, 63, 65, 85]

WUNDERLICH, F THOMAS, WILDNER, H, RAJEWSKY, KLAUS, & EDENHOFER, FRANK. 2001. New variants of inducible Cre recombinase: a novel mutant of Cre-PR fusion protein exhibits enhanced sensitivity and an expanded range of inducibility. *Nucleic acids research*, **29**(10), E47. [26]

WUNDERLICH, F THOMAS, LUEDDE, T, SINGER, S, SCHMIDT-SUPPRIAN, M, BAUMGARTL, J, SCHIRMACHER, P, PASPARAKIS, M, & BRUNING, J C. 2008. Hepatic NF-κB essential modulator deficiency prevents obesity-induced insulin resistance but synergizes with high-fat feeding in tumorigenesis. *Proceedings of the national academy of sciences*, **105**(4), 1297–1302. [7]

WUNDERLICH, F THOMAS, STRÖHLE, PETER, KÖNNER, A CHRISTINE, GRUBER, SABINE, TOVAR, SULAY, BRÖNNEKE, HELLA S, JUNTTI-BERGGREN, LISA, LI, LUO-SHENG, VAN ROOIJEN, NICO, LIBERT, CLAUDE, BERGGREN, PER-OLOF, & BRÜNING, JENS C. 2010. Interleukin-6 Signaling in Liver-Parenchymal Cells Suppresses Hepatic Inflammation and Improves Systemic Insulin Action. *Cell metabolism*, **12**(3), 237–249. [32, III]

XU, HAIYAN, BARNES, GLENN T, YANG, QING, TAN, GUO, YANG, DASENG, CHOU, CHIEH J, SOLE, JASON, NICHOLS, ANDREW, ROSS, JEFFREY S, TARTAGLIA, LOUIS A, & CHEN, HONG. 2003. Chronic inflammation in fat plays a crucial role in the development of obesity-related insulin resistance. *The journal of clinical investigation*, **112**(12), 1821–1830. [20]

YAMAMOTO, KOH, YAMAGUCHI, MITSUKO, MIYASAKA, NOBUYUKI, & MIURA, OSAMU. 2003. SOCS-3 inhibits IL-12-induced STAT4 activation by binding through its SH2 domain to the STAT4 docking site in the IL-12 receptor beta2 subunit. *Biochemical and biophysical research communications*, **310**(4), 1188–1193. [15]

YASUKAWA, H, MISAWA, H, SAKAMOTO, H, MASUHARA, M, SASAKI, A, WAKIOKA, T, OHTSUKA, S, IMAIZUMI, T, MATSUDA, T, IHLE, J N, & YOSHIMURA, A. 1999. The JAK-binding protein JAB inhibits Janus tyrosine kinase activity through binding in the activation loop. *The embo journal*, **18**(5), 1309–1320. [10]

YASUKAWA, HIDEO, OHISHI, MASANOBU, MORI, HIROYUKI, MURAKAMI, MASAAKI, CHINEN, TAKATOSHI, AKI, DAISUKE, HANADA, TOSHIKATSU, TAKEDA, KIYOSHI, AKIRA, SHIZUO, HOSHIJIMA, MASAHIKO, HIRANO, TOSHIO, CHIEN, KENNETH R, & YOSHIMURA, AKIHIKO. 2003. IL-6 induces an anti-inflammatory response in the absence of SOCS3 in macrophages. *Nature immunology*, **4**(6), 551–556. [12]

YOSHIKAWA, TAKESHI, TAKATA, AKEMI, OTSUKA, MOTOYUKI, KISHIKAWA, TAKAHIRO, KOJIMA, KEN-TARO, YOSHIDA, HARUHIKO, & KOIKE, KAZUHIKO. 2012. Silencing of microRNA-122 enhances interferon-α signaling in the liver through regulating SOCS3 promoter methylation. *Scientific reports*, **2**, 637. [13]

YOSHIMURA, A, OHKUBO, T, KIGUCHI, T, JENKINS, N A, GILBERT, D J, COPELAND, N G, HARA, T, & MIYAJIMA, A. 1995. A novel cytokine-inducible gene CIS encodes an SH2-containing protein that binds to tyrosine-phosphorylated interleukin 3 and erythropoietin receptors. *The embo journal*, **14**(12), 2816–2826. [10]

YOSHIOKA, YOKO, HASHIMOTO, ETSUKO, YATSUJI, SATORU, KANEDA, HIROYUKI, TANIAI, MAKIKO, TOKUSHIGE, KATSUTOSHI, & SHIRATORI, KEIKO. 2004. Nonalcoholic steatohepatitis: cirrhosis, hepatocellular carcinoma, and burnt-out NASH. *Journal of gastroenterology*, **39**(12), 1215–1218. [4]

YU, CHENG-RONG, MAHDI, RASHID M, EBONG, SAMUEL, VISTICA, BARBARA P, GERY, IGAL, & EGWUAGU, CHARLES E. 2003. Suppressor of cytokine signaling 3 regulates proliferation and activation of T-helper cells. *The journal of biological chemistry*, **278**(32), 29752–29759. [15]

ZHANG, J G, FARLEY, A, NICHOLSON, S E, WILLSON, T A, ZUGARO, L M, SIMPSON, R J, MORITZ, R L, CARY, D, RICHARDSON, R, HAUSMANN, G, KILE, B J, KENT, S B, ALEXANDER, W S, METCALF, D, HILTON, D J, NICOLA, N A, & BACA, M. 1999. The conserved SOCS box motif in suppressors of cytokine signaling binds to elongins B and C and may couple bound proteins to proteasomal degradation. *Proceedings of the national academy of sciences of the united states of america*, **96**(5), 2071–2076. [10]

ZHANG, REN, DHILLON, HARVEEN, YIN, HUALI, YOSHIMURA, AKIHIKO, LOWELL, BRADFORD B, MARATOS-FLIER, ELEFTHERIA, & FLIER, JEFFREY S. 2008. Selective inactivation of Socs3 in SF1 neurons improves glucose homeostasis without affecting body weight. *Endocrinology*, **149**(11), 5654–5661. [19]

ZHANG, Y, BUCHHOLZ, F, MUYRERS, J P, & STEWART, A F. 1998. A new logic for DNA engineering using recombination in Escherichia coli. *Nature genetics*, **20**(2), 123–128. [27, 87]

ZHAO, QIYI, XIAO, XIAO, WU, YAN, WEI, YI, ZHU, LING-YAN, ZHOU, JIA, & KUANG, DONG-MING. 2011. Interleukin-17-educated monocytes suppress cytotoxic T-cell function through B7-H1 in hepatocellular carcinoma patients. *European journal of immunology*, **41**(8), 2314–2322. [84]

ZHENG, NING, SCHULMAN, BRENDA A, SONG, LANGZHOU, MILLER, JULIE J, JEFFREY, PHILIP D, WANG, PING, CHU, CLAIRE, KOEPP, DEANNA M, ELLEDGE, STEPHEN J, PAGANO, MICHELE, CONAWAY, RONALD C, CONAWAY, JOAN W, HARPER, J WADE, & PAVLETICH, NIKOLA P. 2002. Structure of the Cul1-Rbx1-Skp1-F boxSkp2 SCF ubiquitin ligase complex. *Nature*, **416**(6882), 703–709. [10]

6 Appendix

6.1 Plasmid maps

6.1.1 SOCS3-U targeting construct
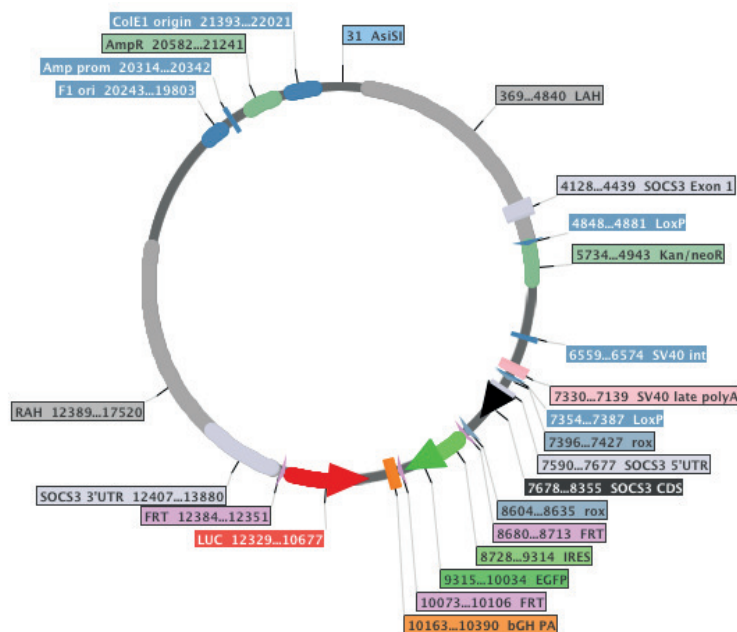
Figure 6.1: **The SOCS3-U targeting construct**
The SOCS3-U targeting construct (22473 bp) with notable features. The left arm of homology (LAH), containing the untranslated exon 1, and the right arm of homology (RAH), containing the 3'UTR, flank the knock-in features. The regulatory region contains a loxP flanked neomycin resistance cassette and the SV40 polyadenylation signal. SOCS3 exon 2, including 5'UTR (in gray) and the SOCS3 coding sequence (black arrow), is flanked by rox sites and followed by the reporter region. The reporter contains an IRES driven GFP, flanked by FRT sites in tandem orientation, and the bovine growth hormone polyadenylation signal. The firefly luciferase coding sequence is encoded on the antisense strand and followed by a FRT site in opposite direction to the other two. Motifs necessary for bacterial replication are depicted together with the AsiSI restriction site for linearization prior to transfection.

6.1.2 SERCA plasmid
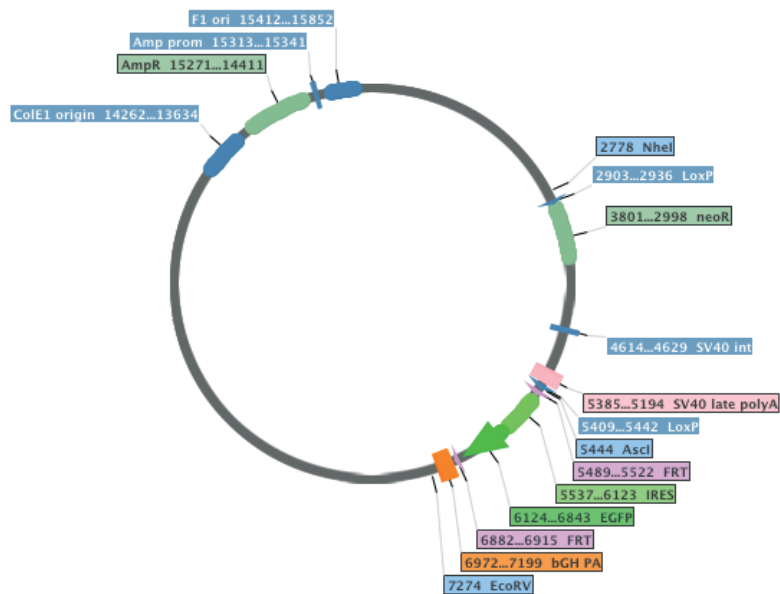
Figure 6.2: **Stop-eGFP-ROSA-CAGs (SERCA)**
Stop-eGFP-ROSA-CAGs (SERCA, 16056 bp) with notable features. AscI restriction site lies in front of the FRT flanked IRES-GFP. NheI and EcoRV restriction sites are used for further cloning. Motifs necessary for bacterial replication are also depicted. [Klisch, 2006]

6.1.3 GK12TK plasmid
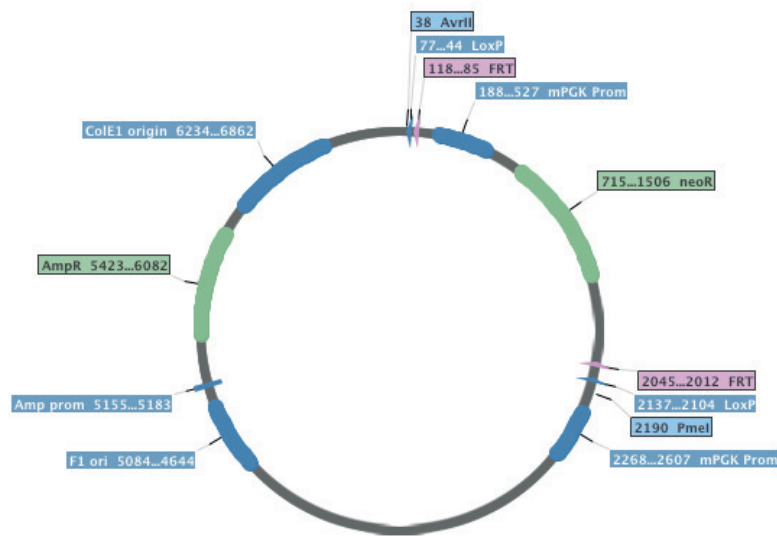
Figure 6.3: **GK12TK**

GK12TK plasmid (7314 bp) with notable features. AvrII and PmeI restriction sites are used for further cloning. Motifs necessary for bacterial replication are also depicted. [Wunderlich *et al.*, 2010]

Danksagung

Erklärung

Die vorliegende Arbeit wurde in der Zeit von Februar 2010 bis Mai 2015 am Institut für Genetik, Universität zu Köln, und am Max-Planck-Institut für Stoffwechselforschung Köln, unter Anleitung von Herrn PD. Dr. Thomas Wunderlich, angefertigt.

Ich versichere, dass ich die von mir vorgelegte Dissertation selbständig angefertigt, die benutzten Quellen und Hilfsmittel vollständig angegeben und die Stellen der Arbeit - einschließlich Tabellen, Karten und Abbildungen -, die anderen Werken im Wortlaut oder dem Sinn nach entnommen sind, in jedem Einzelfall als Entlehnung kenntlich gemacht habe; dass diese Dissertation noch keiner anderen Fakultät oder Universität zur Prüfung vorgelegen hat; dass sie - abgesehen von unten angegebenen Teilpublikationen - noch nicht veröffentlicht worden ist sowie, dass ich eine solche Veröffentlichung vor Abschluss des Promotionsverfahrens nicht vornehmen werde. Die Bestimmungen dieser Promotionsordnung sind mir bekannt.

Köln, Mai 2015

_____
(Philipp Justus Ackermann)

Curriculum vitae

P. Justus Ackermann, M.Sc.

Persönliche Angaben

Name	Philipp Justus Ackermann
Geburtsort	Köln
Geburtstag	29. November 1983
Nationalität	deutsch

Berufserfahrung

07/2014 - *heute*	**Wissenschaftlicher Mitarbeiter**, *Max-Planck-Institut für Stoffwechselforschung, Köln*
02/2010 - 06/2014	**Wissenschaftlicher Mitarbeiter**, *Institut für Genetik, Universität zu Köln*

Ausbildung

02/2010 - *heute*	**Promotion** zum Dr. rer. nat. in Genetik, *Universität zu Köln*
10/2007 - 11/2009	**Master of Science** in Biological Sciences, *Universität zu Köln*
10/2004 - 10/2007	**Bachelor of Science** in Biology, *Universität zu Köln*
09/2003 - 06/2004	Zivildienst, *Hals-Nasen-Ohrenklinik, Universitätsklinikum Köln*
08/1994 - 06/2003	Abitur, *Gymnasium Kreuzgasse, Köln*

Masterarbeit

Titel	Phenotypic characterization of *pcp1Δ* mutants and analysis of their genetic interactions in *Saccharomyces cerevisiae*
Betreuer	Prof. Dr. Thomas Langer

Bachelorarbeit

Titel	Genetic characterization of *YLR168c* in *Saccharomyces cerevisiae*
Betreuer	Prof Dr. Thomas Langer

Praktika

10/2008 - 11/2008	Abteilung Strahlenbiologie, Arbeitsgruppe Astrobiologie, *Deutsches Zentrum für Luft- und Raumfahrt, Köln*
03/2007 - 04/2007	Jean-Uhrmacher Institut für klinische HNO-Forschung, *Universitätsklinikum Köln*

Publikationen

2014	Vera Lepperhof, Olga Polchynski, Klaus Kruttwig, Chantal Brüggemann, Klaus Neef, Florian Drey, Yunjie Zheng, **P. Justus Ackermann**, Yeong-Hoon Choi, F. Thomas Wunderlich, Mathias Hoehn, Jürgen Hescheler, Tomo Šaric. 2014. Bioluminescent Imaging of Genetically Selected Induced Pluripotent Stem Cell-Derived Cardiomyocytes after Transplantation into Infarcted Heart of Syngeneic Recipients. *PLoS One*
	Daniel Sommer, Annika Peters, Tristan Wirtz, Maren Mai, **P. Justus Ackermann**, Yasser Thabet, Jürgen Schmidt, Heike Weighardt, F. Thomas Wunderlich, Joachim Degen, Joachim Schultze & Marc Beyer. 2014. Efficient genome engineering by targeted homologous recombination in mouse embryos using transcription activator-like effector nucleases. *Nature Communications*
2013	Sulay Tovar, Lars Paeger, Simon Hess, Donald A. Morgan, A. Christine Hausen, Hella S. Brönneke, Brigitte Hampel, **P. Justus Ackermann**, Nadine Evers, Hildegard Büning, F. Thomas Wunderlich, Kamal Rahmouni, Peter Kloppenburg and Jens C. Brüning. 2013. K_{ATP}-Channel-Dependent Regulation of Catecholaminergic Neurons Controls BAT Sympathetic Nerve Activity and Energy Homeostasis. *Cell Metabolism*
	Sabine Gruber, Beate K. Straub, **P. Justus Ackermann**, Claudia M. Wunderlich, Jan Mauer, Jens M. Seeger, Hildegard Büning, Lukas Heukamp, Hamid Kashkar, Peter Schirmacher, Jens C. Brüning and F. Thomas Wunderlich. 2013. Obesity Promotes Liver Carcinogenesis via Mcl-1 Stabilization Independent of IL-6Rα Signaling. *Cell Reports*

Konferenz Teilnahmen

03/2014	IGTP Fortbildung der AG West *Köln, Deutschland* **Vortrag:** Altersforschung am übergewichtigen Tier
06/2013	Workshop on Innovative Mouse Models *Leiden, Niederlande* **Poster Award** **Poster:** A universal SOCS3 allele to visualize metabolic changes under obese conditions *in vivo*
09/2012	EMBO-Symposium: Diabetes and Obesity, *Heidelberg, Deutschland* **Poster:** A universal SOCS3 allele to visualize metabolic changes under obese conditions *in vivo*
05/2012	Keystone Symposium: The Role of Inflammation during Carcinogenesis, *Dublin, Irland*
05/2012	SFB832 International Symposium: The Tumor Microenvironment, *Bad Neuenahr, Deutschland*

Köln, Mai 2015